


Spring 5-15-2018

Host Determinants of Protection and Pathogenesis during Chikungunya Virus Infection

Lindsey Elaine Cook

Washington University in St. Louis

Follow this and additional works at: https://openscholarship.wustl.edu/art_sci_etds

 Part of the [Allergy and Immunology Commons](#), [Immunology and Infectious Disease Commons](#), [Medical Immunology Commons](#), and the [Virology Commons](#)

Recommended Citation

Cook, Lindsey Elaine, "Host Determinants of Protection and Pathogenesis during Chikungunya Virus Infection" (2018). *Arts & Sciences Electronic Theses and Dissertations*. 1522.

https://openscholarship.wustl.edu/art_sci_etds/1522

This Dissertation is brought to you for free and open access by the Arts & Sciences at Washington University Open Scholarship. It has been accepted for inclusion in Arts & Sciences Electronic Theses and Dissertations by an authorized administrator of Washington University Open Scholarship. For more information, please contact digital@wumail.wustl.edu.

WASHINGTON UNIVERSITY IN ST. LOUIS

Division of Biology and Biomedical Sciences
Immunology

Dissertation Examination Committee:

Deborah J. Lenschow, Chair

Adrianus C.M. Boon

Michael S. Diamond

Daved H. Fremont

Robert D. Schreiber

Haina Shin

Host Determinants of Protection and Pathogenesis during Chikungunya Virus Infection

by

Lindsey Elaine Cook

A dissertation presented to
The Graduate School
of Washington University in
partial fulfillment of the
requirements for the degree
of Doctor of Philosophy

May 2018
St. Louis, Missouri

© 2018, Lindsey Cook

Table of Contents

List of Figures	iv
List of Abbreviations	vi
Acknowledgments.....	viii
Abstract	xi
Chapter 1 Introduction	1
1.1 Chikungunya virus	2
1.1.1 Overview.....	2
1.1.2 Epidemiology and Transmission.....	2
1.1.3 Symptoms and Treatment	4
1.1.4 Replication Cycle.....	5
1.1.5 Animal Models.....	8
1.1.6 Tropism.....	9
1.1.7 Pathogenesis.....	11
1.2 Type I Interferons.....	14
1.2.1 Overview.....	14
1.2.2 Induction	15
1.2.3 Signaling	17
1.2.4 IFN-I Induction during CHIKV Infection.....	18
1.2.5 IFN-I Action during CHIKV Infection	21
1.2.6 IFN-I Subtypes: evidence for functional differences	24
1.3 Figures.....	29
Chapter 2 Interferons alpha and beta protect against chikungunya virus pathogenesis by distinct mechanisms of action.....	34
2.1 Abstract	35
2.2 Introduction	35
2.3 Results.....	38
2.4 Discussion	45
2.5 Materials and Methods	50
2.6 Figures.....	56

Chapter 3 Therapy with CTLA4-Ig and an antiviral monoclonal antibody controls chikungunya virus arthritis	64
3.1 Abstract	65
3.2 Introduction	65
3.3 Results	68
3.4 Discussion	73
3.5 Materials and Methods	77
3.6 Figures	82
Chapter 4 Summary and Future Directions	92
4.1 Summary	93
4.2 Future Directions	95
4.2.1 When and where are IFN-I subtypes induced during CHIKV infection?	95
4.2.2 How is IFN- α limiting CHIKV replication and dissemination?	97
4.2.3 What is the role of neutrophils in the pathogenesis of CHIKV-infected IFN- β -KO mice?	98
4.2.4 What roles do IFN-I play during chronic CHIKV disease?	101
4.2.5 Are there dual protective and detrimental roles for IFN- β during CHIKV infection?	103
4.3 Materials and Methods	106
4.4 Figures	109
References	112

List of Figures

Chapter 1

Figure 1.1 Replication cycle of CHIKV in mammalian cells.....	29
Figure 1.2 Summary of CHIKV pathogenesis in WT mice.....	30
Figure 1.3 Summary of pathways of IFN-I induction and signaling	31
Figure 1.4 IRF7 participates in a forward feedback loop for IFN-I amplification	32
Figure 1.5 Molecular basis for functional differences among IFN-I subtypes	33

Chapter 2

Figure 2.1 IFN- α and IFN- β both play protective roles in limiting clinical CHIKV disease	56
Figure 2.2 IFN- β -KO, but not IRF7-KO, mice have increased cellular infiltration into the midfoot joint spaces during acute CHIKV infection	57
Figure 2.3 IFN- α , but not IFN- β , limits CHIKV replication and dissemination	58
Figure 2.4 IFN- α and IFN- β exert their protective effects during CHIKV arthritis by signaling on nonhematopoietic cells.....	59
Figure 2.5 IFN- β deficient mice have increased neutrophil recruitment into the ipsilateral foot during CHIKV infection	60
Figure 2.6 Mice lacking IFN- β have increased early IL-9 levels in the ipsilateral foot	61
Figure 2.7 Depletion of neutrophils alleviates the increased foot swelling seen in CHIKV- infected IFN- β -KO mice, but not in IRF7-KO mice.....	62
Figure S2.1 Gating strategy to identify myeloid cells recruited into the ipsilateral foot during CHIKV infection.....	63

Chapter 3

Figure 3.1 Screen of candidate oral and biological DMARDs for treatment of acute CHIKV arthritis in mice	82
Figure 3.2 Combination therapy with CTLA4-Ig and an anti-CHIKV human mAb ameliorates acute CHIKV arthritis in mice	83
Figure 3.3 Viral burden in CHIKV-infected mice treated with CTLA4-Ig and anti-CHIKV mAb	84
Figure 3.4 Cytokine and chemokine analysis in CHIKV-infected mice treated with CTLA4-Ig and anti-CHIKV mAb.....	85
Figure 3.5 Representative H&E staining of the ipsilateral midfoot joints in CHIKV-infected mice treated with CTLA4-Ig and anti-CHIKV mAb.....	86
Figure 3.6 Flow cytometry analysis of infiltrating leukocytes in the feet of mice on day 7 after infection with CHIKV.....	87
Figure 3.7 Clinical assessment of the response to CTLA4-Ig treatment in CHIKV-infected WT and TCR $\beta\delta$ -/- mice.....	88
Figure S3.1 RANKL and OPG expression in CHIKV-infected joints	89

Figure S3.2 Foot swelling with CTLA4-Ig therapy administered before or during CHIKV infection	90
Figure S3.3 Flow cytometry analysis of APC activation in the spleen and ankles of mice on day 7 after infection with CHIKV	91

Chapter 4

Figure 4.1 IRF7-KO mice have increased neutrophil recruitment with elevated CXCL1 and G-CSF	109
Figure 4.2 IFN- α limits persistent CHIKV RNA in the ipsilateral ankle within the first 48 hours following CHIKV infection	110
Figure 4.3 IFN- β may have detrimental effects during chronic CHIKV pathogenesis	111

List of Abbreviations

BMC	bone marrow chimera
ANOVA	analysis of variance
bp	base pairs
BST2	bone marrow stromal antigen 2 (tetherin)
CCL	chemokine (C-C motif) ligand
CHIKV	chikungunya virus
Ckm	muscle creatine kinase
Col1a2	collagen, type I, alpha 2
Cre	Cre recombinase
CXCL	chemokine (C-X-C motif) ligand
CYTOF	cytometry by time of flight (or mass cytometry)
DC	dendritic cell
DENV	Dengue virus
DKO	IRF3 IRF7 double knockout
DMEM	Dulbecco's Modified Eagle Medium
dsRNA	double-stranded RNA
DTR	diphtheria toxin receptor
EAE	experimental autoimmune encephalomyelitis
ECM	extracellular matrix
ECSA	East/Central/South African
FACS	flow cytometry and fluorescence-activated cell sorting
flox	flanked by LoxP sites
GADD34	growth arrest and DNA damage-inducible protein 34
GAPDH	glyceraldehyde-3-phosphate dehydrogenase
H&E	haematoxylin and eosin
IAV	influenza A virus
IFITM3	interferon-induced transmembrane protein 3
IFNAR	interferon alpha/beta receptor
IFN-I	type I interferons
IL	interleukin
ILC	innate lymphoid cells
iNOS/NOS2	inducible nitric oxide synthase
IP	intraperitoneal
IRF	interferon regulatory factor
ISG	interferon stimulated gene
KC	keratinocyte chemoattractant (CXCL1)
KO	knockout
LCMV	lymphocytic choriomeningitis virus

LR	La Reunion
mAb	monoclonal antibody
MAVS	mitochondrial antiviral-signaling protein
MDA5	melanoma differentiation associated protein 5
MIP-2 α	macrophage inflammatory protein 2-alpha (CXCL2)
NSP	non-structural protein
PAMP	pathogen associated molecular pattern
PBS	phosphate buffered saline
PCR	polymerase chain reaction
pDC	plasmacytoid dendritic cell
PFU	plaque forming unit
PKR	protein kinase R
poly I:C	polyinosinic-polycytidylic acid
PRR	pattern recognition receptor
qRT-PCR	quantitative real-time PCR
RA	rheumatoid arthritis
RIG-I	retinoic acid-inducible gene I
RNAseq	RNA sequencing
RRV	Ross River virus
SEM	standard error of the mean
SINV	Sindbis virus
ssRNA	single-stranded RNA
STAT	signal transducer and activator of transcription
TLR	Toll-like receptor
TRIF	TIR-domain-containing adapter-inducing interferon- β
TSLP	thymic stromal lymphopoietin
VEEV	Venezuelan equine encephalitis virus
WNV	West Nile virus
WT	wild type

Acknowledgments

I am indebted to a number of individuals and groups who made this work possible. First and foremost, I would like to thank my thesis advisor, Debbie Lenschow, for over 5 years of guidance and mentorship. I have greatly benefitted from her hands-off, yet approachable mentorship style. She allowed me to struggle and produce perseverance, which ultimately developed me into an independent and better scientist. This journey was not without its frustration or trials, but Debbie was always available and willing to offer her guidance and expertise when science or life became challenging. Debbie is a talented scientist, who also demonstrates great work-life balance and dedication to her family. I am thankful to have such a positive and successful career role model.

Next, I would like to thank my thesis committee for their support and constructive feedback at our various committee meetings over the last 4-5 years: Dr. Bob Schreiber, who served as chair of my committee, Dr. Jacco Boon, Dr. Mike Diamond, Dr. Daved Fremont, and Dr. Haina Shin. Their guidance has been essential in the outcome of this dissertation, and working in such close proximity to leaders in the field of immunology and virology has profoundly shaped the way I do and think about science. I thank Dr. Paul Allen, Dr. Gene Oltz, and Dr. Gwen Randolph who have all served as directors of the Immunology Program during my graduate school career. I would also like to thank Dr. Eynav Klechevsky and Dr. Brian Edelson for allowing me to rotate in their labs. Both rotation experiences were valuable and worthwhile in my training as a scientist. Lastly, I thank the student coordinator for the Immunology Program, Melanie Relich, for her hard work and diligence in helping each and every student successfully persevere to the end.

Washington University has an incredibly collaborative environment, and my dissertation work has greatly benefited from the expertise of many labs. Our lab has a longstanding collaboration with Mike Diamond's lab, and I am incredibly grateful for being included in the CTLA4-Ig therapy project, which substantially contributed to my dissertation. Getting to work with Jonathan Miner, an experienced postdoc and co-first author on this project, was an invaluable training experience. Jonathan is a natural mentor, and I greatly benefitted from putting together and submitting the manuscript with him. This study also included collaboration with Dr. James Crowe (Vanderbilt), who generously provided the human anti-CHIKV 4N12 mAb, as well as other members of the Diamond Lab: Jun Hong, Amber Smith, Raeann Shimak, Subhajit Poddar, and Justin Richner. I also thank the Diamond Lab members who regularly attend CHIKV focus meetings for their constructive discussion: Julie Fox and Sharmila Nair. I also thank Dr. Sandeep Tripathy and Dr. Tony French for their valuable discourse at joint lab meetings for the last 5 years.

The current and past members of the Lenschow Lab have made my time in the lab an incredibly positive experience. I would like to thank former lab members who were present for my rotation and early days in lab: Anjali Rohatgi, Dave Morales, Scott Werneke, Jessea Campbell, and Mari Rodriguez. I am deeply appreciative of their patience, assistance, and guidance. I am especially indebted to Anjali who mentored me during my rotation, and I strive to be a dedicated scientist and kind person, as she was to me. I owe a huge thanks to current lab members for their friendship and collaboration: Kristen Monte, Yi-Chieh (EJ) Perng, Alissa Young, Marissa Locke, and Brad Hiller. EJ and Alissa have been my co-workers for almost the entirety of my time in the Lenschow Lab. Their encouragement and scientific advice have helped me persevere through the more challenging moments of my scientific career. Lastly, a very special thanks for Kristen, our lab manager and a dear friend. She has always been available as an extra set of hands for long

experiments or as a lunch buddy for Kampai Sushi. I am deeply thankful for each and every member of the Lenschow Lab.

My dear classmates, the Immunology cohort of 2012, are amazing people and scientists, whom I count myself fortunate to know, and it is hard to imagine what my graduate school experience would have been like without them. Mike Buck, Chelsea Parker Harp, Christina (O'Neill) Park, Justin Perry, Jing Qui, Jaleisa Turner, and You Zhou will always be considered friends and colleagues. I sincerely thank Chelsea and Mike for their deep friendship, and I look forward to where our careers and lives will carry us.

I cannot thank my family enough for loving me and supporting me. My parents, Jan Ouellette and Steve Cook, have always believed in me and worked hard to provide me with everything I needed to become the scientist I am today. I dearly love all the new people who have been added to our family, especially my stepfather, Pascal Ouellette, and stepmother, Joann Cook. Thank you both for welcoming me into your lives and hearts. It is so special to get share my passion for immunology with my sister and best friend, Melissa, and I thank her for the many years of comradery and love. I thank my roommate, Beth Davey, for being my social justice sister-in-arms and dear friend. Lastly, thank you to my St. Louis faith community at The Journey Hanley Road: for faithfully embodying the sacrificial love Christ.

Greater love has no one than this, that someone lay down his life for his friends.

– John 15:13

Lindsey E. Cook

Washington University in St. Louis

May 2018

ABSTRACT OF THE DISSERTATION

Host Determinants of Protection and Pathogenesis during Chikungunya Virus Infection

by

Lindsey Elaine Cook

Doctor of Philosophy in Biology and Biomedical Sciences

Immunology

Washington University in St. Louis, 2018

Professor Deborah J. Lenschow, Chairperson

Chikungunya virus (CHIKV) is a mosquito-transmitted alphavirus that causes acute and chronic polyarthritis. The virus has rapidly emerged over the last decade, and in 2013, CHIKV spread to the Western Hemisphere for the first time, infecting more than 1.8 million people. CHIKV targets the joints and musculoskeletal tissues, resulting in severe myalgia and symmetric polyarthritis that clinically mimics rheumatoid arthritis. Currently, no approved treatment is effective in preventing or controlling CHIKV infection or disease. Pathogenesis of CHIKV is still poorly understood but is thought to reflect an interplay between viral replication and detrimental immune responses. CHIKV patients have increased numbers of circulating CD4⁺ and CD8⁺ T cells, and mice lacking or depleted of CD4⁺ T cells show reduced foot swelling and arthritis during acute CHIKV infection, suggesting that CD4⁺ T cells contribute to the pathology of arthritis. Additionally, monocytes and/or macrophages are also thought to promote disease because depletion of macrophages with clodronate liposomes or inhibiting production of monocyte chemoattractant protein-1 (MCP-1) with bindarit improved symptoms in animal models. Though immunopathology appears to play an important role in CHIKV pathogenesis, not all host responses are detrimental. Central to controlling CHIKV and other alphavirus infections is the type I

interferon (IFN-I) response, as mice lacking the IFN-I receptor rapidly succumb to infection. IFN-I are well known for their antiviral and immunomodulatory properties, but their mechanism of action during CHIKV infection is poorly understood.

IFN-Is are composed of 14 IFN- α subtypes and single forms of IFN- β , IFN- ϵ , IFN- κ , and IFN- ω , and despite their central role in protection against a number of viruses, little is known about the biological roles of individual IFN-I subtypes during viral infection. To address this issue we used genetic deletion mutants and blockade with antibodies targeting specific IFN subtypes to determine the contributions of IFN- α and IFN- β during acute CHIKV infection. We found that both IFN- α and IFN- β play important protective roles in limiting clinical CHIKV disease, but they do so by distinct mechanisms. The loss of IFN- α (through IRF7 knockout or IFN- α blocking Abs) resulted in increased CHIKV replication and dissemination. In contrast, loss of IFN- β (through IFN- β knockout or IFN- β blocking Abs) had minimal impact on viral replication and dissemination. Instead, the loss of IFN- β lead to increased neutrophil recruitment and elevated IL-9 induction. Further, the increased clinical disease observed in IFN- β knockout mice could be rescued with neutrophil depletion. Thus, our findings suggest distinct protective roles for the IFN-I subtypes during CHIKV infection, with IFN- α functioning to limit early viral replication and spread and IFN- β modulating neutrophil-mediated immunopathology.

Previous data have shown that immune cells and proinflammatory cytokines contribute to CHIKV arthritis in mice. Because chronic CHIKV arthritis is clinically similar to seronegative rheumatoid arthritis, we examined the efficacy of several U.S. Food and Drug Administration (FDA)-approved rheumatoid arthritis therapies in a mouse model of CHIKV infection. We identified CTLA4-Ig (abatacept) as a disease-modifying antirheumatic drug (DMARD) with efficacy during acute CHIKV arthritis. CTLA4-Ig, which blocks T cell activation, reduced T cell

accumulation in the joints of infected animals without affecting viral replication. When paired with the neutralizing anti-CHIKV human monoclonal antibody, 4N12, it was highly effective at reducing joint inflammation, periarticular swelling, migration of inflammatory leukocytes, and infection, even when administered several days after virus inoculation. Thus, combination of anti-inflammatory and antibody-based antiviral therapy may serve as a model for treating humans with arthritis caused by CHIKV or other related viruses.

Collectively, these data provide important mechanistic insight into the host factors that control and promote CHIKV pathogenesis. Continued pursuit of defining interactions between CHIKV and the host immune responses will be paramount in developing effective therapeutics and vaccines to combat CHIKV and other emerging tropical diseases, which remain a global health and economic burden.

Chapter 1

Introduction

1.1 Chikungunya virus

1.1.1 Overview

Chikungunya virus (CHIKV) is a mosquito-transmitted alphavirus that causes acute and chronic polyarthritis. The virus has rapidly emerged over the last decade, with millions of people infected worldwide. CHIKV targets the joints and musculoskeletal tissues, resulting in severe myalgia and symmetric polyarthritis that can last for months to years after infection in some patients. Currently, no approved treatment is effective in preventing or controlling CHIKV infection or disease. Pathogenesis of CHIKV is still poorly understood but is thought to reflect interplay between viral replication and detrimental immune responses.

1.1.2 Epidemiology and Transmission

CHIKV was first isolated from a febrile patient in Tanzania in 1952, and its name comes from a Makonde phrase that means “to become contorted” or “that which bends up,” which describes the posture of those suffering from debilitating CHIKV arthritis¹. In endemic rural areas, CHIKV is maintained in an enzootic cycle involving nonhuman primates and mosquitoes, occasionally causing short-lived sporadic outbreaks in urban areas of Africa, which rely on human-mosquito-human transmission². Three lineages of CHIKV have been defined: East/Central/South African (ECSA), West African, and Asian. The West African strain has mostly been associated with enzootic transmission and occasional small outbreaks of human disease confined to West Africa. In contrast, the ECSA and Asian genotypes have rapidly expanded to new regions and have caused numerous urban outbreaks.

Beginning in 2004 a severe outbreak with the ECSA strain began in the coastal region of Kenya on Lamu Island and Mombasa. CHIKV then quickly spread to surrounding countries and

islands of the Indian Ocean. During this outbreak, the French island of La Réunion experienced a particularly severe outbreak, with over one third of the population infected with CHIKV between 2005 and 2006^{3,4}. During the La Réunion outbreak, more severe disease manifestations, such as encephalopathy and mortality, were observed^{5,6}. Studies comparing a clinical isolate from the La Réunion outbreak (LR OPY2006) to a previous strain (Senegal, 1983) revealed that increased infection of myofibers may have contributed to the increased disease severity seen on La Réunion⁷. When CHIKV re-emerged in India, millions of people were infected, and an infected traveler returning to Italy from India resulted in a small outbreak there, which was the first instance of local CHIKV transmission in Europe⁸. In 2013, the Asian strain of CHIKV emerged in the Caribbean on the island of Saint Martin, and since its introduction to the Americas, there have been over 1.8 million suspected cases in South and Central America⁹. With its introduction to the Western Hemisphere, the United States has seen an increase in the number of imported cases, and for the first time, local transmission was reported in Florida¹⁰.

Historically, CHIKV was primarily transmitted by the *Aedes aegypti* mosquito, but in 2006 the ECSA genotype acquired a single mutation (A226V) in its E1 envelope glycoprotein that enhanced its replication in the *A. albopictus* mosquito, which has more temperate geographical spread than *A. aegypti*¹¹. Interestingly, the Asian strain is genetically constrained in its ability to adapt to the *A. albopictus* mosquito¹². Transmission by *A. albopictus* played an important role in outbreaks that occurred in Italy, and increases the potential for outbreaks in other more temperate regions like the United States⁸. Despite the unprecedented rapid spread of the ECSA in the Indian Ocean region, it was the Asian lineage that emerged in the Caribbean and the Americas, and thus, the outbreaks in the Western Hemisphere have primarily been transmitted by *A. aegypti*. In 2014, the ECSA was reported to have been introduced in Brazil, raising concerns for the potential of

increased spread into the United States, where *A. albopictus* has great geographical range¹³. Collectively, in little more than a decade, CHIKV has reemerged as a global pathogen, infecting millions of people and causing economic damage in more than 50 countries^{2,14}.

1.1.3 Symptoms and Treatment

After being bitten by a mosquito carrying CHIKV and an incubation period of 2-6 days, infections in humans can manifest with fever, a maculopapular-like rash, malaise, myalgia, and severe polyarthralgia and polyarthritis^{15,16}. During the ongoing outbreak, there were also reports of more severe symptoms, particularly in neonates, the elderly, or patients with other underlying medical conditions. These severe clinical features include neurologic and cardiac manifestations, and for the first time, there were reports of fatality associated with CHIKV infection^{5,6}. Unlike other arthritogenic viruses, CHIKV infections are 90-95% symptomatic¹⁷. Patients presenting with acute CHIKV arthralgia usually experience symmetrical joint pain in the peripheral joints, such as wrists, knees, ankles, and the small joints of the hand. Joint pain is often accompanied with arthritis, with joints displaying swelling and tenderness. Acute disease is usually self-limiting and typically resolves in 7-10 days, however a large subset of patients can develop chronic symptoms that last from months to years after infection. There are reports that anywhere from 20 to 60% of infected individuals can develop chronic arthritis symptoms following CHIKV infection¹⁸⁻²¹. Epidemiological predictions suggest that the number of people in the Americas suffering from chronic CHIKV symptoms is 400,000²². Chronic CHIKV arthritis is clinically similar to patients with seronegative rheumatoid arthritis (RA), with the hands, wrists, feet, and ankles primarily affected²³.

There are currently no approved specific antiviral therapies or vaccines available for CHIKV infection. Treatment for acute and chronic symptoms is primarily supportive care to

reduce fever and pain. A couple of small studies have reported improvement of CHIKV symptoms with chloroquine phosphate treatment, an antimalarial drug, but a study with a large cohort of patients from La Réunion found no improvement²⁴⁻²⁶. In recent years, studies have begun to address the need for new therapeutic options in CHIKV infection. A number of compounds have been showed to inhibit CHIKV replication in cell culture, and several treatment strategies in animal models of CHIKV infection have provided some hope for alleviation of CHIKV symptoms²⁷. Monoclonal neutralizing antibodies isolated from infected patients have been protective when administered prophylactically or therapeutically in highly susceptible neonatal mice or immunocompromised mice^{28,29}. Furthermore, a loss-of-function screening approach identified a number of pro-viral host factors with pre-existing small-molecule inhibitors available³⁰. Several of these small-molecule inhibitors were efficacious *in vivo*, and the protective effects were enhanced when used in combination. Collectively, these studies demonstrate that targeting viral and/or host pathways may be promising, but much work remains to be done to develop and test effective treatment options for those suffering with CHIKV arthritis, particularly for those suffering from chronic symptoms.

1.1.4 Replication Cycle

CHIKV and other alphaviruses are members of the *Togaviridae* family of viruses, and as such, they are enveloped viruses with a positive-sense, single stranded RNA genome. The CHIKV genome is approximately 11,800 base pairs in length and contains a 5' untranslated region, followed by nonstructural genes, structural genes with a subgenomic promoter, and a 3' untranslated region. Replication in mammalian cells takes place in the cytosol and in virally-induced cytopathic vacuoles³¹. The replication cycle of CHIKV is summarized in Figure 1.1.

Alphaviruses enter susceptible cells by clathrin-mediated endocytosis, but the specific mechanistic events for CHIKV binding and entry are still unclear³². Bona fide receptors have yet to be identified, but glycosaminoglycans may serve as attachment factors for many susceptible cell types^{33–35}. Once CHIKV enters the endosomal compartment, the increased acidic environment inside the endosome induces a conformational change in the virion envelope that exposes the E1 glycoprotein fusion loop³⁶. This allows fusion of the virion envelope with the endosome membrane, releasing the nucleocapsid into the cytosol. Alphavirus capsid proteins bind the host's large ribosomal subunit, and this interaction is thought to actively disassemble the nucleocapsid and release the RNA genome into the cytosol^{37,38}.

The CHIKV genome contains two open reading frames that encode for two polyproteins, which are then cleaved into multiple proteins. First, the genome is translated by host machinery to produce the nonstructural polyprotein P1234. This precursor is autocleaved by protease activity located in nsP2 into P123 and nsP4, which make up a short-lived replicase that synthesizes a full-length negative-sense RNA template³¹. Early negative-strand synthesis by the short-lived P123/nsP4 replicase takes place at the plasma membrane in small, vesicular compartments called spherules for a number of alphaviruses, including CHIKV^{39–43}. The nsPs localize at the neck of the spherules, which might serve to help shield double-stranded RNA (dsRNA) intermediates from recognition by the host. The spherules are eventually internalized into large cytopathic vacuoles (CPV-I), and P123 accumulation leads to complete processing of the polyprotein into nsP1, nsP2, and nsP3, which together with nsP4 uses the negative-sense template for amplification of genomic positive-sense RNA and transcription of subgenomic (26S) positive-sense RNA that encodes the structural polyprotein.

The host machinery begins to translate the subgenomic RNA, and as the capsid protein is translated, it is quickly released by autoproteolysis to begin forming nucleocapsids containing a single genomic RNA molecule. Translation of the subgenomic RNA continues to generate an E3-E2-6K-E1 product and a minor product (E3-E2-TF) that is the result of ribosomal frameshifting^{44,45}. The N-terminus of E3 contains a signal peptide that directs the 2 polyprotein products into the host secretory pathway, and host protease cleavage yields pE2 (E3-E2), 6K or transframe (TF), and E1. The roles of 6K and TF are still unclear. They do not seem to be incorporated into virions, but may have ion-channel properties and play important roles in viral budding⁴⁶. E1 and E3-E2 continue through the secretory pathway and undergo several post-translational modifications, including N-linked glycosylation, and E3 is released by the host protease furin. E1 and E2 can now begin to form spikes on the plasma membrane³¹.

A second type of cytopathic vacuole (CPV-II) forms late in infection. Here, cytoplasmic nucleocapsids associate with internalized E1 and E2 spikes, and a mature virion egresses and buds from the cell^{47,48}. It is worth noting that CPV-I and CPV-II formation appears to be specific to mammalian cells infected with CHIKV. The CHIKV virion contains a lipid bilayer envelope around an icosahedral nucleocapsid shell, which consists of 240 capsid copies and the genomic RNA. The E1 and E2 glycoproteins form heterodimers on the envelope surface that are further arranged into trimers to form an icosahedral lattice⁴⁹. There is some evidence that CHIKV may be spread by apoptotic blebs to uninfected neighboring cells *in vitro*, which would help avoid detection by antibodies and aid infection of some non-permissive cells. Macrophages were demonstrated to be infected after phagocytosing CHIKV-containing apoptotic blebs *in vitro*⁵⁰.

1.1.5 Animal Models

In the last 10-15 years, significant progress has been made to delineate the mechanisms underlying disease pathogenesis. These advances have been made possible with the development and use of animal models that recapitulate many aspects of human disease. The most commonly used model is a mouse model of CHIKV arthritis. In this model adolescent and adult immunocompetent mice are inoculated with CHIKV directly into the rear footpad, mimicking the effects of a mosquito bite. This arthritis mouse model recapitulates many aspects of acute human disease including viremia, viral replication in the joint and muscle tissues, and histopathological signs of synovitis and myositis⁵¹⁻⁵³. This route of CHIKV infection in mice causes a biphasic pattern of foot swelling in the inoculated foot. In a WT mouse, the first peak of foot swelling occurs 2-3 days post infection (dpi) and is thought to arise from robust viral replication which drives cell death, local proinflammatory cytokine production, and edema. The second peak (6-7 dpi) occurs as infectious virus is cleared from the tissues and blood and is associated with an influx of inflammatory infiltrates into the joint spaces and surrounding soft tissues that drive cytokine production, synovitis, myositis, and edema^{51,52}. Though clinical foot swelling resolves by 10-12 dpi, this model does encompass some aspects of chronic CHIKV disease. CHIKV RNA persists in the joints of mice to at least 120 dpi, and there are signs of myositis and synovitis by histopathology^{54,55}. The pathogenesis of CHIKV in the arthritis model is further discussed in section 1.1.7 and summarized in Figure 1.2

Other animal models have also been useful in determining mechanisms of CHIKV pathogenesis. Infection of neonatal mice results in severe CHIKV disease that exhibits age-dependent mortality. The severe symptoms observed in neonatal mice mimics many aspects of human infants infected with CHIKV, including dissemination to the central nervous system⁵⁶⁻⁵⁸.

Infection of adult cynomolgus macaques results in high viremia, viral dissemination, viral persistence, and pathological features similar to human disease, and aged rhesus macaques show persistent virus in the spleen^{59,60}. The cumulative work from all of these models reveal that CHIKV symptoms are the result of both extensive viral replication in the musculoskeletal and joint tissues, as well as pathology driven by aspects of the host immune response (described in detail below). Careful mapping of the viral and host determinants of pathogenesis will be needed to aid in the development of effective therapeutics and vaccines to combat this global pathogen.

1.1.6 Tropism

Tropism: Cell Culture

When the severe CHIKV outbreak began in 2004, very little was known about CHIKV biology. Early work sought to define the cell tropism of CHIKV *in vitro*. An early study tested a large panel of immortalized and primary human cells for their ability to support CHIKV replication⁶¹. They demonstrated that a variety human epithelial-derived cell lines, such as HeLa and 293T cells, and primary fibroblasts (Hs 789.sk skin cells and MRC5 lung cells) were highly susceptible to CHIKV infection. Additionally, an endothelial cell line isolated from bone marrow (TrHBMEC cells), but not the brain (hCMEC/D3 cells), supported CHIKV replication. CHIKV infection of cell lines and primary cells was highly cytopathic and associated with apoptosis. In contrast, CHIKV did not replicate in lymphoid and monocyte cell lines, primary lymphocytes and monocytes, or monocyte-derived dendritic cells. In this study, primary monocyte-derived macrophages were the only immune cell population tested that was able to support CHIKV growth, albeit to a much lesser extent than the epithelial and fibroblast cells⁶¹. Because the skin is the first site of infection, another group sought to determine the response of keratinocytes to CHIKV infection and found that human keratinocytes are refractory to CHIKV infection at a post-fusion

step, but they were still able to produce cytokines and chemokines following CHIKV exposure⁶². Additional work has shown that CHIKV can also infect primary human osteoblast cultures, which leads to the production IL-6 and receptor activator of nuclear factor kappa-B ligand (RANKL) and inhibition of osteoprotegerin⁶³.

Tropism: Acute Infection

After inoculation of immunocompetent mice in the skin, CHIKV RNA was detected by *in situ* hybridization in the ipsilateral foot at 3 days post infection (dpi) in cells lining blood vessels, skeletal muscle cells, cells in the dermis consistent with fibroblast morphology, cells in the synovial membrane, and cells of the periosteum⁶⁴. By 5 dpi, the cells lining the blood vessels remained positive, but staining was diminished in the dermis and absent in the muscle. These data and the observations from cell culture infections suggest that CHIKV targets a wide variety of cells in the musculoskeletal and joint tissues, which is consistent with the clinical disease manifestations. Whether immune cells, particularly monocytes and macrophages, are actively infected during acute CHIKV infection remains unclear and controversial. Work from Lisa Ng's group showed that monocytes isolated from viremic patients were positive for CHIKV antigen staining by flow cytometry, and this antigen positivity was lost when the samples were taken from the same patients during the chronic phase⁶⁵. However, time-course analysis of infection of human monocytes *in vitro* suggest that monocytes might not support productive release of infectious particles. Over time, the percent of infected monocytes marginally increased over the 0 hour time point (35% versus 10%). Additionally, the viral load determined by RT-PCR remains constant over time, and infectious virus in the supernatant substantially decreases over time⁶⁵. Though the authors concluded that monocytes could "sustain virus growth," these data are more consistent with a model in which CHIKV can bind and enter monocytes, but this ultimately yields a

nonproductive infection. Nonproductively infected cells can be important sources of cytokines and chemokines, and it may be that nonproductive-infected monocytes are important sources of IFN-I (further discussed in section 1.2.4).

Tropism: Chronic Disease

Tropism for chronic CHIKV infection is still not well understood. CHIKV has not been cultured from patient synovial fluid, but a biopsy of synovial tissue from a patient experiencing chronic symptoms showed CHIKV antigen-positive perivascular macrophages and large numbers of activated CD56⁺CD69⁺ NK cells and CD4⁺ T cells clustered around the CHIKV⁺ macrophage⁶⁶. Additionally, aged rhesus macaques show CHIKV RNA persistence in their spleens, and additionally, a study with cynomolgus macaques showed that macrophages in the spleen were positive for CHIKV antigen^{59,60}. These studies suggest that persistent viral RNA and/or antigen may be sustaining immune activation, which promotes continuous proinflammatory cytokine and chemokine production. The sensitivity of assays used to detect CHIKV antigen or viral RNA has made it difficult to identify the source and nature of persistent CHIKV RNA. Unpublished data from our lab using a CHIKV-Cre fate-reporter system suggest that while CHIKV is highly cytopathic *in vitro*, many cells are able to survive CHIKV infection *in vivo*. These cells seem to be CD45-negative and are mostly located in the muscle and to a lesser extent in the dermis. Much more work is needed to characterize the cellular players in harboring persistent CHIKV RNA.

1.1.7 Pathogenesis

Acute Pathogenesis: Innate Immune Responses

Evidence from patient samples and from animal models suggest that a robust innate immune response is mounted following CHIKV infection. Several groups have characterized proinflammatory cytokines and chemokines from serum of CHIKV patient cohorts. There have

been some discrepancies between the various cohorts, but IL-1 β , IL-6, IFN- α , CCL2/MCP-1, CXCL9/MIG, and CXCL10/IP-10 are among those that were upregulated in CHIKV patients relative to healthy controls⁶⁷⁻⁶⁹. Macrophages and monocytes are rapidly recruited to the site of infection in animal models⁵². Clodronate depletion of macrophages had a protective effect on clinical disease, but worsened viremia, suggesting the macrophages may have a dual role in promoting pathogenesis while also controlling viral replication⁵¹. Consistent with this, a study showed that treatment with Bindarit, an inhibitor of CCL2 synthesis, reduced cellular infiltration and CHIKV-associated bone loss⁷⁰. However, the role of macrophages and monocytes may be more complex, as mice deficient for CCR2, the receptor for CCL2, developed much more severe and prolonged CHIKV arthritic disease that was due to compensatory recruitment of neutrophils and eosinophils⁷¹. Indeed, recent work demonstrated that monocytes were protective in both RRV and CHIKV infection due to their type I interferon production (discussed in section 1.2.4)⁷². More careful characterization of infiltrating myeloid cells and their effector functions during CHIKV infection will be valuable for clarifying these findings.

Natural killer (NK) cells also infiltrate into the joint and muscle tissues following CHIKV infection⁵². Two separate studies have identified elevated NK cell percentage or activation in PBMCs isolated from patients^{73,74}. Careful evaluation of the function of NK cells during CHIKV pathogenesis has not been done, but one study did note that NK cells mediated worse disease with an East-Central-South-African (ECSA) genotype of CHIKV, but not with an Asian lineage of CHIKV, suggesting that there might be strain-specific effects of NK cell involvement in pathogenesis⁷⁵. Another innate-like cell type often involved in skin immune responses is $\gamma\delta$ T cells. One study showed that TCR $\gamma\delta$ -KO mice had worsened foot swelling at 7 dpi, accompanied with elevated proinflammatory cytokines and altered cellular recruitment, but no change in viral load

was observed⁷⁶. This finding implies a protective immunomodulatory role for $\gamma\delta$ T cells in CHIKV infection. Innate lymphoid cells are involved in a number of acute inflammatory models, including RA, but they have not been evaluated in CHIKV pathogenesis⁷⁷.

Acute Pathogenesis: Adaptive Immune Responses

Adaptive immune responses are involved in both protection and pathogenesis during CHIKV disease. Neutralizing antibodies are required for clearing infectious virus, whereas CD4⁺ T cells play a critical role in promoting pathogenesis. This is demonstrated in *Rag1*^{-/-} mice, which fail to control viremia and sustain infectious virus replication in their periphery for greater than 3 months post infection⁵⁴. Coincidentally, *Rag1*^{-/-} animals are also largely protected from clinical disease. Further characterization, of CD4-KO and CD8-KO mice determined that it was CD4⁺ T cells contributing to pathogenesis and antibodies responsible for clearing virus, whereas CD8⁺ T cells seem to be dispensable. Passively administering CHIKV neutralizing antibodies to *Rag1*^{-/-} mice eliminates infectious virus, but after administration was stopped, infectious virus re-emerged, suggesting that neutralizing antibodies are able to control, but not clear CHIKV^{54,55}. A pathogenic role for CD4⁺ T cells is reinforced with the observation that expansion of T regulatory cells with an IL-2/anti-IL-2 complex prior to CHIKV infection alleviated disease by inhibiting CHIKV-specific effector CD4⁺ T cells⁷⁸. These findings from animal models are supported by a study of a patient cohort, which found greater percentages of activated effector CD4⁺ and CD8⁺ T cells in peripheral blood mononuclear cells (PBMCs) isolated from patients with persistent CHIKV polyarthritis and patients with untreated, active rheumatoid arthritis (RA) compared to healthy controls²³. Taken altogether, there is profound evidence that adaptive immune responses play important roles in the early stages of acute CHIKV disease.

Chronic pathogenesis

It is known that CHIKV RNA, but not infectious virus, persists in the joints and musculoskeletal tissues of patients and animals infected with various strains of CHIKV^{52,55,66}. Furthermore, mice infected with a CHIKV strain engineered to express firefly luciferase still showed bioluminescence at chronic time points⁷⁹. It is possible that this persistent RNA is continuously stimulating an inflammatory response. Consistent with this theory, a number of IFN-related and proinflammatory genes were upregulated in CHIKV-infected foot tissue at 30 dpi compared to day 0 samples⁵⁵. High levels of IFN- α was observed in PBMCs isolated from chronic CHIKV patients, and another group found that persistent arthralgia was associated with elevated levels of IL-6 and GM-CSF^{66,68}. There is still much to be done to delineate the mechanisms of chronic CHIKV pathogenesis.

1.2 Type I Interferons

1.2.1 Overview

Type I interferons (IFN-I) are a family of multifunctional cytokines originally named for their ability to interfere with viral replication *in vitro*, and now they are recognized as major effector cytokines with important roles in both innate and adaptive immune responses^{80,81}. General properties of IFN-I include eliciting an antiviral state through the induction of interferon stimulated genes (ISGs) and modulating innate and adaptive immune responses through both direct and indirect effects. IFN-I in mice consist of 14 IFN- α subtypes and single forms of IFN- β , IFN- ϵ , IFN- κ , and IFN- ω . Despite signaling through a shared receptor and possessing a similar spectrum of functions, *in vitro* studies and recent work *in vivo* highlight that there are different potencies of shared functions and some unique properties among the individual subtypes. The multigene nature

of IFN-I is conserved across many species, suggesting that having multiple IFN subtypes is beneficial for the host.

1.2.2 Induction

Host cells possess many cell intrinsic and cell extrinsic mechanisms for detecting a viral infection and coordinating an IFN-I response. Pattern recognition receptors (PRRs) detect conserved pathogen-associated molecular patterns (PAMPs), such as nucleic acids during viral infection⁸². The nucleic acid sensors can be found in the cytosol of many cell types or in specialized endosomal compartments of immune cells and some nonhematopoietic cells^{83,84}. Nucleic acid-sensing PRRs are able to induce IFN-I through several distinct pathways, depending on the sensor and cell type, but most pathways ultimately converge on the activation of IRF3 or IRF7 (summarized in Figure 1.3)^{82,85}.

DNA Sensors

Cytosolic sensors of DNA include DNA-dependent activator of IFN-regulatory factors (DAI)⁸⁶ and cyclic GMP-AMP synthase (cGAS)^{87,88}, whereas Toll-like receptor 9 (TLR9) recognizes cytosine-guanosine motifs in DNA within endosomes⁸⁹. Most cytosolic DNA sensor signaling pathways converge on the activation of stimulator of IFN genes (STING), which is located on the endoplasmic reticulum. Activation of STING results in the phosphorylation and activation of TANK-binding kinase 1 (TBK1)⁹⁰. TBK1 phosphorylates IRF3 or IRF7, allowing for their translocation into the nucleus. In contrast, TLR9 signals through MyD88 (myeloid differentiation primary response 88) to activate the E3 ubiquitin ligase TRAF6 (TNF receptor associated factor 6). TRAF6 can then induce proinflammatory cytokines via the activation of NF- κ B (nuclear factor kappa-light-chain-enhancer of activated B cells) or induce type I IFN production through IRF7 activation⁹¹.

RNA Sensors

Cytosolic RNA sensors include retinoic acid-inducible gene I (RIG-I), which recognizes short dsRNA and RNA with 5' triphosphate ends and melanoma differentiation-associated protein 5 (MDA5), which detects long dsRNA⁹¹. TLR3 and TLR7/8 are located in endosomes and recognize dsRNA and single-stranded RNA, respectively⁸². RIG-I and MDA5 signal through mitochondrial antiviral-signaling protein (MAVS), which when associated with the mitochondria leads to IFN-I induction via TBK1-mediated activation of IRF3/7, whereas when it is associated with the peroxisome, it leads to induction of a distinct set of antiviral genes. TLR3 signals through TRIF (TIR-domain-containing adapter-inducing interferon- β) to induce IFN-I downstream of TBK1-mediated activation of IRF3⁹¹.

IRF3 and IRF7

Initially, most cells respond to PRR signals to activate interferon regulatory factor 3 (IRF3), which can act on the promoters of the IFN- β and IFN- α 4 subtypes^{92,93}. These initial IFN-I subtypes signal in autocrine and paracrine means to modulate expression of ISGs that include antiviral effector molecules and regulators that promote the antiviral response. IRF7 is among the transcriptional regulators induced by the early IFN-I subtypes, and it participates in a positive feedback loop that induces the other IFN- α subtypes, thus amplifying and diversifying the IFN-I response (Figure 1.4)^{94,95}. The central role of IRF7 in inducing the IFN- α subtypes is demonstrated in IRF7 deficient mice, which fail to produce many of the IFN- α subtypes in response to viral infection, including CHIKV^{64,96-98}. A recent study from the laboratory of Jean-Laurent Casanova identified a compound heterozygous null mutation in *IRF7* in a patient who suffered from a life-threatening primary influenza A infection⁹⁹. The patient's leukocytes and plasmacytoid DCs (pDCs) produced very little type I and type III interferons and supported higher viral replication

in response to influenza infection; however, IFN- β was still mildly induced in the patient's stimulated cells. Thus, IRF7 is a master regulator of IFN-I, particularly IFN- α subtypes, in both mice and humans. An exception to this IRF7 paradigm is pDCs, which are specialized cells of the immune system capable of producing large amounts of IFN-I during a viral infection¹⁰⁰. Unlike most other cell types, pDCs constitutively express IRF7, enabling them to produce large amounts of IFN- α subtypes directly downstream of TLR7 or TLR9 signaling. The importance of pDCs for production of IFN-I during an infection can depend on the route of infection (systemic versus peripheral) and tropism of the virus^{101,102}.

1.2.3 Signaling

All type I IFN subtypes bind to and signal through a shared heterodimeric IFN- α/β receptor (IFNAR), which is composed of the subunits IFNAR1 and IFNAR2. IFNAR expression is fairly ubiquitous, enabling most cell types to respond to IFN-I. Ligand binding of IFNAR induces a conformational change in the receptor that causes auto-phosphorylation and activation of the tyrosine kinases Janus kinase 1 (JAK1) and tyrosine kinase 2 (TYK2), which are constitutively associated with IFNAR2 and IFNAR1, respectively¹⁰³. Activated JAK1 and TYK2 then regulate the phosphorylation and activation of various signal transducer and activator of transcription (STAT) proteins¹⁰⁴.

In canonical IFN-I signaling, STAT1 and STAT2 are phosphorylated and then form a complex with IRF9. This complex is called the IFN-stimulated gene (ISG) factor 3 (ISGF3), which can enter the nucleus and bind to IFN-sensitive response elements (ISREs) in the promoters of ISGs¹⁰⁴. Type I IFN signaling can also regulate genes downstream of type II IFN (IFN- γ) by phosphorylating and activating STAT1 homodimers that bind to IFN- γ -activated site (GAS) enhancer elements in the promoters of some ISGs¹⁰⁵. Additional C-terminal serine phosphorylation

of STAT1 and STAT2 is required for full transcriptional activation of ISGs but is not required for STAT nuclear translocation or DNA binding^{106,107}. Ultimately, IFN-I signaling culminates in transcriptional regulation of hundreds of genes. These ISGs function to elicit an antiviral state in infected and neighboring cells. IFN-I are also known to have immunomodulatory and pleiotropic effects, depending on the cell type and context¹⁰⁸.

There are many pathways independent of STAT activation that are induced upon IFN-I stimulation, and these pathways play important roles in regulating the pleiotropic effects of IFNs. In brief, TYK2-mediated phosphorylation of the scaffolding protein insulin receptor substrate 1 (IRS1) allows for activation of the PI3K (phosphatidylinositol-4,5-bisphosphate 3-kinase) pathway, resulting in a broad range of biological effects including interleukin-10 (IL-10) production and protein kinase C delta (PKC- δ) activation^{109,110}. PKC- δ is thought to be important in serine phosphorylation of STATs, as pharmacological inhibition of PI3K blocks STAT1 phosphorylation at Ser727 and reduces STAT1-dependent transcription¹¹¹. TYK2 can also recruit and phosphorylate the adaptor molecule CRKL (Crk-like protein), leading to the activation of the p38 MAPK (mitogen-activated protein kinase) pathway, which is required for IFN-I-mediated production of genes under ISRE and GAS regulation¹¹².

1.2.4 IFN-I Induction during CHIKV Infection

CHIKV has evolved mechanisms to counteract IFN-I action, highlighting the importance of IFN-I in combating CHIKV. CHIKV nsP2 translocates into the nucleus and degrades the host RNA polymerase II subunit RPB1, which results in general host cell transcriptional shut-off and cytopathic effects in mammalian cells¹¹³. Additionally, nsP2 is able to directly antagonize IFN-I signaling by preventing phosphorylated STAT1 from entering the nucleus by mechanisms that are still unclear^{114,115}. Despite this antagonism, human patients infected with CHIKV mount a robust

innate immune response, including the induction of IFN-I and other cytokines and chemokines, and this is recapitulated in animal models^{56,58}.

Nonhematopoietic Cells Induce IFN-I via MAVS

Most cells are able to produce IFN-I *in vitro*, but induction *in vivo* is more complicated. One study generated a series of BMCs to characterize cell type-dependent PRR pathways responsible for IFN-I induction *in vivo*⁹⁷. IRF3/7 DKO mice fail to make sufficient IFN-I and succumb to CHIKV infection with slightly delayed kinetics compared to IFNAR1-KO mice. DKO → WT BMCs were able to survive infection and control viral dissemination, indicating a role for nonhematopoietic cells in producing IFN-I during CHIKV infection. *In vitro* evidence indicated that MAVS is critical for IFN-I induction in mouse embryonic fibroblasts (MEFs) following CHIKV infection¹¹⁶. Although DKO → MAVS^{-/-} BMCs survive infection, they showed enhanced viremia and dissemination. In contrast, the viral loads in MAVS^{-/-} → DKO BMCs were almost identical to that of WT → DKO. These findings suggest that MAVS plays an antiviral role in nonhematopoietic cells, but is less important for IFN-I responses in hematopoietic cells. An antiviral role for MAVS pathways is further demonstrated in MAVS global knockout mice, which develop more severe clinical disease and enhanced viral replication^{64,116}. It is also worth noting that RIG-I^{-/-} or MDA5^{-/-} mice do not show these clinical or virologic phenotypes, suggesting that RIG-I and MDA5 have redundant roles in CHIKV infection.

Hematopoietic Cells Induce IFN-I

There is also evidence that immune cells can produce IFN-I during CHIKV infection. WT → DKO BMCs were able to survive infection and only showed limited increase in viral dissemination compared to WT → WT BMCs⁹⁷. These results demonstrate that hematopoietic cells can be a sufficient source of IFN-I to effectively control CHIKV infection. That same study

performed multiple BMCs to determine the hematopoietic-specific PRR pathways responsible for protecting DKO recipients that fail to induce sufficient IFN-I. TLR7^{-/-} → DKO and MyD88^{-/-} → DKO BMCs survived infection and controlled viral replication similarly as WT → DKO BMCs. This was surprising, given that MyD88^{-/-} mice develop worse clinical disease and mildly worse viral loads compared to WT mice^{64,116}. These data suggest that hematopoietic cells induce sufficient IFN-I for DKO recipients via a MyD88-independent pathway.

Several studies have characterized the role of TLR3 during CHIKV infection and found conflicting results. One group reported increased viremia and worsened clinical disease, characterized by severe infiltration of neutrophils and F4/80⁺ macrophages/monocytes in TLR3^{-/-} mice¹¹⁷. This group also generated TLR3^{-/-} → WT BMCs which recapitulated the viremia in the TLR3 global knockout mice, but showed no change in clinical disease. This suggests that TLR3 may have an antiviral role in immune cells and an anti-inflammatory role in nonhematopoietic cells. Strikingly, a second group reported no virologic phenotype in TLR3^{-/-} mice, but this discrepancy could be due to differences in route of infection or the age of animals¹¹⁶. An antiviral role for TLR3, is supported by the observation that TRIF^{-/-} mice develop worse foot swelling and viremia after CHIKV infection⁶⁴. All together, these data suggest that in immune cells, TLR3 may play an antiviral role by means of a MyD88-independent, TRIF-dependent pathway. There also seems to be a role for MyD88 in nonhematopoietic cells that impacts clinical disease but not viral load. These effects could be mediated downstream of IL-1 β , which also signals via MyD88. More work is needed to delineate the roles these PRR pathways in nonhematopoietic and immune cells play in pathogenesis of CHIKV disease.

Recently, the laboratory of Tem Morrison demonstrated that monocytes play an important role in limiting disease severity and viral dissemination during alphavirus infection⁷². This study

made use of transgenic mice expressing the diphtheria toxin receptor (DTR) under the control of CCR2 expression, to allow for specific deletion of CCR2⁺ cells, namely monocytes. Loss of monocytes worsened clinical disease and viral loads following infection with a related alphavirus, Ross River virus (RRV). Additionally, they generated CCR2-DTR → DKO BMCs and demonstrated that monocytes are the critical immune cell for inducing protective IFN-I. Unfortunately, they did not perform these same BMC experiments with CHIKV, but they did demonstrate that depletion of monocytes also resulted in more severe clinical disease and viral dissemination during CHIKV infection. Other work demonstrated that CHIKV is able to bind and enter monocytes and induce IFN-I production, but ultimately yields a nonproductive infection (discussed further in section 1.1.6)⁶⁵. Together these data imply that similar to RRV infection, monocytes may be an essential hematopoietic source of IFN-I during CHIKV infection, but more work is needed to confirm this. This would be consistent with the observation that both human and mouse pDCs stimulated with CHIKV *in vitro* produced very little IFN-I compared to stimulation with poly I:C, an agonist of TLR3, or influenza A, suggesting that another cell type is likely responsible for producing IFN-I¹¹⁶.

1.2.5 IFN-I Action during CHIKV Infection

IFN-I Signals on Nonhematopoietic Cells

Mice that lack IFNAR1, and thus all IFN-I activity, are extremely susceptible to CHIKV and other alphavirus infections, indicating that IFN-I are critical host factors for controlling CHIKV infection^{56,64,97,116,118–120}. Loss of both IRF3 and IRF7 (DKO) fail to produce sufficient IFN-I and die from uncontrolled CHIKV replication and hemorrhagic shock-like symptoms, similar to what is observed in IFNAR1 deficient mice⁶⁴. The kinetics of lethality are slightly delayed in the DKO mice compared to the IFNAR1-KO phenotype, suggesting that other factors,

such as IRF1 or IRF5, may also induce some IFN-I during CHIKV infection, though insufficient to control infection. Another study generated reciprocal WT \rightarrow IFNAR1^{-/-} and IFNAR1^{-/-} \rightarrow WT BMCs to determine the cell type-dependent IFNAR expression responsible for controlling CHIKV infection¹¹⁶. They found that IFN-I signaling is required on nonhematopoietic cells to control CHIKV infection. However, the authors did not evaluate pathogenesis or viral load, so there is possibility of some involvement of IFN-I signaling on immune cells during CHIKV infection. Altogether, these findings are unsurprising given that the cellular targets of CHIKV are primarily nonhematopoietic cells, such as fibroblasts and muscle cells.

Functions of ISGs in CHIKV Infection

IFN-I ultimately exert their biological properties by inducing ISGs, but only a short list of ISGs have been studied in the context of CHIKV infection. Viperin (encoded by the gene *Rsad2*) was found to restrict CHIKV replication *in vitro*, and *Rsad2*^{-/-} mice were more susceptible to CHIKV infection¹²¹. Protein kinase R (PKR) transcription is regulated by both IFN-I signaling and various stress responses, and then it requires activation by the presence of dsRNA. Once active, PKR phosphorylates the eukaryotic translation initiation factor (eIF2 α) to inhibit cellular mRNA translation, but it can also indirectly aid in activation of multiple transcription factors, such as STAT1¹²². Studies have demonstrated that PKR is activated during CHIKV infection *in vitro*, which leads to the upregulation of several genes that promote IFN-I production, such as GADD34. Cells lacking PKR or GADD34 supported increased CHIKV replication and induced very little IFN- β ^{123,124}. Furthermore, neonatal mice lacking GADD34 were more susceptible to CHIKV-induced lethality compared to WT mice and supported higher viral loads in multiple tissues, establishing important anti-CHIKV properties for PKR and GADD34 *in vivo*.

Additionally, IFITM3 has been demonstrated to block CHIKV fusion in cells, and BST2 (also known as tetherin) has been shown to block CHIKV budding. Both IFITM3 and BST2 play antiviral roles during CHIKV infection *in vivo*, as mice that lack either IFITM3 or BST2 displayed worsened disease and higher viral replication in several tissues¹²⁵⁻¹²⁷. ISG15 is one of the most rapidly and abundantly upregulated genes in response to IFN-I. It contains two ubiquitin-like domains, and similar to ubiquitin, it can be conjugated to viral and host proteins¹²⁸. ISG15-KO neonatal mice are much more susceptible to CHIKV-induced lethality, but displayed similar viral loads throughout infection. Rather than functioning to limit viral replication, as it does in several other viral systems, the absence of ISG15 during neonatal CHIKV infection promoted a cytokine storm phenotype⁵⁸. Collectively these studies have begun to define the mechanistic basis for ISG-mediated modulation of CHIKV replication and pathogenesis, but much work remains to characterize the roles of ISGs during CHIKV infection.

In summary, there has been substantial effort to characterize the pathways and cell types that induce IFN-I during CHIKV infection, the cells that respond to IFN-I, and the mechanistic actions of some ISGs. This collective work has yielded a model in which IFN-I signaling is absolutely required on nonhematopoietic cells to control CHIKV infection. Both hematopoietic cells, likely monocytes, and nonhematopoietic cells can produce sufficient IFN-I to control CHIKV, though they utilize distinct pathways to do so. Hematopoietic cells likely utilize the TLR3-TRIF pathway, whereas nonhematopoietic cells rely on the RIG-I/MDA5-MAVS pathways. A central role for nonhematopoietic cells, like fibroblasts and muscle, for supporting viral replication and coordinating immune responses sets CHIKV apart from other alphaviruses. Related alphaviruses such as RRV, Sindbis virus (SINV), and Venezuelan equine encephalitis virus (VEEV), as well as the flavivirus West Nile virus (WNV), are all able to infect and induce

IFN-I production in dendritic cells^{118,129,130}. Thus, CHIKV infection could serve as a unique model to study IFN-I responses in nonhematopoietic cells.

1.2.6 IFN-I Subtypes: evidence for functional differences

IFN-I are pleiotropic cytokines with broad biological activities that include upregulating cell-intrinsic antiviral defense mechanisms, modulating proinflammatory cytokine production, and augmenting innate and adaptive cellular responses. Despite signaling through a single, shared receptor, the IFN-I subtypes have been documented to have distinct properties both *in vitro* and *in vivo*. Examples and mechanisms of these functional differences are discussed below.

Functional differences in vitro

All IFN-I subtypes bind to IFNAR, but with varying affinities. For example, IFN- α 2 has nanomolar binding affinity to IFNAR2 and micromolar affinity for IFNAR1, whereas IFN- β exhibits picomolar binding affinity for IFNAR2 and nanomolar affinity for IFNAR1^{131,132}. Differences in binding affinities among the IFN subtypes manifest as differences in dissociation constants. IFN- β has about a 100 second half-life in a ternary complex with both receptors, and IFN- α 2 has a half-life of about 1 to 5 seconds^{133,134}. Careful mapping of structural and biochemistry properties have revealed that for some IFN-I properties, such as antiproliferative activity, different potencies among the subtypes are ascribed to differential binding affinities and dissociation rates for the receptor. These properties that are highly dependent on cellular context and affinity are designated as “tunable” IFN properties. For example, IFN- β has the highest known natural affinity for IFNAR and has been shown to be the most potent inhibitor of osteoclastogenesis of monocytic precursors *in vitro*¹³⁵. In contrast, “robust” IFN-I properties, such as antiviral activity, only marginally improve with increased affinity and are programmed for maximal output by all subtypes irrespective of affinity or cellular context¹³⁶. The ability of IFN-I signaling to have graded

responses to multiple ligands likely contributes to the pleiotropic activities ascribed to IFN-I and provides a molecular explanation for how IFN-I subtypes can have unique properties (summarized in Figure 1.5).

Lessons from IFN- ϵ

Prior to 2013, the function of IFN- ϵ remained uncharacterized. A study published in *Science* showed that unlike the other type I IFN subtypes, IFN- ϵ is not induced by Toll-like receptor ligands. Rather, it is constitutively expressed by the epithelium of reproductive organs, with its expression further regulated by sex hormones¹³⁷. Likely a consequence of its unique regulation, IFN- ϵ is the only type I IFN subtype shown to play a protective role against *Chlamydia* infection, whereas the other subtypes may worsen disease^{137,138}. IFN- ϵ signals through IFNAR like the other IFN-I subtypes, but with some notable differences. A recent paper demonstrated that unlike other studied IFN-I subtypes, IFN- ϵ displays higher affinity for the IFNAR1 subunit compared to IFNAR2¹³⁹. Additionally, IFN- ϵ was the only subtype shown to have cross-species reactivity for human IFNAR, which had also been previously shown for canine IFN- ϵ ¹⁴⁰. Collectively, these studies demonstrate that IFN- ϵ has distinct biological properties both *in vitro* and *in vivo*, and these distinctions are relevant for human disease.

IFN- β deficient mice

Some of the first attempts to delineate properties of individual IFN-I subtypes *in vivo* came with the generation of mice that specifically lack the IFN- β subtype¹⁴¹. IFN- β -KO mice are more susceptible than wild type (WT) mice to West Nile virus (WNV), an encephalitic flavivirus¹⁴². The increased lethality in the IFN- β ^{-/-} mice was accompanied with elevated viral replication in some, but not all tissues. WNV was similarly controlled in the serum and spleen by IFN- β -KO and WT mice, and consistent with this, IFN-I activity in the serum was comparable between the two

genotypes. Onset of viral replication was similar in certain peripheral tissues, such as the central nervous system (brain and spinal cord) and kidneys, but viral loads accumulated to higher levels in the IFN- β deficient mice. This suggests that for some tissues, IFN- β functions to limit replication within those tissues, but not the viral seeding of those tissues. In striking contrast, the lymph nodes displayed very early and severely elevated replication, suggesting an early antiviral role of IFN- β in select tissues. Furthermore, WNV infection of cell cultures generated from IFN- β -KO mice revealed that macrophages and dendritic cells supported significantly higher WNV replication compared to WT cells, whereas the phenotype was minimal or non-existent in cultured fibroblasts and neurons, suggesting that there might be cell-type specificity for requirement of certain IFN-I subtypes. Taken together, these data suggest that during WNV infection IFN- β has a protective, antiviral role in limiting replication in certain cell types and tissues, and of note, the virologic phenotype in IFN- β -KO mice was not as severe as what has been described for WNV infection in mice lacking other components of the IFN-I system (*Ifnar*^{-/-}, *Irf3*^{-/-}, or *Irf7*^{-/-} mice)^{96,130,143}.

Several other studies have also identified a protective, antiviral role for IFN- β during viral infection. One study demonstrated that IFN- β -KO mice were more susceptible to 3 different doses of intranasal inoculation of vaccinia virus, a member of *Poxviridae* with a dsDNA genome¹⁴⁴. Similar to what was observed with WNV infection, only certain tissues displayed increased viral loads, namely the lung and brain, but not the spleen. Another study demonstrated a protective role for IFN- β in coxsackievirus B3 infection¹⁴⁵. Coxsackievirus group B belong to the *Picornaviridae* family of positive-sense, ssRNA viruses that cause viral myocarditis. When infected with coxsackievirus B3, 70% of IFN- β ^{-/-} mice succumbed to infection by 5 dpi, whereas 100% of WT mice survived. Interestingly, the viral loads at 4 dpi (just before lethality) were not different in the heart and only slightly elevated in the liver and spleen in the IFN- β -KO mice; however, IFN- β -

KO mice did show increased inflammation and infiltrates by histology in the heart compared to WT mice, suggesting that IFN- β might have protective antiviral and immunomodulatory functions in this context.

One of the most intriguing and complicated viral systems to study IFN-I biology might be influenza A (IAV) infection. Some studies have reported that IFN-I directly correlates with disease severity, whereas other studies indicated that IFN-I inversely correlated with pathology¹⁴⁶. Pretreatment of mice with IFN 8 hours prior to infection protected mice from severe infection, but only in mice that expressed the IAV-restricting ISG MX1¹⁴⁷. In contrast, treatment of MX1-negative mice with exogenous IFN-I increased morbidity and mortality during IAV infection by upregulation of tumor necrosis factor-related apoptosis-inducing ligand (TRAIL)¹⁴⁸. These findings highlight that during IAV infection, IFN-I have a complex role, and whether they play a beneficial or detrimental role may depend on the genetic background of the mouse, dose or route of the inoculum, and concentration of IFN-I induced. C57BL/6 mice are MX1-negative and susceptible to influenza infection. One study generated C57BL/6 mice that do express MX1 but are deficient for IFN- β ¹⁴⁹. In this MX1-positive genetic background, IFN- β was shown to play a protective antiviral role, as mice lacking IFN- β showed greater lethality and higher viral burden in the lung following IAV infection. Taken altogether, the current model of IFN-I activity during IAV infection is that moderate, transient expression of IFN-I induces a protective antiviral response, whereas excessive or prolonged IFN-I induction is detrimental by exacerbating inflammation.

IFN- α versus IFN- β during LCMV Infection

The lack of IFN- α deficient mice has hindered the direct functional comparison of IFN- α versus IFN- β *in vivo*, but the recent development of blocking monoclonal antibodies (mAb)

specific for either IFN- α or IFN- β is making those studies possible⁹⁸. In a study with lymphocytic choriomeningitis virus (LCMV) persistent infection (clone 13), Oldstone and colleagues demonstrated that IFN- β is dispensable for controlling early LCMV replication and spread, suggesting that other subtypes, such as the IFN- α 's, are the dominant subtypes contributing to the antiviral responses. Indeed, blockade of IFN- α worsened viral loads. In contrast, IFN- β was found to be detrimental to the host and responsible for promoting LCMV persistence¹⁵⁰. Specific blockade of IFN- β improved antiviral T cell responses that led to accelerated virus clearance, recapitulating what is observed with blockade of IFNAR1 during LCMV infection^{151,152}. Infection of dendritic cells is an important step for establishment of persistent LCMV infection, and mice that were treated with anti-IFNAR1 or anti-IFN- β mAb showed decreased infection of CD8 α ⁻ dendritic cells, suggesting a mechanism for viral clearance. Whereas studies have been performed to assess the specific role of the IFN- β subtype, this was the first report to directly compare the properties of IFN- α and IFN- β and observe distinguishable biological functions.

Collectively, these studies highlight that cellular source, timing, concentration, and context of expression can drastically impact the function of an IFN-I subtype. IFN-I are both the targets of and used as therapeutics for a number of diseases, such as hepatitis C infection, multiple sclerosis, and some cancers, and careful study of the functions of individual subtypes may lead to more effective treatments with less off-target effects¹⁵³.

1.3 Figures

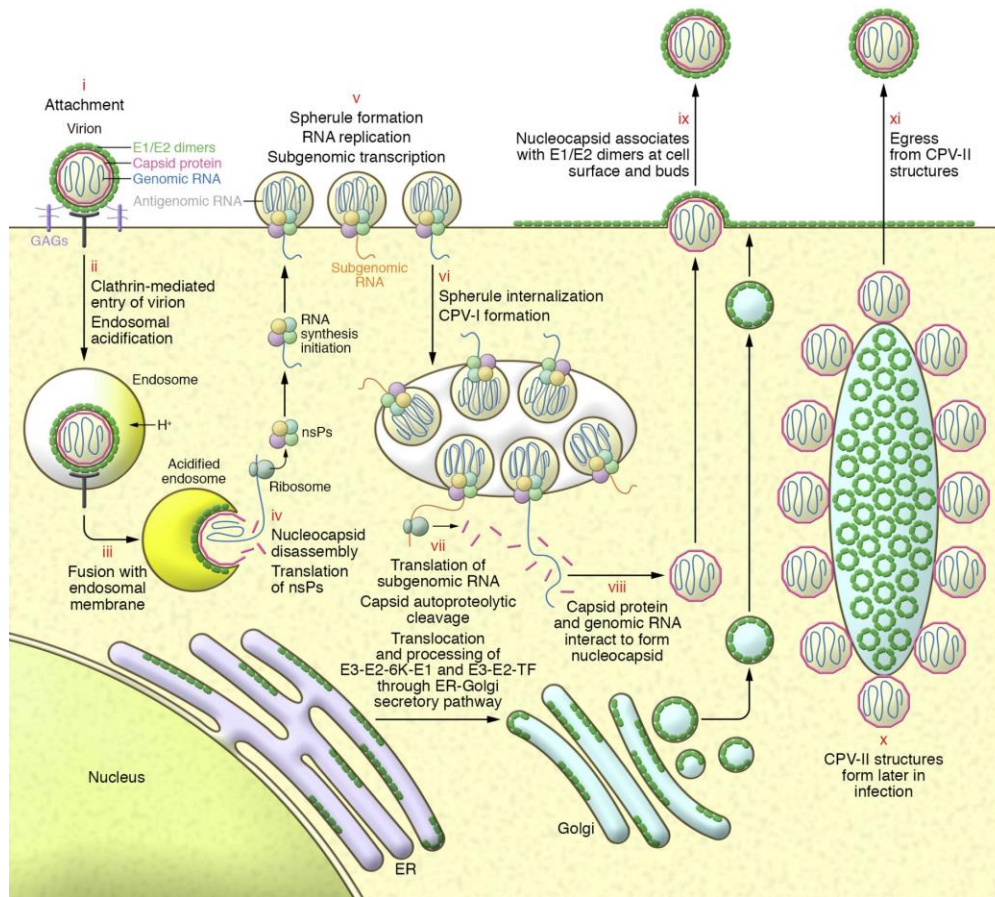


Figure 1.1 Replication cycle of CHIKV in mammalian cells

This figure was taken from Silva, L. A. & Dermody, T. S. Chikungunya virus: epidemiology, replication, disease mechanisms, and prospective intervention strategies. *J. Clin. Invest.* 127, 737–749 (2017). In brief, CHIKV replication in mammalian cells is characterized by i-iii) receptor-mediated endocytosis and pH-dependent fusion, iv-v) early replication of negative-strand genome occurs in spherules, vi-viii) formation of large cytopathic vacuoles (CPV-I) where subgenomic and genomic RNA are transcribed and translated, resulting in accumulation of nucleocapsids and E1/E2 dimers at the cell surface, and x-xi) nucleocapsids associate with internalized E1/E2 spikes (CPV-II) to form mature virions, which egress and bud from the cell.

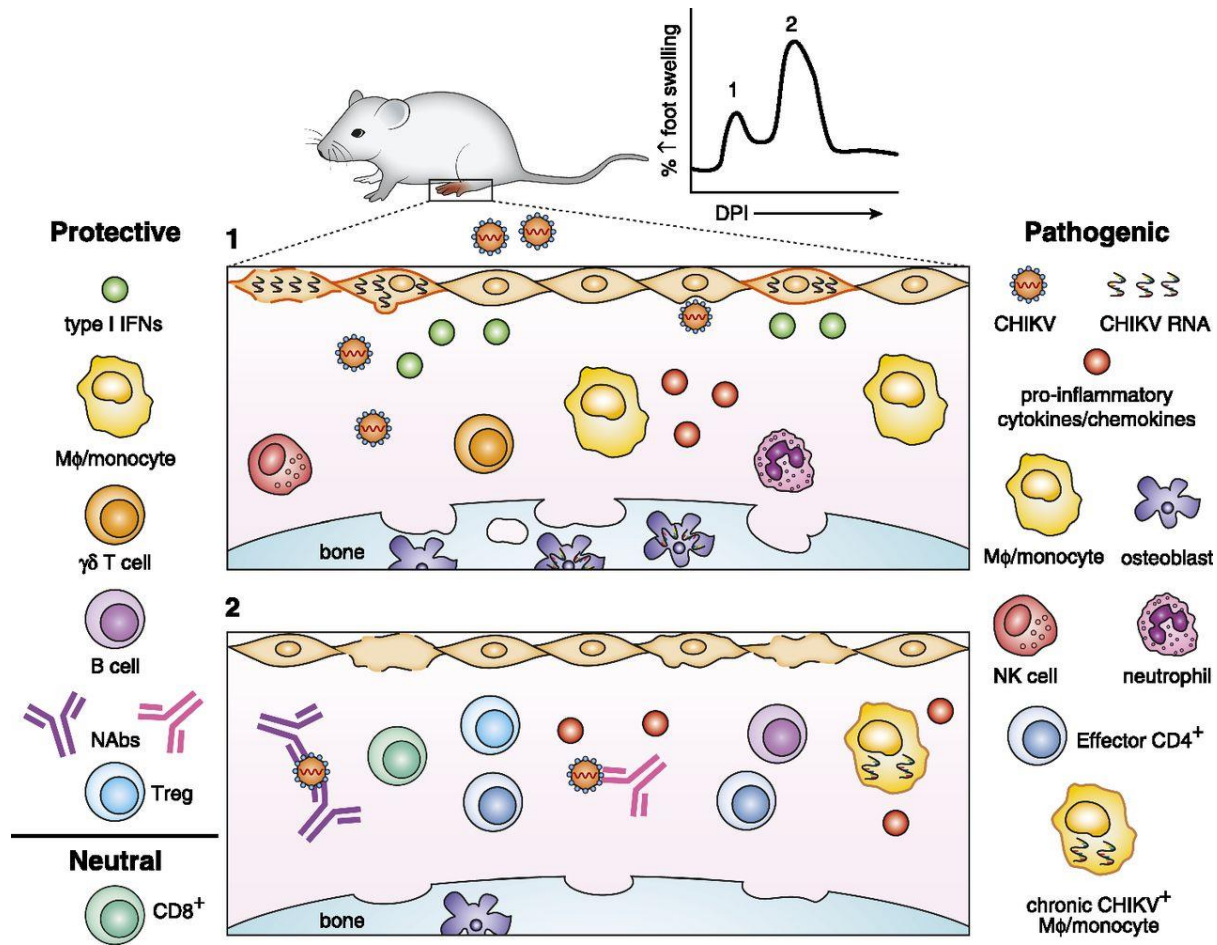


Figure 1.2 Summary of CHIKV pathogenesis in WT mice

This figure was taken from Fox, J. M. & Diamond, M. S. Immune-Mediated Protection and Pathogenesis of Chikungunya Virus. *J. Immunol.* 197, 4210–4218 (2016). Infection of WT mice with CHIKV in the foot produces a biphasic swelling response that is accompanied with histological signs of arthritis, myositis, and synovitis. The first peak of foot swelling at 2-3 dpi is thought to arise from robust viral replication which drives cell death, local proinflammatory cytokine production, and edema (box 1). The second peak at 6-7 dpi occurs as infectious virus is cleared from the tissues and blood and is associated with an influx of inflammatory infiltrates into the joint spaces and surrounding soft tissues that drive cytokine production, synovitis, myositis, and edema (box 2).

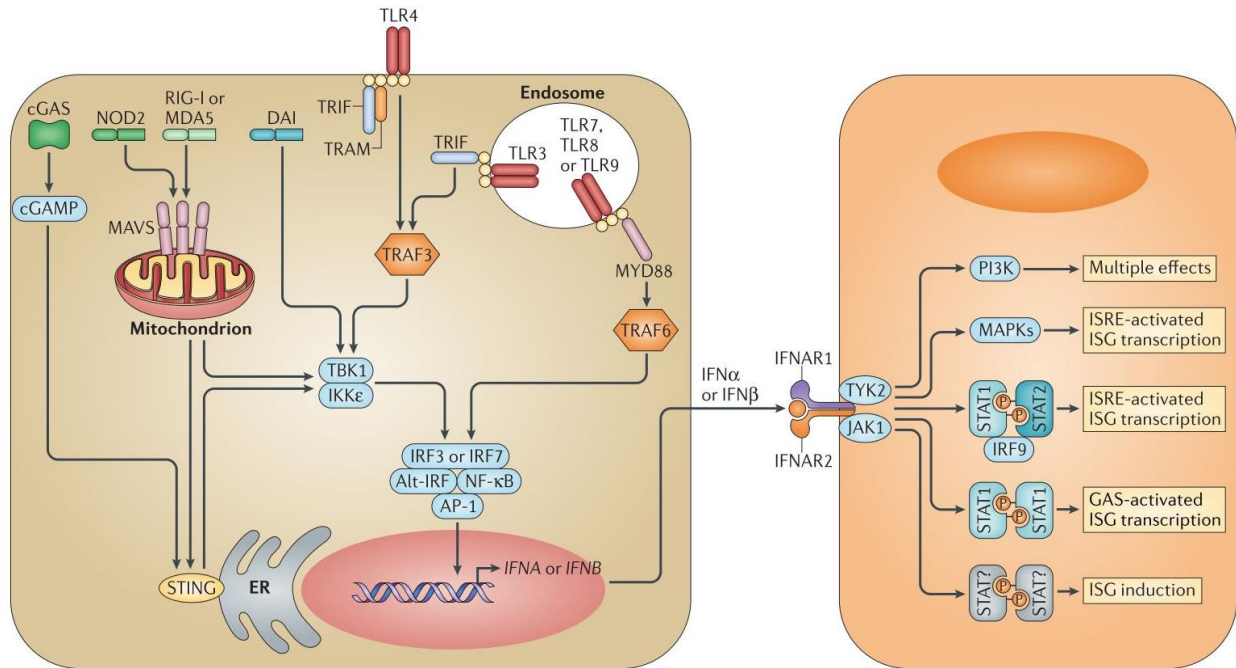


Figure 1.3 Summary of pathways of IFN-I induction and signaling

This figure was taken from McNab, F., Mayer-Barber, K., Sher, A., Wack, A. & O'Garra, A. Type I interferons in infectious disease. *Nat. Rev. Immunol.* **15**, 87–103 (2015). Briefly, pattern recognition receptor signaling pathways converge on the activation of IRF3 and/or IRF7 to induce IFN-I production. IFN-I then exert pleiotropic effects by signaling through IFNAR to induce various JAK/STAT signaling pathways and IFN-stimulated genes (ISGs). IFN-I can also activate other pathways, such as PI3K and MAPKs.

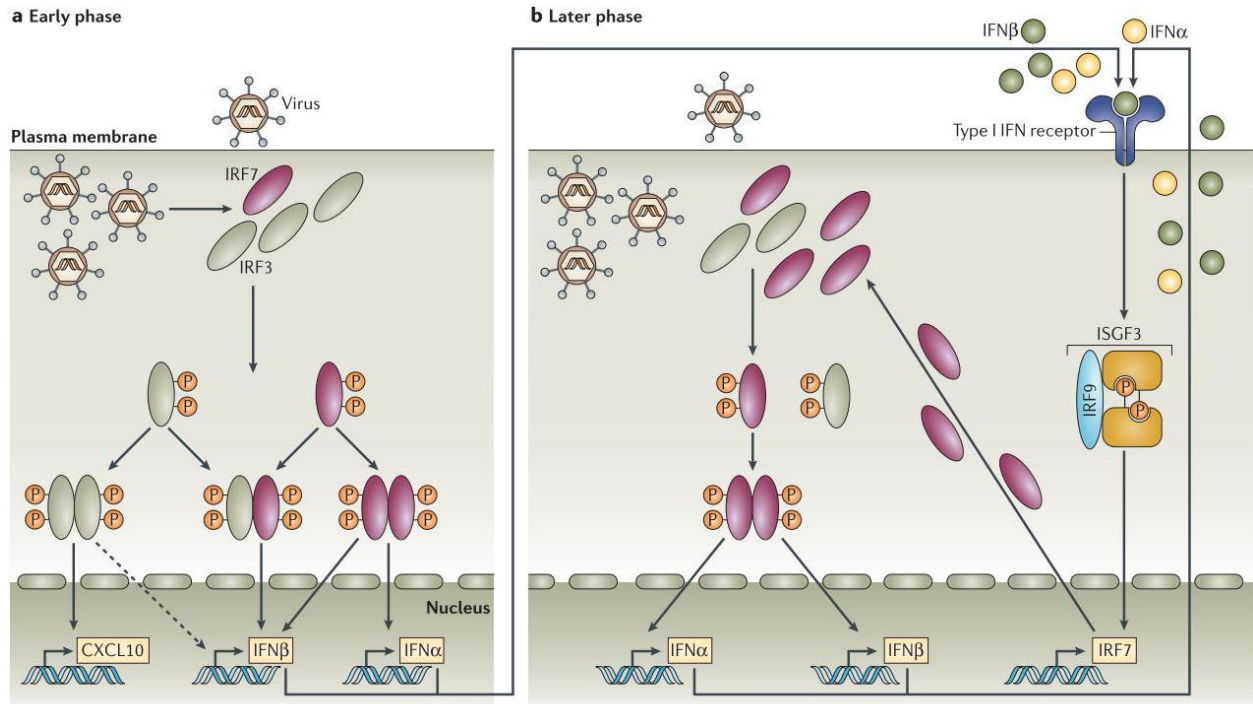


Figure 1.4 IRF7 participates in a forward feedback loop for IFN-I amplification

This figure was taken from Honda, K. & Taniguchi, T. IRFs: master regulators of signalling by Toll-like receptors and cytosolic pattern-recognition receptors. *Nat. Rev. Immunol.* **6**, 644–658 (2006). In the early phase of IFN-I induction, IRF3 (or IRF7 in some cells, such as pDCs) acts on the promoter of IFN- β (and IFN- α 4, not depicted). Secreted IFN-I signals through IFNAR to upregulate IRF7, which can then bind the promoters of the other IFN- α subtypes, as well as IFN- β , to amplify the IFN-I response.

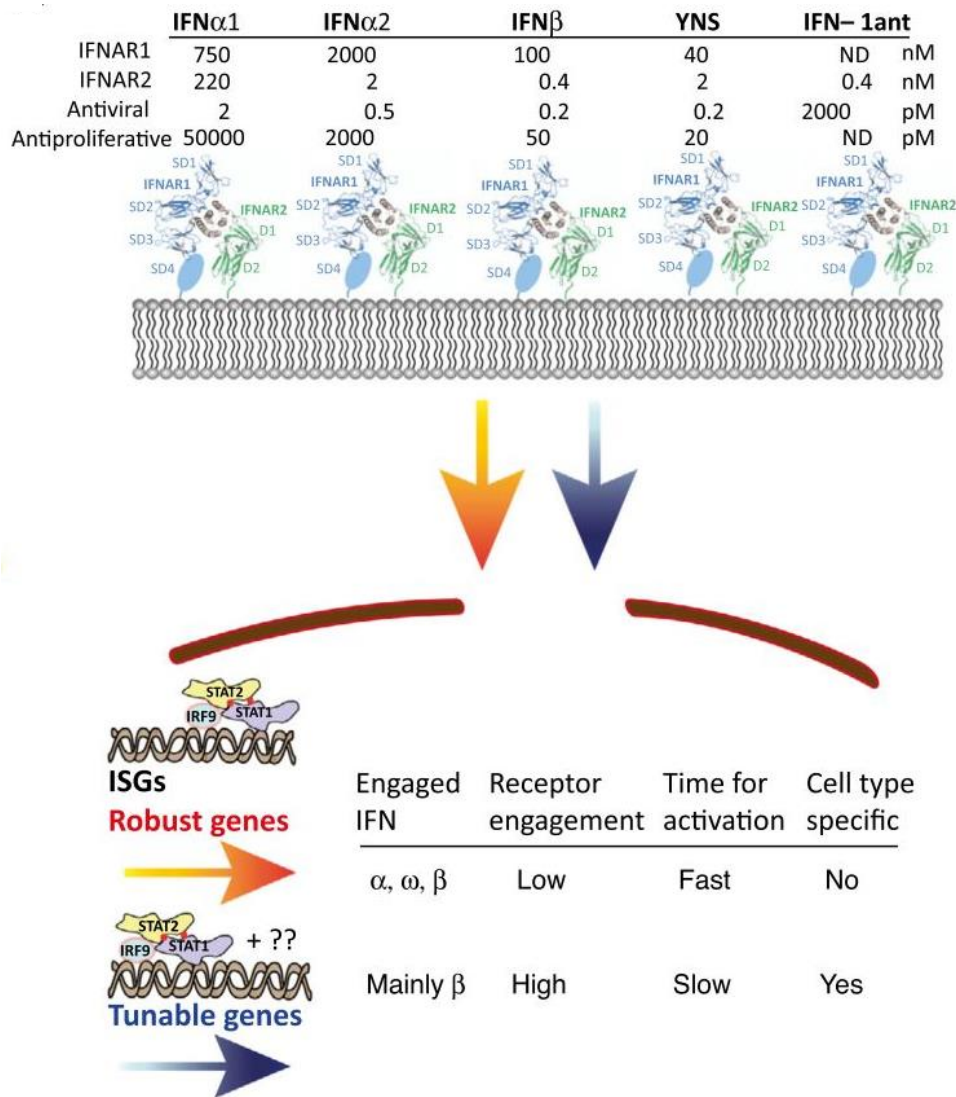


Figure 1.5 Molecular basis for functional differences among IFN-I subtypes

This figure was taken from Schreiber, G. & Piehler, J. The molecular basis for functional plasticity in type I interferon signaling. *Trends Immunol.* **36**, 139–149 (2015). Upper panel: The affinities (K_D) for each receptor subunit and EC_{50} values for antiviral and antiproliferative activities are listed for three natural IFN-I subtypes (IFN- α 1, IFN- α 2, and IFN- β) and two engineered IFN- α mutants (YNS and IFN-1ant). Lower panel: Some IFN-I properties are “robust” and do not correlate with affinity to the receptor, whereas “tunable” IFN-I properties require longer or continuous activation of the receptor, display a linear correlation with affinity for the receptor, and may be cell type specific.

Chapter 2

Interferons alpha and beta protect against chikungunya virus pathogenesis by distinct mechanisms of action

This chapter contains data from a manuscript in preparation for submission.

L. E. Cook, M. C. Locke, A. R. Young, K. Monte, M. L. Hedberg, R. M. Shimak, D. J. Veiss, M. S. Diamond, D. J. Lenschow. Interferon alpha limits chikungunya virus replication, but not interferon beta, which controls immunopathology mediated by neutrophils. (2018).

2.1 Abstract

Type I interferons (IFN-I) possess a wide range of biological activity and are important in protection against a number of viruses, including alphaviruses. Despite signaling through a shared receptor, there are well documented biochemical and functional differences among the different IFN-I subtypes. Work with lymphocytic choriomeningitis virus (LCMV) persistent infection previously demonstrated that IFN- α and IFN- β have distinguishable biological activities, with IFN- α functioning to limit viral replication and IFN- β playing a detrimental role by promoting persistent infection. Herein, we demonstrate that IFN- α and IFN- β both play protective roles during acute CHIKV infection, but they do so by distinct mechanisms. IFN- α limits CHIKV replication and dissemination, but in contrast, IFN- β protects from CHIKV pathogenesis by limiting immunopathology mediated by neutrophils. Our findings support the accumulating evidence that the IFN-I subtypes have distinct biological activities, and we identify a novel mechanism for the differential activity of IFN- β compared to the IFN- α 's.

2.2 Introduction

Type I interferons (IFN-I) are a family of multifunctional cytokines, and in mice they consist of 14 IFN- α subtypes and single forms of IFN- β , IFN- ϵ , IFN- κ , and IFN- ω . Their broad pleiotropic properties include upregulating cell-intrinsic antiviral defense mechanisms, modulating proinflammatory cytokine production, and augmenting innate and adaptive cellular responses. All IFN-I exert their effects by binding to the shared heterodimeric IFN- α/β receptor (IFNAR), which is composed of the subunits IFNAR1 and IFNAR2. Engaging IFNAR activates Janus kinase (JAK) and signal transducer and activator of transcription (STAT) signaling programs to modulate the expression of hundreds of interferon stimulated genes (ISGs)¹⁰⁴. Conservation of

the IFN-I family's multigene nature across many species suggests that expression of multiple IFN subtypes is beneficial for the host defense. However, the physiological roles of the individual subtypes remain poorly understood.

IFN-I are rapidly induced in response to infection with viruses and other pathogens. Host pattern recognition receptors (PRR) that recognize nucleic acids are important sensors of viral infection. For many cells, the immediate response to PRR signaling leads to the production of IFN- β and IFN- α 4 subtypes via activation of interferon regulatory factor 3 (IRF3). These initial IFN-I subtypes signal in autocrine and paracrine means to modulate expression of ISGs that include antiviral effector and regulator molecules. IRF7 is among the transcriptional regulators induced by the early IFN-I subtypes, and it participates in a positive feedback loop that induces the other IFN- α subtypes, thus amplifying and diversifying the IFN-I response^{85,94,95}. The central role of IRF7 in inducing the IFN- α subtypes is demonstrated in IRF7 deficient mice, which fail to produce many of the IFN- α subtypes in response to viral infection^{64,96-98}.

Despite possessing a similar spectrum of activities, the IFN-I subtypes display unique properties and different potencies of shared functions. Structural and biochemistry studies have ascribed these distinct properties to differential binding affinities and dissociation rates for the IFN-I receptor¹⁵⁴⁻¹⁵⁷. The ability of IFNAR to have graded responses to multiple ligands likely contributes to the wide range of biological activity documented for IFN-I, but until recently, the physiological relevance of these biochemical differences was unclear. In a study with lymphocytic choriomeningitis virus (LCMV) persistent infection, Oldstone and colleagues demonstrated that IFN- β is dispensable for controlling LCMV replication and spread, suggesting that other subtypes, such as the IFN- α 's, are the dominant subtypes contributing to the antiviral response. Instead, IFN- β was found to be detrimental to the host and responsible for promoting LCMV persistence.

Specific blockade of IFN- β improved antiviral T cell responses that lead to accelerated virus clearance, recapitulating what is observed with blockade of IFNAR1 during LCMV infection¹⁵⁰⁻¹⁵². Infection of dendritic cells is an important step for establishment of persistent LCMV infection, and mice that were treated with anti-IFNAR or anti-IFN- β mAb showed decreased infection of CD8 α^- dendritic cells, suggesting a mechanism for viral clearance. Taken together, the biochemical evidence and work with LCMV demonstrate that IFN- α 's and IFN- β have distinguishable biological activities and that these differences can have profound implications for viral pathogenesis.

Chikungunya virus (CHIKV) is a mosquito-transmitted alphavirus capable of causing explosive outbreaks of acute fever, rash, polyarthritis, arthralgia, and myositis^{2,8}. These symptoms reflect an interplay between extensive viral replication and damage mediated by immune cells, such as macrophages and activated CD4⁺ T cells^{51,53,79}. However, not all immune responses are detrimental. Neutralizing antibodies and IFN-I have been shown to be important in controlling CHIKV infection, and mice that lack IFNAR rapidly succumb to infection due to hemorrhagic shock and uncontrolled virus dissemination^{17,64}. Despite their central role in limiting alphavirus infection, little is known about the contributions of individual IFN-I subtypes to protection against CHIKV infection. To explore this question we used genetic deletion mutants and antibody blockade to determine the contributions of IFN- α and IFN- β during acute CHIKV infection. Both IFN- α and IFN- β protect the host during acute CHIKV infection. However, our findings suggest distinct roles for the IFN-I subtypes during CHIKV infection, with IFN- α limiting early viral replication and spread and IFN- β controlling neutrophil-mediated immunopathology. Thus, these results define a novel mechanism by which IFN- β can have distinguishable biological activity from the IFN- α 's.

2.3 Results

IFN- α and IFN- β both play protective roles in limiting clinical CHIKV disease. Human patients and mice infected with CHIKV mount a robust innate immune response, including the induction of IFN-I and other cytokines and chemokines^{56,58}. Loss of IFNAR1 in mice leads to uncontrolled viral replication and dissemination, with mice succumbing to infection by 3-4 days post infection (dpi) from hemorrhagic shock-like symptoms^{56,58,64}. Evidence shows that the IFN-I subtypes have distinct biological properties, but there have been no studies performed to determine the roles of individual subtypes in CHIKV pathogenesis.

To address this, we evaluated the pathogenesis of CHIKV in wild type C57BL/6J (WT), IFN- β knockout (KO), and IRF7-KO mice. IRF7-KO mice have previously been shown to lose IFN- α amplification during CHIKV infection with minimal impact on IFN- β production⁶⁴. Animals were infected subcutaneously in the left rear foot with 10^3 plaque forming units (PFU) of a clinical isolate of CHIKV (La Réunion, 2006) and monitored daily for clinical foot swelling. Previous studies have described a biphasic swelling response in the CHIKV-infected foot of WT mice, with a first peak usually observed 2-3 dpi and a second, larger peak at 6-7 dpi. Mice that lack IFN- β developed much more severe foot swelling that mimics the kinetics of swelling seen in WT mice (Fig. 2.1A, $p < 0.0001$). In contrast, mice that lack IRF7 develop a large initial peak of swelling at 3 dpi and a delayed second peak at 11 dpi (Fig. 2.1A, $p < 0.0001$). Both IFN- β -KO and IRF7-KO mice also displayed prolonged foot swelling out to at least 15 dpi compared to WT mice, which typically clear swelling by about 12 dpi (Fig. 2.1A). These data highlight that IFN- β and IFN- α both play important protective roles to limit clinical disease during CHIKV infection,

but the differences in the kinetics of swelling between the IFN- β -KO and IRF7-KO mice suggest that different mechanisms may underlie these phenotypes.

Though IRF7 has previously been shown to play a critical role in IFN- α production, it is also known to regulate a number of antiviral genes independent of IFN production, for example tetherin (also known as BST-2 or CD317)¹⁵⁸. Therefore, to evaluate if the phenotype in IRF7 deficient mice was due to loss of IFN- α , we made use of a pan-IFN- α blocking antibody (TIF-3C5) and an IFN- β specific blocking antibody (HD β -4A7) to more directly assess the impact of the IFN subtypes on CHIKV pathogenesis^{98,150}. WT mice were treated with the blocking antibodies one day before and again one day after CHIKV infection and monitored for foot swelling in the ipsilateral foot. Monoclonal antibody (mAb) blockade of IFN- α or IFN- β mimicked the early swelling trends observed in the IRF7 and IFN- β deficient mice, respectively. At 3 dpi, both the IFN- α and IFN- β mAb blockade groups displayed an increase in foot swelling compared to the isotype control treated group (Fig. 2.1B, $p < 0.0001$). However, the foot swelling at later acute time points (7-14 dpi) in the IFN-I blockade groups were less severe than the genetic deletion models, which could be due to the limited dosing regimen or partial blockade. These data confirm that the early foot swelling phenotypes in IFN- β -KO and IRF7-KO mice are due to loss of IFN- β and IFN- α , respectively. Taken together, these results suggest that IFN- β and IFN- α have distinct, non-redundant roles in protection from CHIKV clinical disease.

IFN- β -KO, but not IRF7-KO, mice have increased cellular infiltration into the midfoot joint spaces during acute CHIKV infection. In a WT mouse, the first peak of foot swelling (2-3 dpi) is thought to arise from robust viral replication which drives cell death, local proinflammatory cytokine production, and edema. The second peak (6-7 dpi) occurs as infectious virus is cleared from the tissues and blood and is associated with an influx of inflammatory

infiltrates into the joint spaces and surrounding soft tissues that drive cytokine production, synovitis, myositis, and edema^{51,53,55,79}. To determine if the increased foot swelling observed with loss of IFN- α or IFN- β was associated with worsened arthritis and inflammation, we next evaluated histological sections for overall inflammation of the joints and musculoskeletal tissues in the ipsilateral foot of WT, IFN- β -KO, and IRF7-KO mice at 7 dpi infection in a blinded manner. We found that 100% of the IFN- β -KO mice showed severe inflammation (score of 3) in the infected foot, whereas there was more variability in the severity of inflammation in the WT and IRF7-KO mice (Fig 2.2A and 2.2C). Additionally, IFN- β -KO mice, but not IRF7-KO mice, showed increased cellular infiltration into the midfoot joint spaces at 7 dpi compared to WT mice (Fig. 2.2D, $p < 0.01$). These data demonstrate that while both IFN- β -KO and IRF7-KO mice develop severe CHIKV-induced foot swelling, only the IFN- β -KO mice appear to show increased pathology, especially as measured by cellular infiltration into the mid-foot joint spaces.

IFN- α , but not IFN- β , limits CHIKV replication and dissemination. To further investigate the differential roles of IFN- α and IFN- β , we next determined the infectious viral load in the ipsilateral foot and distal tissues at various times post infection by plaque assay. Analysis of the ipsilateral foot revealed that mice lacking IFN- β supported CHIKV replication at similar levels as WT mice (Fig. 2.3A). Clearance of infectious virus was similar between WT and IFN- β -KO mice, with detectable virus cleared from both strains by 10 dpi (Fig. 2.3A). In contrast, mice lacking IRF7 had 1 log₁₀ higher CHIKV viral load in the ipsilateral foot at 2 and 3 dpi compared to WT mice (Fig. 2.3A, $p < 0.01$) and had delayed clearance of infectious virus compared to WT or IFN- β -KO mice, with 2 log₁₀ more infectious virus at 7 dpi (Fig. 2.3A, $p < 0.001$).

We next evaluated the impact of loss of IFN- β or IRF7 on CHIKV dissemination to distant tissues. Overall, we observed minimal difference between WT and IFN- β -KO mice in viral titers

in several disseminated tissues. CHIKV titers in the serum of IFN- β -KO mice were the same as WT mice at all time points examined. Likewise, we observed no difference in the time of onset of replication in the distant tissues of IFN- β -KO mice, and only in the muscle did we observe a significant change in the overall magnitude of viral replication compared to WT mice at 3 dpi (Fig. 2.3A, $p < 0.0001$). Conversely, IRF7-KO mice displayed a substantial increase in CHIKV dissemination. IRF7-KO mice had substantially higher and prolonged viremia compared to WT and IFN- β -KO mice, with 2 \log_{10} more virus at 2 dpi and a 5 \log_{10} increase at 3 dpi in the serum (Fig. 2.3A, $p < 0.0001$). Additionally, CHIKV spread to distant sites much more quickly and sustained elevated viral loads in IRF7-KO mice compared to WT mice. For example, IRF7-KO contralateral ankles rapidly develop a 3 \log_{10} increase in replication at 2 dpi, at a time when replication is only just detectable in WT and IFN- β -KO mice. Additionally, whereas IFN- β -KO and WT mice have cleared CHIKV from the opposite ankle at 7 dpi, there is still $10^{4.5}$ pfu of virus present in the IRF7-KO mice. These data suggest that IFN- β is dispensable for controlling CHIKV replication and spread, and that other IFN-I subtypes, such as the IFN- α 's, are the dominant subtypes eliciting antiviral responses.

Administering mAb blockade of either pan-IFN- α or IFN- β recapitulated the virologic phenotypes we observed in the genetic knockout models. Blockade of IFN- β in WT mice had minimal impact on viral load in the ipsilateral foot or in distal sites compared to mice treated with an isotype control mAb (Fig. 2.3B). Treatment of WT mice with the IFN- α blocking mAb resulted in an elevated viral load in the inoculated ankle at 7 dpi, more severe viremia, and a substantial increase in dissemination to the muscle and distal joints, similar to what we observed in IRF7 deficient mice (Fig. 2.3B). These data suggest that IFN- α is important for controlling early viral replication and spread, whereas IFN- β is dispensable for these effects. In contrast, the absence of

IFN- β led to increased foot swelling and increased inflammatory cell infiltrates into the joint spaces without impacting viral loads, suggesting that IFN- β may primarily function as an immunomodulatory molecule during CHIKV. Taken together, these findings demonstrate that IFN- α and IFN- β are both protective during CHIKV infection but mediate their effects by distinct mechanisms of actions.

IFN- α and IFN- β exert their protective effects during CHIKV arthritis by signaling on nonhematopoietic cells. Previous studies using bone marrow chimeras have demonstrated that IFN signaling is required in nonhematopoietic cells to survive CHIKV infection¹¹⁶. However, these studies evaluated only survival and did not determine the impact of IFN-I signaling on immunopathology in the CHIKV arthritis model. To address this question, we utilized Vav-Cre transgenic mice crossed onto the IFNAR1^{flox/flox} background, which removes IFN-I signaling from immune cells and endothelial cells¹⁵⁹. Infecting Vav-Cre positive mice with 10³ pfu CHIKV in the footpad resulted in no lethality and did not yield any significant difference in clinical disease, as measured by foot swelling, compared to Cre negative littermate controls (Fig. 2.4A). To determine if loss of IFN-I signaling in hematopoietic cells impacts the ability to control viral replication or spread, we assessed the viral load in the ipsilateral foot and distant tissues at several times post infection. We did not observe significant differences in viral replication in the ipsilateral ankle or distant tissues, though there was a slight delay in clearance of CHIKV from the serum (Fig. 2.4B, $p < 0.05$). Taken together, these data suggest that IFN- α and IFN- β mainly signal on nonhematopoietic cells to exert their respective protective effects during CHIKV arthritis.

IFN- β deficient mice have increased neutrophil recruitment into the ipsilateral foot during CHIKV infection. Mice lacking IFN- β begin to develop increased foot swelling by 2 dpi, but tissues support a similar level of CHIKV replication (Fig. 2.1-2.3). This led us to hypothesize

that IFN- β protects from CHIKV pathogenesis by modulating the innate immune response. Therefore, we first sought to determine how the absence of IFN- β affected early (2-3 dpi) cellular recruitment into the ipsilateral foot tissue. Previous studies have demonstrated that macrophages, monocytes, and neutrophils are among the early cells recruited to the infected foot and that altering the balance of these infiltrating cells can drastically impact disease^{51,52,71,72}. To quantitate differences in immune cell infiltration into the foot, infected WT or IFN- β -KO mice were sacrificed at 2 or 3 dpi, and the infected foot was disarticulated and digested to generate a single cell suspension²³. We stained the cell suspension for various surface cell identifying markers and analyzed the cells were analyze by flow cytometry to determine the total number of immune cells (CD45⁺), inflammatory monocytes (Ly6C⁺ CD11b⁺ Ly6G⁻), neutrophils (Ly6G⁺ CD11b⁺), and macrophages (F4/80⁺ MERTK⁺) (fig. S2.1). At 2 dpi, we observed an increase in the total number of neutrophils (4-fold), as well as a significant increase in the percentage of neutrophils among CD45⁺ immune cells in mice lacking IFN- β compared to WT mice (Figure 2.5A, $p < 0.05$ and $p < 0.0001$). By 3 dpi, there was no longer a difference in neutrophil number, though there was still an increase in percentage of neutrophils at this time point (Fig. 2.5A, $p < 0.0001$). We did not observe a difference in total number of CD45⁺ cells, monocytes, or macrophages between WT and IFN- β KO mice, but we did see a minor decrease in the percentage of monocytes at 2 dpi (Fig. 2.5A, $p < 0.05$). Consistent with the histological observations, these results suggest that IFN- β functions to limit immunopathology during CHIKV infection by modulating neutrophil infiltration into the ipsilateral foot.

Mice lacking IFN- β have increased early IL-9 levels in the ipsilateral foot. We next assessed local cytokine and chemokine levels to determine the basis for increased neutrophil recruitment in the infected feet of IFN- β -KO mice. Using a multiplexed assay, we measured

cytokine and chemokine levels in the ipsilateral foot at 2 and 3 dpi in WT and IFN- β -KO animals. We did not observe elevated proinflammatory cytokines, such as IL-6, IL-1 β , or TNF- α , or common neutrophil chemoattractants, such as CXCL1 (KC) or CXCL2 (MIP-2) in the IFN- β -KO mice. In a panel of 25 cytokines and chemokines the only analyte significantly elevated in IFN- β -KO foot tissue was IL-9 at 2 dpi (Fig. 2.6, $p < 0.0001$). Previous studies have shown that IL-9 can contribute to acute inflammation in certain models including rheumatoid arthritis¹⁶⁰. Importantly, IL-9 has been linked to neutrophil survival and function in a model of arthritis, and furthermore, in the context of experimental autoimmune uveoretinitis (EAU), treatment with IFN- β inhibited IL-9 production by splenocytes^{161,162}. Thus, elevated IL-9 points to a potential mechanism for increased neutrophil numbers present in the IFN- β -KO mice.

Depletion of neutrophils alleviates the increased foot swelling seen in CHIKV-infected IFN- β -KO mice, but not in IRF7-KO mice. Because we observed an increase in number and percentage of infiltrating neutrophils in the infected foot of IFN- β KO mice at 2 and 3 dpi, which correlates with when we first begin to see differences in clinical disease, we sought to determine if neutrophils are responsible for the increased clinical disease severity in the IFN- β KO. We depleted neutrophils by intraperitoneal administration of anti-Ly6G mAb (clone 1A8) one day before infection and every other day through 7 dpi in WT, IFN- β -KO, and IRF7-KO mice. Neutrophil depletion was confirmed by flow cytometric analysis of the blood 6 or 8 dpi (data not shown). Neutrophil depletion had no effect on foot swelling in WT or IRF7-KO mice, but it alleviated the increased foot swelling observed in the IFN- β -KO mice to WT levels. The beneficial effects of neutrophil depletion began at 2 dpi in the IFN- β -KO mice (Fig. 2.7, $p < 0.01$), and this protective effect persisted throughout the course of acute infection. Importantly, neutrophil depletion had no effect on foot swelling in IRF7-KO mice, highlighting that distinct mechanisms

are driving pathology in IFN- β -KO versus IRF7-KO mice (Fig. 2.7). This observation demonstrates that neutrophils are required for exacerbated CHIKV clinical disease in the IFN- β deficient mice.

2.4 Discussion

IFN-I signaling is critical for the protection against a number of RNA and DNA viruses. Most of what is known about IFN-I biology comes from *in vitro* studies or the use of animals that lack all IFN-I signaling through IFNAR1 deletion. Neither of these approaches have allowed delineation of the roles of individual IFN-I subtypes in physiological context. Recent work with lymphocytic choriomeningitis virus (LCMV) persistent infection demonstrated that IFN- α and IFN- β have unique and distinguishable biologic functions, with IFN- β being mainly responsible for promoting viral persistence¹⁵⁰. Blockade of IFN- β during LCMV infection improved antiviral T cell responses and ultimately decreased infection of CD8 α ⁻ dendritic cells (DCs) at later time points. In this study we show that both IFN- α and IFN- β play distinct protective roles during acute CHIKV infection. We demonstrate that the IFN- α subtypes are sufficient for limiting viral CHIKV replication and spread, whereas IFN- β is dispensable for controlling viral replication and instead primarily functions to limit immunopathology by an apparent novel mechanism.

We demonstrate that the loss of IFN- α by mAb blockade or deletion of IRF7 increased CHIKV replication and dissemination to distant tissues, supporting an important antiviral role for the IFN- α 's during CHIKV infection. Previous work showed that during LCMV infection blockade of IFN- α led to increased viral loads late in infection¹⁵⁰. Similarly, IRF7-KO mice infected with West Nile virus (WNV), an encephalitic flavivirus also transmitted by mosquitoes, showed increased lethality compared to WT mice, and increased susceptibility was associated with

lowered IFN- α induction and severe viral dissemination^{96,98}. WNV and Dengue virus (DENV), another encephalitic flavivirus, both require IFN-I signaling on hematopoietic cells to control infection^{130,163}; however, our findings demonstrate that the antiviral effects of the IFN- α 's during CHIKV infection are primarily through their action on nonhematopoietic cells (Fig. 2.4). This is supported by previous bone marrow chimera studies that demonstrated that IFN signaling is required in nonhematopoietic cells to survive CHIKV infection¹¹⁶. Detailed characterization of CHIKV tropism in *Ifnar1*^{-/-} mice compared to WT mice in the arthritis model has not been done; however, IRF3/IRF7 double KO (DKO) mice, which closely resemble the phenotype of IFNAR1-KO mice during CHIKV infection, have been evaluated. DKO mice showed increased CHIKV RNA staining of many similar cell types as WT mice in the ipsilateral foot, but also showed spread to the epidermis, presumably due to infection of keratinocytes, which was not observed in WT mice⁶⁴. This is in contrast with what has been observed with loss of IFN-I during other alphavirus infections. IFNAR1 deletion during infection with a related alphavirus, Sindbis virus (SINV), permitted infection of macrophage-DC-like cells, which normally restrict SINV infection in WT mice¹¹⁸. Furthermore, related alphaviruses Ross River virus (RRV), SINV, and Venezuelan equine encephalitis virus (VEEV) are all able to infect and induce IFN-I production in DCs, whereas this has not been observed for CHIKV^{61,118,129,130}. The reason for these differences is not fully understood, but it may depend on the receptors or co-receptors for CHIKV entry, which still have not been identified. So while IFN-I, particularly the IFN- α 's, appear to play important antiviral roles in multiple viral infections, the cell types involved in these protective pathways are different depending on the context.

Nonhematopoietic cells that are likely important for CHIKV pathogenesis include synovial and skin fibroblasts and various muscle cell types, which have all been shown to support robust

CHIKV replication^{56,61,64}. There have been surprisingly few studies performed to determine how these cell types contribute to CHIKV pathogenesis. There is accumulating evidence that stromal cells participate in coordinating immune responses during various disease states, such as rheumatoid arthritis (RA)¹⁶⁴. Synovial fibroblasts are the main stromal cells of the synovium, and they are responsible for producing the extracellular matrix (ECM) component of synovial fluid and maintaining lubrication of the joint. Cultured human fibroblast-like synoviocytes from RA patients were shown to express TLR3, TLR7, RIG-I, and MDA5, and consequently, stimulation with polyinosinic-polycytidylic acid (poly I:C) induced IRF3 activation and IFN-I production¹⁶⁵. CHIKV can infect myoblasts, and certain strains, including La Réunion, are able to infect myofibers⁷. Muscle cells are able to participate in innate immune responses, as IL-1 β was shown to induce nitric oxide synthase 2 (NOS2 or iNOS) in rat skeletal myoblasts, and human skeletal muscle biopsies showed a linear correlation between IL-1 β levels and iNOS expression¹⁶⁶. Keratinocytes are infected by many arboviruses, including WNV and DENV^{167,168}; however, human keratinocytes are refractory to CHIKV infection at a post-fusion step but are still able to produce cytokines and IFN-I following CHIKV exposure, suggesting that they also might be an important contributor to inflammation during CHIKV infection⁶². Extensive *in vitro* work has demonstrated that different cell types can differentially respond to IFN-I signaling¹⁵⁷. Clearly, nonhematopoietic cells represent important responders to IFN-I during CHIKV infection *in vivo*, and much more work is needed to characterize the cell type-specific protective antiviral ISGs and proinflammatory pathways that are induced in these cells in response to CHIKV infection and IFN-I signaling.

Whereas IFN- α was important for limiting viral replication, we demonstrate that loss of IFN- β exacerbates acute CHIKV disease but without having much impact on viral loads at the site

of inoculation or in distant tissues, suggesting that IFN- β primarily functions as a beneficial immunomodulatory molecule. This is distinct from what was observed with LCMV infection, where IFN- β was also dispensable for controlling viral replication but ultimately played a detrimental role for the host and promoted LCMV persistence¹⁵⁰. In that study, specific blockade of IFN- β improved antiviral T cell responses and led to accelerated virus clearance, presumably through decreased infection of CD8 α^- dendritic cells, suggesting that IFN- β likely signals on DCs^{150,169}. Additionally, IFN- β has well described beneficial immunomodulatory activity in the treatment of multiple sclerosis and its mouse model, experimental autoimmune encephalomyelitis (EAE), and in that context, IFN-I signaling was required in myeloid cells to exert protective effects and limit autoimmunity^{170,171}. In contrast, we demonstrate that IFN- β is protective in CHIKV infection by signaling on nonhematopoietic cells and ultimately limits neutrophil recruitment into the site of inflammation (Fig. 2.4 and 2.5). Furthermore, depletion of neutrophils completely reversed the exacerbation of clinical CHIKV disease seen in the IFN- β -KO mice. Dysregulated neutrophil recruitment has been previously documented to increase acute CHIKV disease severity. Mice deficient for the chemokine (C-C motif) receptor 2 (CCR2) or Toll-like receptor 3 (TLR3) both developed more severe and prolonged CHIKV arthritis associated with early and severe neutrophil infiltration^{71,117}. Increased neutrophil recruitment in the CCR2-KO mice was accompanied with increased expression of inflammatory mediators. However, we were surprised to see unaltered, or even slightly lowered, levels of many proinflammatory cytokines and chemokines in the ipsilateral foot tissue of IFN- β -KO mice, including the known neutrophil-attracting chemokines CXCL1 (KC) and CXCL2 (MIP-2 α)⁷¹. Unexpectedly, IL-9 was the only significantly altered cytokine out of 25 tested analytes by multiplex assay (Fig. 2.6). More work

needs to be done to determine if IL-9 is directly involved in the worsened CHIKV disease of IFN- β -KO mice.

IL-9 is generally described as a type 2 immunity cytokine, and as such, it has a protective role during helminth infections; however, it has also been shown to contribute to pathogenesis during autoimmune inflammation, such as rheumatoid arthritis and allergic responses^{160,172}. Despite being originally characterized as a T cell cytokine, an IL-9 fate reporter mouse revealed that type 2 innate lymphoid cells (ILC2s) are the predominant source of IL-9 during a lung inflammation model¹⁷³. We observed elevated IL-9 prior to the generation adaptive immune responses (2 dpi), which suggests that ILC2s are a potential source of IL-9 in the IFN- β -KO mice. ILC2s are known to produce IL-9 when they are stimulated with IL-25, IL-33, and thymic stromal lymphopoietin (TSLP), which are typically secreted by damaged epithelium barriers¹⁷⁴. Synovial fibroblasts isolated from RA patients have been shown to produce both IL-33 and TSLP^{175,176}. Unfortunately, these cytokines were not in our multiplex panel, but future studies will determine if IL-33, IL-25, and TSLP are also dysregulated in IFN- β -KO mice during acute CHIKV infection. Previous work in a mouse model of experimental autoimmune uveoretinitis (EAU) showed that *in vivo* IFN- β treatment dampened IL-9 production by *ex vivo* stimulated splenocytes by an unknown mechanism, suggesting that IFN- β may indirectly regulate ILC2 responses in multiple biological contexts¹⁶². Altogether, our findings suggest a model in which IFN- β signals on synovial cells or other nonhematopoietic cells in the foot tissue to modulate IL-9 induction, presumably by ILC2s, during acute CHIKV infection. ILC2s have not been evaluated during CHIKV infection, but our findings suggest that evaluating the contribution of ILC2s and IL-9 in acute CHIKV pathogenesis may reveal important interactions between nonhematopoietic cells and innate immune responses.

The current model of IFN-I-mediated protection during CHIKV infection is that IFN-I signaling is absolutely required in nonhematopoietic cells to control and survive infection, yet how these different cell types respond to IFN-I and CHIKV infection is poorly understood^{97,116}. IFN-I signaling is incredibly complex, and the functional outcome depends on many factors, including concentration, IFN-I subtype affinity and half-life with the receptor, IFNAR surface levels, and the cell type and biological context. Our studies add to the accumulating evidence that IFN-I subtypes have distinct properties *in vivo* and that even the mechanisms underlying the differential functions can vary depending on the biological context. Similar to other systems, we found that the IFN- α 's are sufficient to control CHIKV replication and dissemination. In contrast, IFN- β functioned to modulate the host immune response by a novel mechanism to protect against neutrophil-mediated immunopathology during acute CHIKV infection. There are a number of therapeutic agents approved for a variety of diseases that either target or augment the IFN-I pathway. Our studies highlight that careful delineation of the biological activities of the IFN-I subtypes may lead to more efficacious therapies with less off-target effects and also help explain why the multigene nature of IFN-I is conserved across many species.

2.5 Materials and Methods

Mice

All animal experiments were performed in accordance and with approval of Washington University Institutional Animal Care and Use Committee guidelines, and all mouse infection studies were performed in an animal biosafety level 3 laboratory. All experiments were performed with 4-week-old male mice. C57BL/6J (WT), interferon beta knockout (*Ifnb*^{-/-}), and interferon regulatory factor 7 knockout (*Irf7*^{-/-}) mice were bred and maintained in our mouse colony before

being transferred to the animal biosafety level 3 laboratory for CHIKV experiments. For some experiments, 4-week-old *Vav-Cre^{+/-}Ifnar1^{fl/fl}* or *Vav-Cre⁻Ifnar1^{fl/fl}* littermate controls were used, which were also bred and maintained in our colony and genotyped prior to use in experiments. *Ifnb^{-/-}*, *Irf7^{-/-}*, and *Vav-Cre⁺Ifnar1^{fl/fl}* mice bred onto the C57BL/6J background were generously provided by Michael S. Diamond (Washington University School of Medicine).

Virus experiments

A recombinant strain of CHIKV (LR2006 OPY1) was generously provided by S. Higgs (Kansas State University) and generated from *in vitro* transcribed cDNA, as previously described¹⁷⁷. At 4 weeks of age, mice were inoculated in the left rear footpad with 10³ PFU of the LR2006 OPY1 strain of CHIKV in a volume of 10 µl. Infected mice were monitored daily for foot swelling with digital calipers for 14-15 days. At the termination of experiments, mice were sedated with a ketamine-xylazine cocktail and euthanized, and perfused via intracardiac injection with PBS. Tissues (ipsilateral left ankle, contralateral right ankle, and ipsilateral quadriceps muscle) were harvested into 0.65 mL PBS and then stored at -80°C until processing for viral burden. “Ankle” refers to distal foot with the skin and digits removed, and “foot” refers to the distal foot with cutaneous and subcutaneous tissues everted but still attached to the distal digits. For serum analysis, blood was collected at the time of sacrifice and centrifuged for 10 min at 10,000g and stored at -80°C.

Tissue viral burden

Organs were harvested into 0.65 ml of PBS and homogenized with 1.0 mm diameter zirconia-silica beads with 2 pulses of 3,000 rpm for 30 seconds with a MagNA Lyser (Roche) prior to plaque assay on BHK cells. 200 µL of serial dilutions of organ homogenates or serum in DMEM with 1% FBS was added to BHK cells (5x10⁵ cells for 6 well plates) and incubated for 1 hr at 37°C

with rocking every 20 min. An MEM-agar overlay was then added to the cells and incubated for approximately 60 hrs at 37°C or until plaques were visible by visual examination. Plates were then fixed with 1% formaldehyde (30 min at room temperature), and agar plugs were removed. Plaques were visualized using a 1% crystal violet solution and counted.

Histopathological analysis

The ipsilateral feet of infected mice were treated with Nair® to remove the fur, and then the mice were sacrificed with a ketamine-xylazene cocktail and perfused by intracardiac injection of PBS at the indicated day post infection. The infected whole foot tissue (with the skin intact) was dissected above the ankle and fixed in 4% paraformaldehyde for 48 hours, followed by decalcification in 10 mL of 14% acid-free EDTA (pH 7.2) for 10-14 days, with the buffer changed every couple of days. Decalcified tissues were dehydrated with increasing ethanol gradients (30%, 50%, and then 70%) and subsequently embedded in paraffin with 5-um sections prepared. Tissue sections were stained with hematoxylin and eosin (H&E). Embedding, sectioning, and staining were performed by the Musculoskeletal Histology and Morphometry Core.

For quantification of cells into the joint space, H&E slides were imaged with a Zeiss Axio Imager Z2 microscope equipped with a color CCD camera (Washington University Center for Cellular Imaging). The investigator was not blinded to the identity of the samples at the time of imaging, but all mid-foot synovial caps were imaged and then blinded for quantification by another investigator. The data are represented as the number of cells per high-power field (HPF). For overall inflammation scoring, the slides were blinded and scored by a pathologist. The pathologist noted the absence or presence of joint space inflammation, myositis, and tenosynovitis and then gave an overall inflammation score based on the following criteria: 0, no inflammation; 1, mild inflammation; 2, moderate inflammation; 3, severe inflammation.

Immune cell flow cytometry analysis

Mice were sacrificed 2 or 3 days after inoculation and perfused with PBS. The inoculated foot was disarticulated at the ankle without fracturing the bone. Cutaneous and subcutaneous tissue were everted but still attached to the distal foot and digits during digestion. Tissues were incubated for 2 hours at 37°C in 5 mL digestion buffer with manual shaking every 20-30 min. Digestion buffer consisted of RPMI (Sigma), type IV collagenase (2.5 mg/ml) (Sigma), DNase I (10 mg/ml) (Sigma), 15 mM Hepes (Corning), and 10% FBS (BioWest). Digested tissues were passed through a 70-um cell strainer and washed once with 40 mL PBS containing 4% FBS. The number of viable cells was quantified by trypan blue staining.

The single cell suspension was transferred to a 96-well plate and incubated with anti-mouse CD16/CD32 (Clone 93; BioLegend) for 10 min at 4°C and then surface-stained in PBS containing 4% FBS for 1 hour at 4°C with two separate panels of antibodies. All antibodies are from BioLegend unless otherwise specified. Panel 1 consisted of anti-MHC-II PerCP-Cy5.5 (1:400, M5/114.15.2), anti-CD45 FITC (fluorescein isothiocyanate) (1:400, 30-F11), anti-CD11b Brilliant Violet 605 (1:200, M1/70), anti-CD3e (1:200, 145-2C11) and anti-CD19 (1:400, 1D3, BD Biosciences) Brilliant Violet 510 (dump gate), anti-CD11c Pacific Blue (1:200, N418), anti-F4/80 APC-Cy7 (1:200, BM8), anti-Ly6C Alexa Fluor 700 (1:200, HK1.4), anti-MERTK PE (phycoerythrin) (1:200, 2B10C42), anti-Ly6G PE-Cy7 (1:200, 1A8), and Fixable Viability Dye eFluor 506 (1:500, eBioscience). Gating strategy for myeloid cells is illustrated in figure S2.1.

Panel 2 (data not shown) included anti-CD45 FITC (1:200, 30-F11), anti-CD11c Pacific Blue (1:200, N418), anti-CD19 APC-Cy7 (1:400, 6D5), anti-CD8 α Alexa Fluor 700 (1:200, 53-6.7), anti-CD3 ϵ APC (1:200, 145-2C11), anti-CD4 PE-Cy7 (1:400, GK1.5), anti-NK1.1 PE (1:200, PK136), and Fixable Viability Dye eFluor 506 (1:500, eBioscience). Cells were washed

and fixed at 4°C for 10 min in 4% paraformaldehyde (Electron Microscopy Sciences). The fixed cells were washed and resuspended in PBS containing 4% FBS. Cells were run on a LSR Fortessa (Becton Dickinson) flow cytometer and analyzed using BD FACSDiva and FlowJo V10 software.

In vivo IFN blockade

BL6 mice were administered 1 mg of anti-mouse pan-IFN- α (TIF-3C5), 1 mg of anti-mouse IFN- β (HDb-4A7), or 1mg isotype control (PIP) (Leinco, St. Louis, MO) at 24h prior to and again 24h post infection by an intraperitoneal route.

In vivo neutrophil depletion

BL6, IFN- β -KO, or IRF7-KO mice were treated with 0.25 mg of anti-mouse Ly6G (1A8) or isotype control (Leinco, St. Louis, MO) at 1 day before and every other day through 7 days post infection by intraperitoneal route. Neutrophil depletion was verified by whole blood staining at 6 or 8 dpi (data not shown).

Cytokine and chemokine analysis

Foot tissues (with the cutaneous and subcutaneous tissues everted but still attached to the distal foot and digits) were harvested from euthanized infected mice at days 2 and 3 and collected in 500 μ L PBS with 0.1% BSA added and then homogenized using a MagNA Lyser (Roche). Cytokine and chemokine levels in the homogenates were measured using Luminex technology with a mouse 25-plex assay, as per the manufacturer's instructions (Millipore).

Quantification and Statistical Analysis

All statistical analyses were performed with GraphPad Prism 7 software (San Diego, CA). For foot swelling over time and viral burden analysis (3 experimental groups), two-way ANOVA with Dunnet's post-hoc multiple comparisons analysis was used. For cytokine/chemokine and infiltrate analyses (2 experimental groups), two-way ANOVA with Sidak's post-hoc multiple

comparisons was used. For histological scoring and cells/HPF quantification one-way ANOVA with Tukey's post-hoc multiple comparisons test was used. All sample sizes were determined based on our extensive experience with this model. $P < 0.05$ indicated statistically significant differences.

2.6 Figures

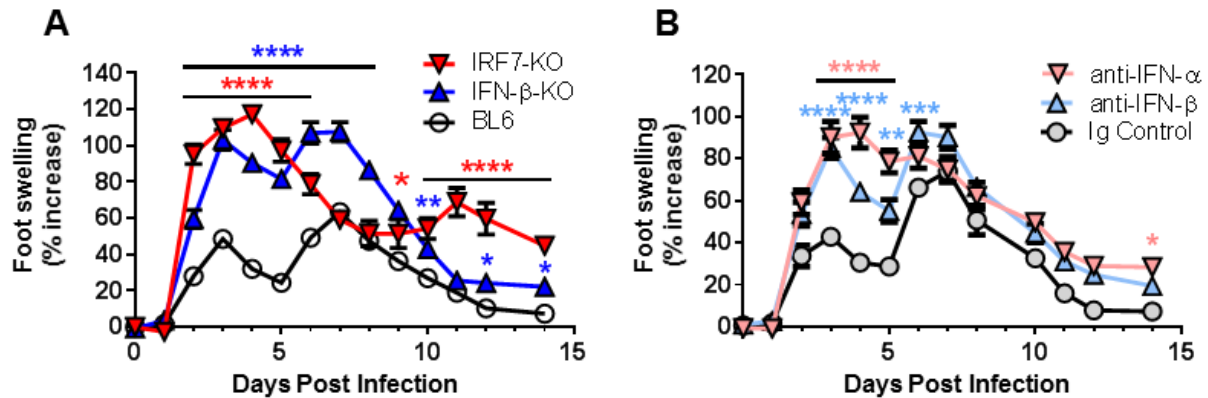


Figure 2.1 *IFN- α and IFN- β both play protective roles in limiting clinical CHIKV disease*

Mice were inoculated with 10^3 pfu of CHIKV (La Réunion) subcutaneously in the left rear foot pad. (A-B) Foot swelling was measured daily for WT, IFN- β -KO, or IRF7-KO mice (A) or WT mice treated with 1 mg of anti-mouse IFN- α (TIF-3C5), 1 mg anti-mouse IFN- β (HD β -4A7), or 1 mg isotype control antibody at 24 hours prior to and post infection by intraperitoneal (IP) route (B). Data are reported as percent increase in foot area (vertical x horizontal mm²) over baseline. Data are pooled from at least 2 independent experiments with $n = 18-22$ mice per group (A) or $n = 10$ mice per group (B). All data are represented as mean \pm SEM, and if no error bar is present that indicates the error is smaller than the height of the symbol. *, $p < 0.05$; **, $p < 0.01$; ***, $p < 0.001$; ****, $p < 0.0001$ (2-way repeated measure ANOVA with Dunnett's post-hoc multiple comparisons analysis).

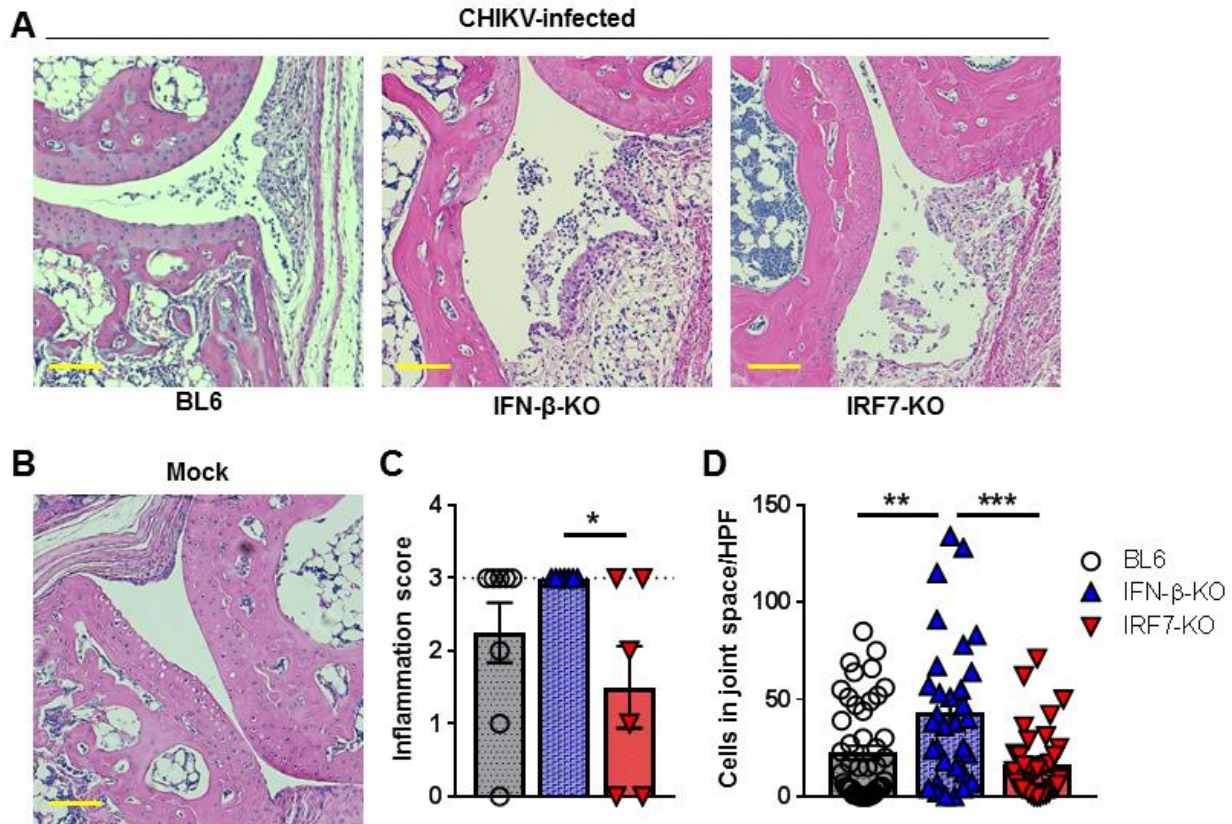


Figure 2.2 *IFN-β-KO, but not IRF7-KO, mice have increased cellular infiltration into the midfoot joint spaces during acute CHIKV infection*

Infected (10^3 pfu CHIKV) or mock-inoculated animals were sacrificed at 7 dpi, and histology of the ipsilateral foot was performed. (A-B) Representative hematoxylin and eosin (H&E) staining of the ipsilateral mid-foot joints in CHIKV-infected (A) or mock-inoculated mice (B) at 7 dpi (scale bar = 100 μ m). (C) H & E slides were scored on a scale of 0 to 3 by a blinded pathologist for overall inflammation, taking into consideration joint space inflammation, myositis, and synovitis for scoring. Criteria were: 0, no inflammation; 1, mild inflammation; 2, moderate inflammation; 3, severe inflammation. (D) A blinded investigator counted the number of inflammatory cells per high-power field (HPF) in the midfoot synovial spaces. Data are depicted as the mean \pm SEM. Histological results are at least two independent experiments pooled with $n = 4-6$ per group. *, $p < 0.05$; **, $p < 0.01$; ***, $p < 0.001$ (1-way ANOVA with Tukey's post-hoc multiple comparisons analysis).

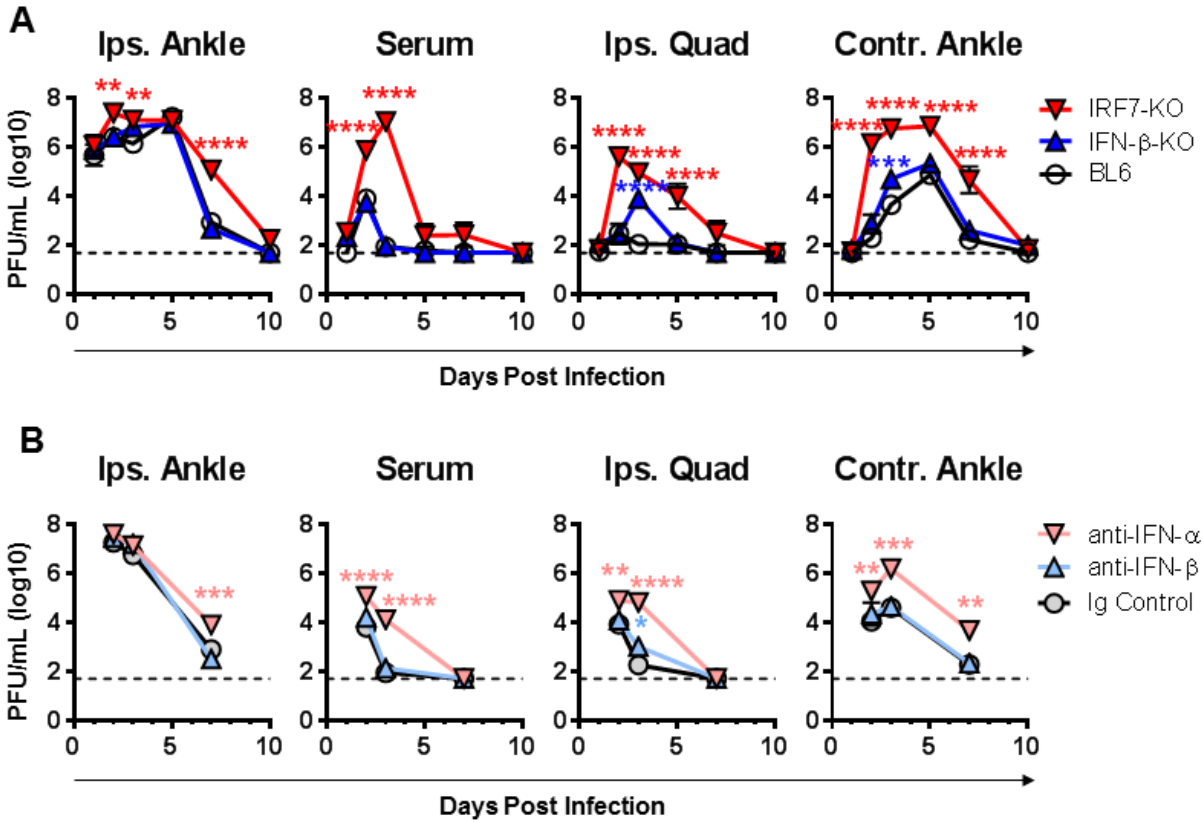


Figure 2.3 *IFN- α , but not IFN- β , limits CHIKV replication and dissemination*

Mice were inoculated with 10^3 pfu of CHIKV and then sacrificed and perfused with PBS at the indicated time points. Infectious virus in the joints, muscle, and serum were determined by plaque assay in BHK cells in (A) WT, IFN- β -KO mice, or IRF7-KO mice or (B) WT mice administered 1 mg anti-IFN- α , 1 mg anti-IFN- β , or 1 mg isotype control by IP route at 24 h prior to and 24 h post infection. Dashed line represents the limit of detection. Data are represented as median \pm SEM. *, $p < 0.05$; **, $p < 0.01$; ***, $p < 0.001$; ****, $p < 0.0001$ (2-way ANOVA followed by Dunnett's post-hoc multiple comparisons test).

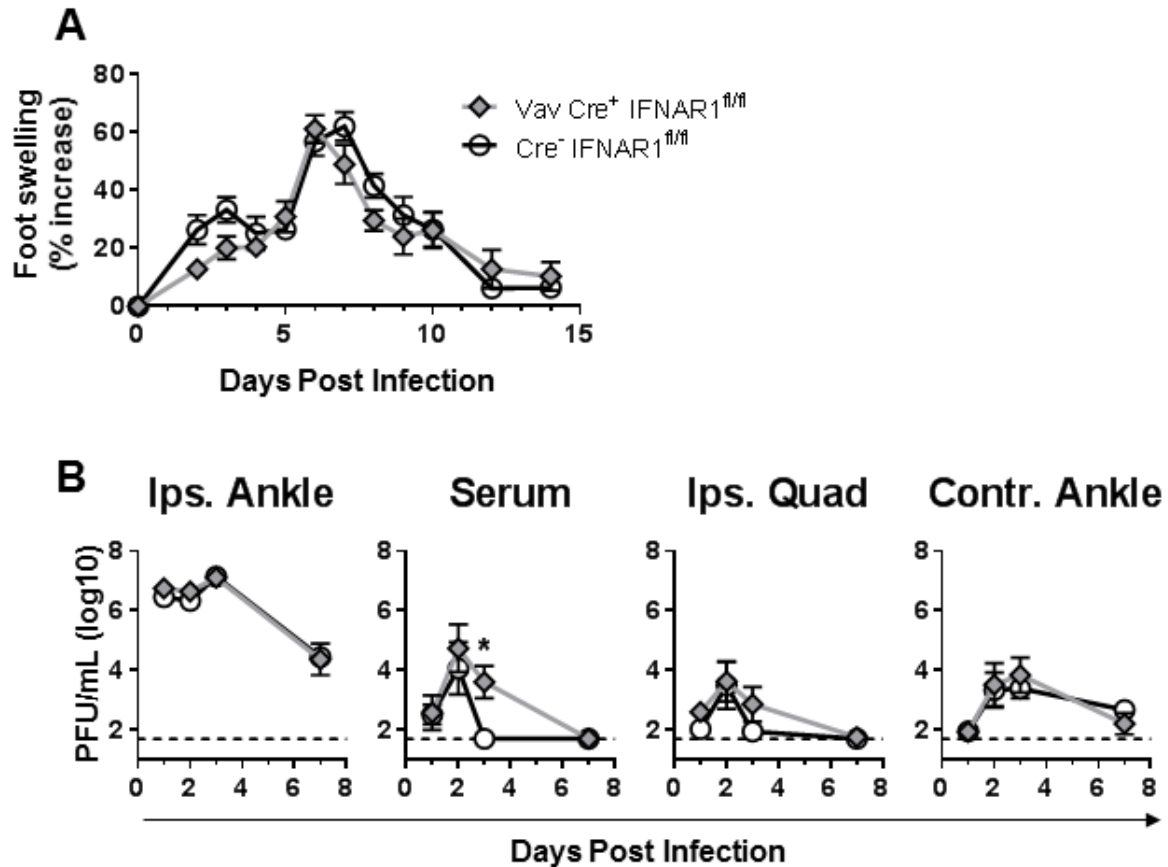


Figure 2.4 *IFN- α and IFN- β exert their protective effects during CHIKV arthritis by signaling on nonhematopoietic cells*

Vav-Cre⁺ IFNAR1^{fl/fl} mice or Cre⁻ IFNAR1^{fl/fl} littermate controls were infected with 10³ pfu of CHIKV (La Réunion). **(A)** Foot swelling was measured daily with digital calipers. Results are pooled from 2 independent experiments with $n = 6-9$ mice per group. Data are represented as the mean \pm SEM. The results were not statistically significant ($p > 0.05$) by 2-way repeated measure ANOVA with Dunnett's post-hoc multiple comparisons analysis. **(B)** Infectious virus in the joints, muscle, and serum were determined by plaque assay at the indicated time points. Data are represented as median \pm SEM. *, $p < 0.05$ (2-way ANOVA followed by Dunnett's post-hoc multiple comparisons test).

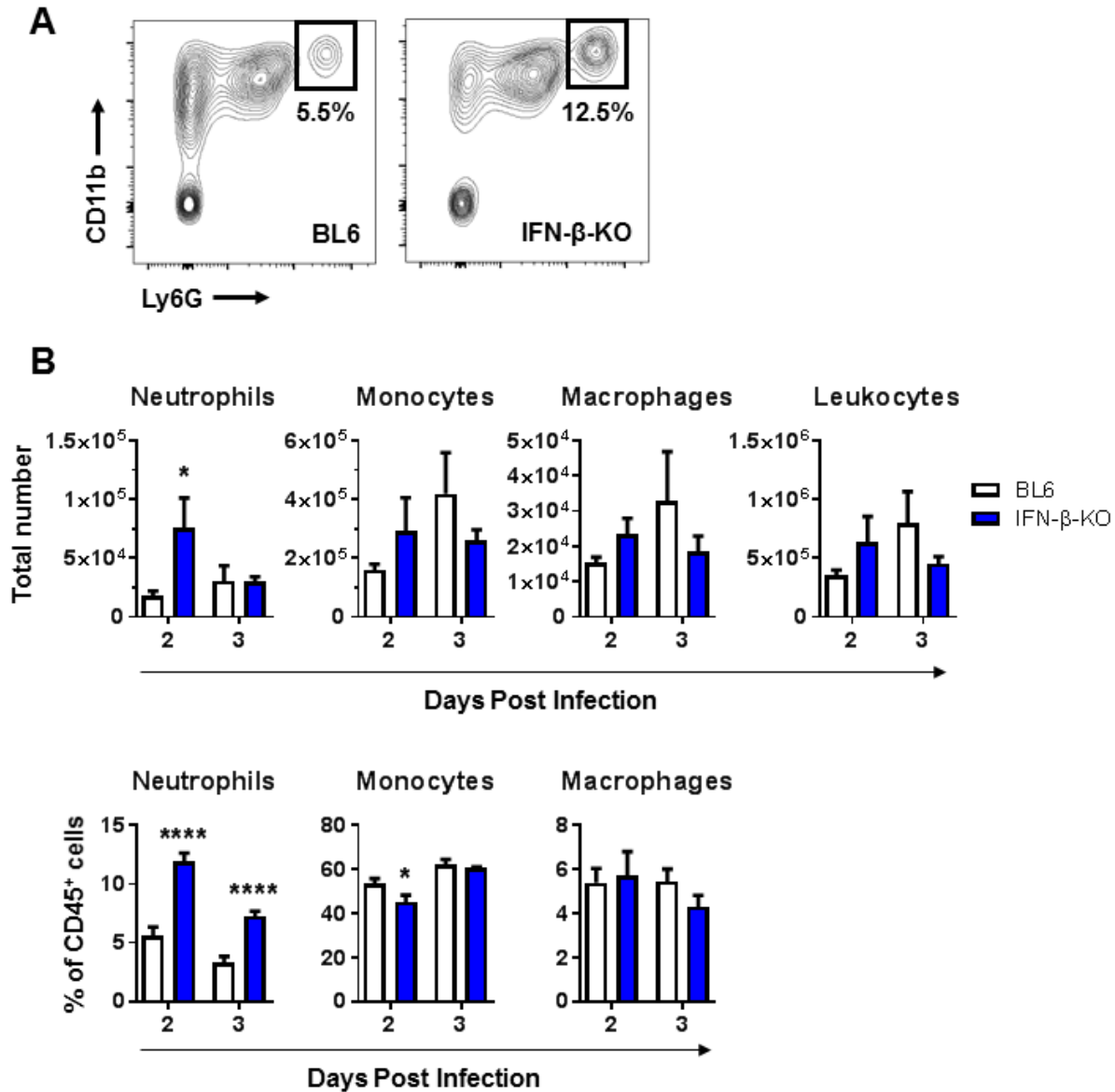
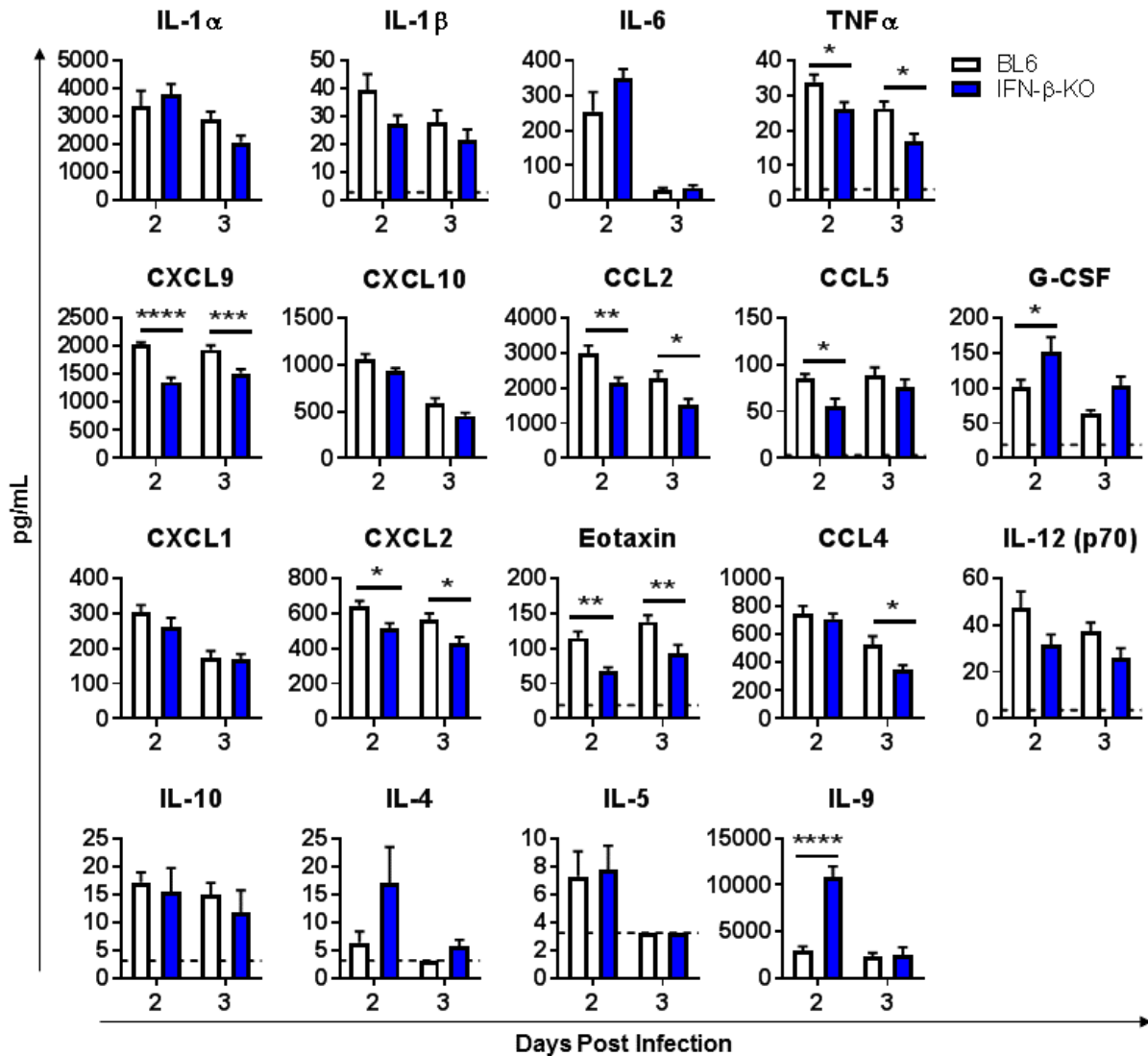


Figure 2.5 *IFN-β* deficient mice have increased neutrophil recruitment into the ipsilateral foot during CHIKV infection

Mice were inoculated with 10^3 pfu of CHIKV via a subcutaneous route. The ipsilateral foot tissue was collected at 2 and 3 dpi and digested with Collagenase IV (Sigma). The single cell suspension was surface stained for immune cell markers and analyzed by flow cytometry. (A) Representative FACS plots showing the percentages of CD11b⁺Ly6G⁺ neutrophils isolated from the feet of WT or IFN-β-KO mice at 2 dpi. B. (B) Total number of isolated CD45⁺ leukocytes and total number or percentage of CD11b⁺Ly6G⁺ neutrophils, CD11b⁺Ly6C⁺Ly6G⁻ monocytes, and F4/80⁺MERTK⁺ macrophages. Results are pooled from 2 independent experiments with $n = 6-7$ mice per group. Data represent the mean \pm SEM. *, $p < 0.05$; ****, $p < 0.0001$ (2-way ANOVA with Sidak's post-hoc multiple comparisons test).



Not detected: GM-CSF, IL-7, IFN-γ, IL-12 (p40), IL-13, IL-17

Figure 2.6 Mice lacking IFN-β have increased early IL-9 levels in the ipsilateral foot

Mice were inoculated with 10^3 pfu of CHIKV via a subcutaneous route. Cytokine and chemokine levels on day 2 and 3 in the ipsilateral foot was determined using Luminex technology (Millipore). Results are pooled from two independent experiments with $n = 6-7$ mice per group. Data represent the mean \pm SEM. Dashed line represents limit of detection. *, $p < 0.05$; ****, $p < 0.0001$ (2-way ANOVA with Sidak's post-hoc multiple comparisons test).

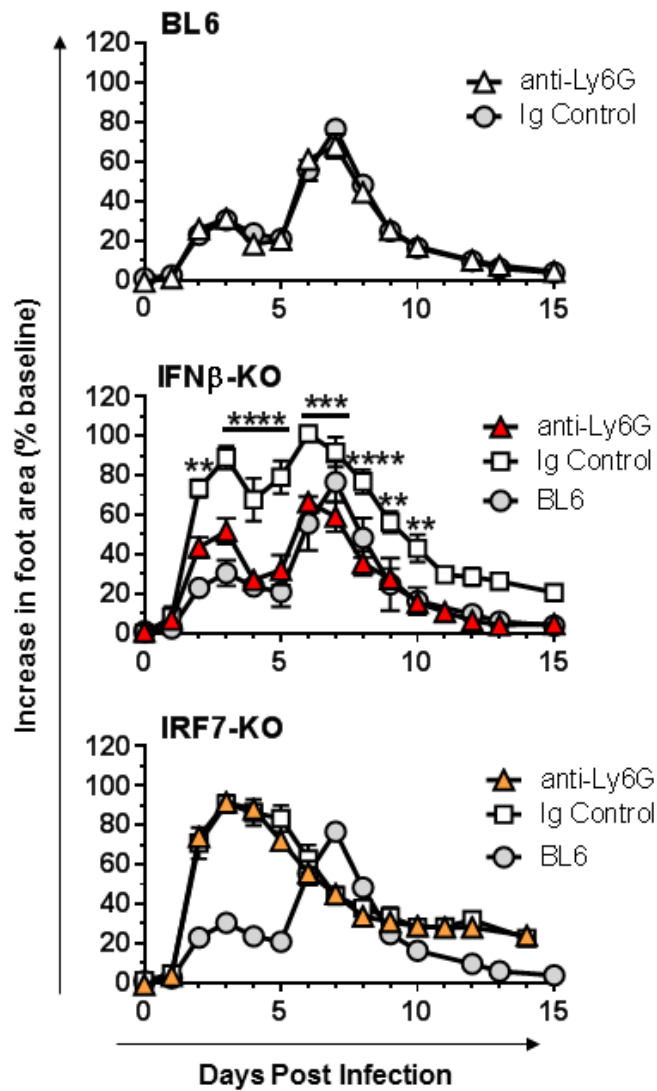


Figure 2.7 Depletion of neutrophils alleviates the increased foot swelling seen in CHIKV-infected IFN- β -KO mice, but not in IRF7-KO mice

WT, IFN- β -KO, or IRF7-KO mice were infected with 10^3 pfu of CHIKV. Mice were administered 0.25 mg anti-Ly6G (1A8) or isotype control antibody by IP route beginning at 1 day before and continued every other day through 7 dpi. Foot swelling was monitored daily and is reported as percent increase in foot area (vertical x horizontal mm²) over baseline. Results are pooled from 2 independent experiments with $n = 5-8$ mice per group. Data are reported as the mean \pm SEM. **, $p < 0.01$; ***, $p < 0.001$; **** $p < 0.0001$ (2-way repeated measure ANOVA with Dunnett's post-hoc multiple comparisons analysis).

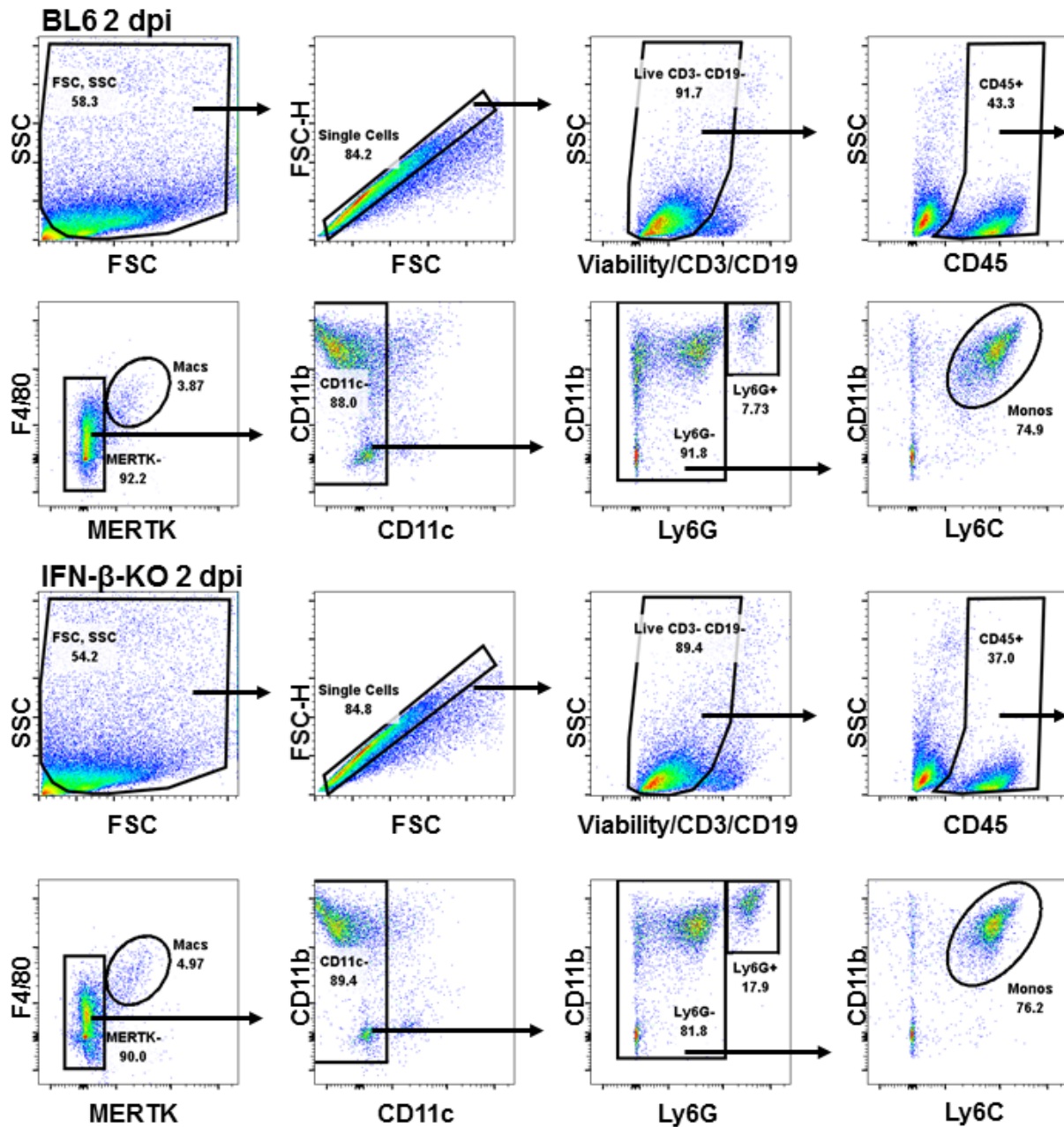


Figure S2.1 Gating strategy to identify myeloid cells recruited into the ipsilateral foot during CHIKV infection

Mice were inoculated with 10^3 pfu of CHIKV via a subcutaneous route. The ipsilateral foot tissue was collected at 2 and 3 dpi and digested with Collagenase IV (Sigma). The single cell suspension was surface stained for immune cell markers and analyzed by flow cytometry. Gating strategy for WT and IFN- β -KO mice at 2 dpi is shown. Gates were drawn based on an unstained sample.

Chapter 3

Therapy with CTLA4-Ig and an antiviral monoclonal antibody controls chikungunya virus arthritis

This chapter contains data published in the following publication with significant contribution from Jonathan Miner.

J. J. Miner*, **L. E. Cook***, J. P. Hong, A. M. Smith, J. M. Richner, R. M. Shimak, A. R. Young, K. Monte, S. Poddar, J. E. Crowe Jr., D. J. Lenschow, M. S. Diamond, Therapy with CTLA4-Ig and an antiviral monoclonal antibody controls chikungunya virus arthritis. *Sci. Transl. Med.* 9, eaah3438 (2017).

*co-first authors

3.1 Abstract

In 2013, chikungunya virus (CHIKV) transmission was documented in the Western Hemisphere, and the virus has since spread throughout the Americas with more than 1.8 million people infected in more than 40 countries. CHIKV targets the joints, resulting in symmetric polyarthritis that clinically mimics rheumatoid arthritis and can endure for months to years. At present, no approved treatment is effective in preventing or controlling CHIKV infection or disease. We treated mice with eight different disease-modifying antirheumatic drugs and identified CTLA4-Ig (abatacept) and tofacitinib as candidate therapies based on their ability to decrease acute joint swelling. CTLA4-Ig reduced T cell accumulation in the joints of infected animals without affecting viral infection. Whereas monotherapy with CTLA4-Ig or a neutralizing anti-CHIKV human monoclonal antibody provided partial clinical improvement, therapy with both abolished swelling and markedly reduced levels of chemokines, proinflammatory cytokines, and infiltrating leukocytes. Thus, combination CTLA4-Ig and antiviral antibody therapy controls acute CHIKV infection and arthritis and may be a candidate for testing in humans.

3.2 Introduction

Chikungunya virus (CHIKV) is a mosquito-transmitted alphavirus that causes severe acute and chronic polyarthritis. CHIKV was first isolated in Tanzania in 1947, but the virus has emerged rapidly over the last decade, causing outbreaks in the islands of the Indian Ocean, in Southern Europe, and in Southeast Asia^{178,179}. In 2013, CHIKV spread to the Western Hemisphere and, by the end of 2015, had infected more than 1.8 million people in North America, Central America, and South America. The acute symptoms of CHIKV infection include fever and rash, which typically resolve within a few days, and joint and muscle pain²³. CHIKV and other arthritogenic

alphaviruses directly invade the synovium to cause inflammatory arthritis, which is characterized by articular swelling and prolonged morning stiffness^{23,52}. CHIKV-induced arthritis in humans can persist, with as many as 60% of individuals progressing to chronic disease that lasts from months to years^{20,23,180,181}. Epidemiological projections suggest that there are currently about 400,000 individuals in the Western Hemisphere with chronic CHIKV arthritis²².

Chronic CHIKV arthritis clinically is similar to seronegative rheumatoid arthritis (RA), an autoimmune disease characterized by symmetrical joint pain, swelling, and morning stiffness^{23,182–184}. Treatment with newer disease-modifying antirheumatic drugs (DMARDs) has been effective in preventing the bone erosions and deformities seen in patients with untreated RA. Whether chronic CHIKV arthritis causes erosive disease remains controversial, although there are reports of bone erosions in patients infected with CHIKV¹⁸². Effective treatment of RA relies on early diagnosis, because erosions can occur within months of onset of the disease¹⁸⁵. Because CHIKV and RA exhibit significant clinical overlap, there is potential for confusing the diagnoses and inadvertently treating CHIKV arthritis with DMARD therapy²³.

Over the last 20 years, studies in patients with RA have demonstrated that oral and biological DMARDs prevent joint pain, swelling, and damage. Oral DMARDs include hydroxychloroquine, methotrexate, and sulfasalazine, whereas biological DMARDs include the anticytokine antibodies and Ig chimeras [for example, anti-tumor necrosis factor- α (TNF- α) and anti-interleukin-6 (IL-6) receptor]. Other biological DMARDs block T cell costimulation (CTLA4-Ig) or deplete B cells (anti-CD20). Among the newest drugs used to treat RA is tofacitinib, an oral DMARD that inhibits JAK (Janus kinase)/STAT (signal transducers and activators of transcription) signaling and broadly blunts cytokine responses^{186,187}. However, many DMARDs, by virtue of their immunosuppressive properties, may predispose to serious microbial

infections. Thus, there is a need to determine whether DMARDs are effective, benign, or deleterious in the treatment of CHIKV arthritis. The current standard of care for CHIKV arthritis is treatment with nonsteroidal anti-inflammatory drugs (NSAIDs), although these often do not ameliorate symptoms^{23,26}. One trial compared chloroquine (a DMARD) to meloxicam (an NSAID) and found no difference in efficacy, although a placebo group was not included in the trial design²⁶. Another open-label study examined a combination of hydroxychloroquine and methotrexate in the treatment of CHIKV arthritis and found that some patients partially responded to therapy, although ~50% of patients did not achieve significant improvement in disease score¹⁸⁸.

Subcutaneous inoculation of young wild-type (WT) immunocompetent C57BL/6 mice with pathogenic strains of CHIKV results in acute foot swelling, myositis, and arthritis^{51,52}. In this model, swelling resolves within the first 2 weeks of infection, although mild chronic disease can be observed histologically for weeks to months^{51,52,189}. This finding contrasts with the disease in humans, which are natural hosts and frequently have a protracted clinical disease course. Human patients with CHIKV arthritis have increased numbers of circulating, activated cytolytic CD8⁺ T cells, as do patients with untreated RA²³. Gene expression signatures observed in mouse models of CHIKV arthritis and RA suggested overlapping contributions of T cell-associated pathways in these diseases¹⁹⁰. Mice lacking or depleted of CD4⁺ T cells have reduced foot swelling and arthritis during acute CHIKV infection, suggesting that CD4⁺ T cells contribute to the pathology of arthritis⁷⁹. Inflammatory monocytes also are thought to play an initiating role in CHIKV arthritis in mice, because inhibiting production of monocyte chemoattractant protein-1 (MCP-1) with bindarit improved the disease¹⁹¹. Finally, treatment of mice with anti-CHIKV monoclonal antibodies (mAbs) 1 day before infection prevents arthritis, but whether therapy after infection is

effective has not been studied^{29,192,193}. Moreover, no previous study has tested the efficacy of clinically available DMARDs against CHIKV arthritis in mice.

Here, we examined the efficacy of several U.S. Food and Drug Administration (FDA)–approved RA therapies in a mouse model of CHIKV infection. We identified two DMARDs (CTLA4-Ig and tofacitinib) with efficacy during acute CHIKV arthritis. In particular, CTLA4-Ig, when paired with the neutralizing anti-CHIKV human mAb 4N12, was highly effective at reducing joint inflammation, periarticular swelling, migration of inflammatory leukocytes, and infection even when administered several days after virus inoculation. Thus, combination of anti-inflammatory and antibody-based antiviral therapy may serve as a model for treating humans with arthritis caused by CHIKV or other related viruses.

3.3 Results

Screen of candidate oral and biological DMARDs for treatment of acute CHIKV arthritis in mice. On the basis of previous data showing that immune cells and proinflammatory cytokines contribute to CHIKV arthritis in mice and our study showing that CHIKV arthritis clinically can mimic seronegative RA, we hypothesized that some of the existing FDA-approved therapies for RA might ameliorate acute CHIKV arthritis^{23,79}. To test this idea, we performed a multiarm prospective study (Fig. 3.1A) by inoculating 224 4-week-old WT mice subcutaneously in the left rear foot with 10^3 focus-forming units (FFU) of a pathogenic clinical isolate of CHIKV (La Reunion, 2006). Mice were divided into groups of 28 animals that received one of the following treatments beginning on day 3 after infection: methylprednisolone, naproxen, methotrexate, etanercept (soluble human TNF- α receptor), CTLA4-Ig (abatacept), oral gavage vehicle control, or tofacitinib (JAK inhibitor). All of the biological agents that we used have been

shown previously to have activity in mice^{186,194,195}. We chose day 3 after infection to initiate treatment, because this represents the time point of the first peak of clinically apparent foot swelling in the WT C57BL/6 mouse model of CHIKV infection (Fig. 3.1B). Animals were followed for clinical joint swelling in the ipsilateral foot and viral yield at different times after infection and treatment.

Treatment with CTLA4-Ig or tofacitinib at day 3 ameliorated foot swelling on day 7 after infection at the point of peak clinical disease [Fig. 3.1, C to F; 9.0 mm² (injection control) versus 7.8 mm² (CTLA4-Ig), $P < 0.005$ and 9.3 mm² (oral control) versus 8.5 mm² (tofacitinib), $P < 0.005$]. Other treatments had no significant effect at the dose tested in our experiments. To assess the systemic and local impact on viral burden of DMARD treatment, we evaluated CHIKV RNA levels on day 7 in serum and joint tissues. Remarkably, none of the therapies affected viral RNA levels in the right ankle or left ankle at day 7 or day 28 after infection compared to controls (Fig. 3.1, G to J; $P > 0.1$). Thus, CTLA4-Ig and tofacitinib ameliorate joint and periarticular inflammation in mice during the acute phase without substantively altering the viral burden in inflamed tissues. The beneficial effect of CTLA4-Ig, which blocks T cell activation, is consistent with data suggesting that CD4⁺ T cells contribute to immunopathology associated with CHIKV arthritis^{79,194}.

Combination therapy with CTLA4-Ig and an anti-CHIKV human mAb ameliorates acute CHIKV arthritis in mice. We next tested whether combination immunomodulatory and antiviral therapy might have greater beneficial effects. Potently neutralizing human anti-CHIKV mAbs previously were shown to protect against CHIKV-induced lethality in immunocompromised *Ifnar1*^{-/-} mice, even when administered at late time points after infection²⁸. We administered either a single 600- μ g dose of a control immunoglobulin G (IgG), 300 μ g of CTLA4-Ig, 300 μ g of anti-

CHIKV mAb (4N12, a neutralizing anti-CHIKV human mAb), or 300 μ g each of CTLA4-Ig + anti-CHIKV mAb (Fig. 3.2A) 3 days after CHIKV infection. Whereas either anti-CHIKV mAb or CTLA4-Ig partially reduced foot swelling at day 7, the combination completely abolished it (10.8 mm² versus 6.6 mm², $P < 0.0001$) relative to untreated or control IgG-treated animals (Fig. 3.2, A and B). Thus, anti-CHIKV mAb therapy initiated after disease onset can partially treat the acute clinical arthritis associated with CHIKV infection, and combination therapy with anti-CHIKV mAb and the immunomodulator CTLA4-Ig completely resolves clinical disease in mice within a few days of treatment.

Viral burden in CHIKV-infected mice treated with CTLA4-Ig and anti-CHIKV mAb.

To confirm the activity of the anti-CHIKV mAb in this model, we assessed its effects on viral burden. Treatment with anti-CHIKV mAb (alone or in combination with CTLA4-Ig) at day 3 eliminated infectious virus in the joints of infected mice within 2 days, as we observed a ~10,000-fold reduction in the ipsilateral ankle (Fig. 3.3A; $P < 0.0005$) and a ~100-fold reduction in the contralateral ankle (Fig. 3.3A; $P < 0.05$). Viral burden in mice treated with only CTLA4-Ig was not reduced in either the ipsilateral or contralateral ankle (Fig. 3.3A). Although infectious CHIKV cannot be detected after day 7 in this mouse model (or during the chronic phase in humans), CHIKV RNA persists in joint tissues for months^{23,52,54}. Because persistent viral RNA is a pathogen-associated molecular pattern and may contribute to CHIKV arthritis, we tested whether anti-CHIKV mAb treatment would reduce viral RNA levels^{23,54}. Although we did not observe a reduction in viral RNA levels in the ipsilateral foot joints ($P > 0.1$), other extremity joints exhibited a ~10-fold reduction in viral RNA on day 7 after infection, including the contralateral ankle and ipsilateral wrist (Fig. 3.3B; right ankle, $P < 0.005$; left wrist, $P < 0.05$). On day 28, there was a trend toward reduced RNA in distal joint tissues of animals treated with anti-CHIKV mAb,

although this did not attain statistical significance (Fig. 3.3C; $P = 0.2$). Collectively, these results show that treatment with an anti-CHIKV mAb (alone or in combination with CTLA4-Ig) rapidly eliminates infectious virus within 2 days and reduces but fails to clear viral RNA in affected tissues.

Cytokine and chemokine analysis in CHIKV-infected mice treated with CTLA4-Ig and anti-CHIKV mAb. To begin to define the basis for reduced joint swelling associated with treatment, we analyzed the effects on local cytokine and chemokine production. Using a multiplexed assay, we measured cytokine and chemokine levels in the ipsilateral foot on day 7 after infection in animals that received either control mAb, CTLA4-Ig, anti-CHIKV mAb, or combination therapy with CTLA4-Ig and anti-CHIKV mAb. Monotherapy with CTLA4-Ig reduced levels of CXCL10 and macrophage inflammatory protein-1 β (MIP-1 β) (Fig. 3.4, A and B; $P < 0.05$), whereas treatment with anti-CHIKV mAb reduced levels of MCP-1 (Fig. 3.4C; $P < 0.05$). In comparison, combination therapy had more profound anti-inflammatory effects and resulted in decreased levels of many of the measured chemokines (for example, KC, CXCL10, MCP-1, MIP-1 β , and RANTES; Fig. 3.4, A to I; $P < 0.05$) in the joint tissue.

Histological and immune infiltrate analysis of the ipsilateral midfoot joints in CHIKV-infected mice treated with CTLA4-Ig and anti-CHIKV mAb. Histological analysis of joint tissues in the ipsilateral foot revealed reduced leukocyte infiltration into the midfoot joints of mice receiving CTLA4-Ig and combination therapy with CTLA4-Ig and anti-CHIKV mAb (Fig. 3.5, A to F; yellow arrows, moderate to severe synovitis; white arrows, absent or mild synovitis). We next quantitated the number of inflammatory cells per high-power field (HPF) in the synovial space of the midfoot. CTLA4-Ig and combination therapy with CTLA4-Ig and anti-CHIKV mAb resulted in decreased inflammatory cell infiltration into the synovial space (52 cells per HPF in the

control group, 22 cells per HPF in CTLA4-Ig group, and 9 cells per HPF in the CTLA4-Ig + anti-CHIKV mAb group, $P < 0.05$ and $P < 0.0001$, respectively). Histological analysis did not reveal evidence of bone erosion, proteoglycan loss, or effects on expression of receptor activator of nuclear factor kappa-B ligand (RANKL) and osteoprotegerin (OPG) (fig. S3.1). Consistent with a role for CTLA4-Ig in modulating immune cell recruitment, administration of CTLA4-Ig 1 day before infection resulted in reduced swelling on day 7 but not on day 3 (fig. S3.2), a time point at which subcutaneous edema but not immune cell infiltration is observed. To quantitate differences in immune cell infiltration into the entire foot at day 7 after infection, we analyzed by flow cytometry how CTLA4-Ig and anti-CHIKV mAb treatments affected the total numbers of immune cells in the soft tissues of the ipsilateral foot, which included the skin, muscle, and joints. After treatment with CTLA4-Ig or a combination of CTLA4-Ig and anti-CHIKV mAb, we observed about a three- to fourfold reduction in the number of total $CD45^+$ leukocytes (Fig. 3.6, A and B; $P < 0.0005$) with markedly reduced numbers of $Ly6C^+CD11b^+$ inflammatory monocytes, natural killer cells, and $CD8^+$ T cells, and a nearly complete absence of $CD4^+$ T cells (Fig. 3.6, B to G). By contrast, treatment with the anti-CHIKV mAb alone did not reduce the number of infiltrating $CD45^+$ cells or individual leukocyte subsets into the infected foot (Fig. 3.6, A to G).

Clinical assessment of the response to CTLA4-Ig treatment in CHIKV-infected WT and $TCR\beta\delta^{-/-}$ mice. CTLA4-Ig blocks T cell costimulation, but it can also have immunomodulatory effects on antigen-presenting cells (APCs)^{194,196}. Human CTLA4-Ig, which was used in our studies, binds murine B7.1 and B7.2 antigens and can modulate APC function^{197,198}. We assessed APC activation on day 7 after infection but saw no difference in CD80, CD86, and class II major histocompatibility complex marker expression in APCs isolated from the spleen and feet of control and CTLA4-Ig-treated mice (fig. S3.3). To test whether CTLA4-Ig

exerted its therapeutic benefits via T cells, we compared the response to CTLA4-Ig and a control mAb in CHIKV-infected WT and *TCRβδ*^{-/-} mice, the latter of which lack both αβ and γδ T cells. As we observed a beneficial effect of CTLA4-Ig in WT animals (Fig. 3.7, A and C; P < 0.005) but not in *TCRβδ*^{-/-} mice (Fig. 3.7, B and C; P > 0.9), CTLA4-Ig reduces swelling during acute CHIKV infection in part via its action on T cells.

3.4 Discussion

The worldwide emergence of CHIKV has created a need to identify treatments, as epidemiological estimates suggest there are millions suffering from acute arthritis and at least ~400,000 people in the Western Hemisphere suffering from chronic CHIKV arthritis^{22,180}. We reasoned that established therapies used to treat other forms of inflammatory arthritis (for example, rheumatoid or psoriatic arthritis) also might mitigate CHIKV arthritis. Our experiments identified CTLA4-Ig and tofacitinib as candidate DMARD therapies based on efficacy against acute CHIKV arthritis in mice.

Immunopathology likely contributes to the pathogenesis of CHIKV arthritis. Previous studies using *Rag2*^{-/-} animals suggested that the response depends on B and T cells, because *Rag2*^{-/-} animals had no ipsilateral foot swelling⁷⁹. Leukocyte subsets infiltrating the peripheral joints of CHIKV-infected mice primarily consist of T cells, inflammatory monocytes, and macrophages⁵². When we blocked T cell costimulation with CTLA4-Ig, we observed reduced infiltration of T cells and inflammatory monocytes into the joints of infected animals, although this was not sufficient to eliminate the clinical disease completely. Treatment of *TCRβδ*^{-/-} mice with CTLA4-Ig had no effect on joint swelling, suggesting that CTLA4-Ig ameliorates clinical disease primarily via its action on T cells. These findings are consistent with previous studies

suggesting that joint swelling in the foot of $CD4^{-/-}$ animals is reduced in severity but not completely controlled⁷⁹. Our findings suggest that other inhibitors of $CD4^+$ T cell function also might limit musculoskeletal disease associated with CHIKV infection. Teo et al. recently demonstrated that treatment with fingolimod, an agonist of the sphingosine 1-phosphate receptor, limited infiltration of $CD4^+$ T cells into CHIKV-infected joints and adjacent muscle in mice, resulting in reduced joint swelling and muscle necrosis¹⁹⁹.

Previous studies showed that mouse and human antiviral antibodies could prevent CHIKV arthritis in mice when administered before infection or protect against lethality in highly immunocompromised *Ifnar1*^{-/-} mice^{28,54,192}. We found that treatment of WT mice 3 days after CHIKV infection with an antiviral human mAb reduced but did not eliminate joint swelling, although infectious virus could not be detected in the joints within 2 days of therapy. Foot swelling likely depends on multiple factors including synovitis, myositis, and edema resulting from production of proinflammatory cytokines⁵². The anti-CHIKV mAb eliminated infectious virus within 2 days of its administration and reduced foot swelling without altering leukocyte infiltration into joints of infected animals, suggesting that leukocyte recruitment is not the only factor that affects disease severity in this model. Local cytokine production in specific compartments (for example, serum, muscles, or joints) independently may affect the virus-induced swelling or edema. Future histological studies may define better the precise mechanism by which neutralization of infectious CHIKV by antiviral antibodies ameliorates foot swelling.

The type I interferon (IFN-I) response is important in controlling CHIKV infection. *Ifnar1*^{-/-} mice lacking type I IFN signaling are highly vulnerable to disseminated infection with CHIKV and succumb within days due to high levels of virus in the brain and spinal cord⁵⁶. Remarkably, treatment with tofacitinib, which blocks JAK/STAT signaling that is downstream of

IFNAR1 and other cytokine receptors, reduced clinical disease without ostensible effects on morbidity or mortality. This result may be related to the pharmacodynamics of tofacitinib including its short half-life¹⁸⁶. Tofacitinib therapy may blunt cytokine production and/or leukocyte infiltration without enhancement of CHIKV replication. Nevertheless, because tofacitinib is known to enhance the risk of some viral infections, including varicella zoster virus, future combination therapy studies with tofacitinib and an antiviral mAb may be warranted²⁰⁰.

Anecdotal reports in humans have suggested that methotrexate may be effective for treatment of CHIKV arthritis^{188,201}. In our studies, a low dose of methotrexate did not provide benefit against acute arthritis. It remains possible that methotrexate would show greater benefit if higher doses were used. Mouse models of Ross River virus arthritis previously revealed exacerbation of disease after treatment with etanercept, whereas an uncontrolled study in humans suggested that blockade of TNF- α provided some benefit in 13 patients who were diagnosed with a “chronic rheumatologic disease” after acute CHIKV infection^{201,202}. However, it is important to note that some patients infected with CHIKV may develop rheumatologic disease sporadically or coincidentally after CHIKV infection. In a controlled study of mice infected with CHIKV, we did not find a benefit of etanercept therapy with acute CHIKV arthritis, but we were unable to assess chronic disease because of the histopathological absence of frank arthritis during the chronic phase. In light of our animal model results and the anecdotal nature of previous human studies, it seems that rigorous, blinded, placebo-controlled studies in human patients are necessary to define which DMARD therapies may be safe and optimal in patients with chronic CHIKV arthritis.

CHIKV and related arthritogenic alphaviruses directly invade the joints and leave persistent viral RNA in the joints and surrounding tissues even in the absence of detectable infectious virus⁵⁴. In previous studies, we found that most CHIKV-infected control C57BL/6 mice

did not exhibit histopathological evidence of chronic arthritis 1 month after infection, although there was mild chronic tenosynovitis and myositis in some animals⁵². Because we could readily detect viral RNA in the joints at day 28, our studies suggest that persistent viral RNA may not be sufficient to cause clinically apparent chronic arthritis in mice and that other factors must contribute to pathogenesis. Thus, it remains to be determined whether our combination treatment with an antiviral antibody and CTLA4-Ig has beneficial effects in chronic CHIKV arthritis. Other animal models with more severe chronic disease (for example, nonhuman primates) may be required to address these questions.

The beneficial effects of CTLA4-Ig and antiviral antibody therapy on CHIKV arthritis must be interpreted with caution because there are limitations with the mouse model. Unlike humans, mice are not natural hosts for CHIKV and therefore do not develop the severe, debilitating arthritis that is commonly observed in humans. Because CHIKV causes less severe disease in mice, it remains possible that immunomodulatory therapies, including CTLA4-Ig, may have no or even deleterious effects in humans.

The concept of combination antiviral and immunomodulatory therapy is a unique approach for the treatment of infectious diseases. The near-complete effectiveness of combination therapy in our mouse model of acute CHIKV arthritis has implications for treatment of other viral infections in which both virus- and immune-mediated pathology result in morbidity and mortality (for example, influenza and severe acute respiratory syndrome coronavirus). Given the large number of clinically available biological and small molecular DMARDs, this work may provide greater impetus for studies that test combination antiviral and immunomodulatory therapies for the treatment of infectious diseases.

3.5 Materials and Methods

Study design

We initiated this study to determine whether anti-inflammatory and antiviral therapy control acute CHIKV arthritis in mice. Our initial observation was that treatment with antiviral antibody reduced infectious viral burden in the ipsilateral joint and that therapy with CTLA4-Ig diminished recruitment of T cells and inflammatory monocytes as well as the accumulation of proinflammatory cytokines. Subsequent histological analysis confirmed these findings. We measured viral titers and RNA in tissues, immunologic parameters (including influx of specific cell subtypes into the joints and surrounding tissues), and cytokine levels. Sample sizes and end points were selected on the basis of our extensive experience with these systems. Mice were age- and sex-matched between groups. Histological analysis was performed in a blinded fashion. Initial footpad measurements were performed by three individuals in an unblinded fashion. However, the measurements after CTLA4-Ig treatment were reproduced by a fourth individual who performed a blinded assessment. Investigators were not blinded when conducting virus tissue burden analysis, cytokine measurements, or flow cytometry analysis.

Mouse experiments

All animal experiments were performed in accordance and with approval of Washington University Institutional Animal Care and Use Committee guidelines, and all mouse infection studies were performed in an animal biosafety level 3 laboratory. All experiments were performed with 4-week-old C57BL/6 mice or with $TCR\beta\delta^{-/-}$ mice that were obtained commercially (The Jackson Laboratories).

Virus infection studies

A recombinant LR2006 OPY1 strain of CHIKV was provided by S. Higgs (Kansas State University) and generated from in vitro transcribed cDNA, as previously described¹⁷⁷. At 4 weeks of age, mice were inoculated in the left rear footpad with 10^3 FFU of the LR2006 OPY1 strain of CHIKV in a volume of 10 μ l. Infected mice were monitored daily for foot swelling with digital calipers for 28 days. At the termination of experiments, mice were sedated with a ketamine-xylazene cocktail and euthanized, and perfused via intracardiac injection with PBS. Tissues (injected left ankle, contralateral ankle, and ipsilateral wrist) were harvested and snap-frozen on dry ice and stored at -80°C until processing for RNA isolation. For serum analysis, blood was collected at the time of sacrifice and centrifuged for 10 min at 10,000g and stored at -80°C . In some experiments, serum and joint tissues were isolated from mice on day 5 after infection for subsequent analysis by focus-forming assay.

Tissue viral burden analysis

Focus-forming assays were performed as previously described¹⁹². Briefly, tissue homogenates or serum were incubated for 90 min on a monolayer of Vero cells in 96-well plates, and then cells were overlaid with 1% (w/v) methylcellulose in modified Eagle media supplemented with 4% fetal bovine serum (FBS). Plates were harvested 18 to 24 hours later and fixed with 1% paraformaldehyde (PFA) in PBS. The plates were incubated sequentially with chimeric CHK-9 (500 ng/ml)¹⁹² and horseradish peroxidase-conjugated goat anti-human IgG in PBS supplemented with 0.1% saponin and 0.1% bovine serum albumin. CHIKV-infected foci were visualized using TrueBlue peroxidase substrate (KPL) and quantitated on an ImmunoSpot 5.0.37 macroanalyzer (Cellular Technologies Ltd).

Real-time qRT-PCR analysis

RNA was extracted from tissue using the RNeasy Mini Kit (Qiagen). The quantity of CHIKV RNA was determined by qRT-PCR using the TaqMan RNA-to-CT 1-Step Kit (Applied Biosystems) with an E1-specific primer/probe set²⁰³. Two microliters of the isolated RNA was analyzed by qRT-PCR and compared to a standard curve generated from RNA isolated from a CHIKV stock to determine FFU equivalents.

Therapeutic agents

4N12 is a human IgG1 mAb that neutralizes CHIKV infection and has been described previously²⁸. Antibody was purified from hybridoma supernatants by protein G affinity chromatography. Methotrexate, CTLA4-Ig (abatacept), and etanercept were obtained from the Center for Advanced Medicine Rheumatology Clinic (St. Louis, MO). Naproxen sodium and methylprednisolone acetate were purchased from Sigma. The isotype control antibody [humanized anti-West Nile virus antibody (E16)] was produced in Chinese hamster ovary cells and purified by protein G affinity chromatography²⁰⁴.

Histopathological analysis

Infected mice were sacrificed and perfused by intracardiac injection of 4% PFA at the indicated days after infection. The infected ankle/foot tissue was dissected and fixed in 4% PFA/PBS for 48 hours, followed by decalcification in 14% acid-free EDTA for 10 to 14 days. Decalcified tissues were embedded in paraffin, and 5- μ m sections were stained with hematoxylin and eosin (H&E) and evaluated by light microscopy. Embedding, sectioning, and staining were performed by the Musculoskeletal Histology and Morphometry Core at Washington University School of Medicine. All samples were visualized using a Nikon Eclipse microscope equipped with a QICAM 12-bit camera (QImaging) and processed with QCapture software using the same exposure times.

Cytokine/chemokine analysis

Ankles were harvested from euthanized infected mice at day 7 and collected in 500- μ l PBS and homogenized using a MagNA Lyser (Roche). Cytokine levels were measured using Luminex technology with a Bio-Plex Pro mouse cytokine 13-plex assay (Millipore).

Immune cell analysis

Mice were sacrificed 7 days after inoculation and perfused with PBS. The inoculated foot was disarticulated at the ankle without fracturing the bone. Cutaneous and subcutaneous tissue were everted but still attached to the distal foot and digits during digestion. Tissues were incubated for 2 hours at 37°C in digestion buffer [RPMI, type I collagenase (2.5 mg/ml) (Sigma), DNase I (10 mg/ml) (Sigma), 15 mM HEPES, 10% FBS]. Digested tissues were passed through a 70- μ m cell strainer. The number of viable cells was quantified by trypan blue staining. Isolated cells were incubated with anti-mouse CD16/CD32 (Clone 93; BioLegend) for 10 min at 4°C and then surface-stained in PBS containing 5% FBS for 30 min at 4°C with the following antibodies: anti-CD3e-FITC (fluorescein isothiocyanate) (eBioscience), anti-CD4-PE (phycoerythrin) (BD Biosciences), anti-CD8a-PerCP/Cy5.5 (BioLegend), anti-NK1.1-PE/Cy7 (BioLegend), anti-CD45-Brilliant Violet 605 (BioLegend), anti-Ly6C-Brilliant Violet 421 (BD Biosciences), anti-Ly6G-Alexa Fluor 700 (BioLegend), and anti-CD19-APC/Cy7 (BioLegend). Cells were washed and incubated at room temperature for 30 min in Foxp3 Fixation/Permeabilization buffer (eBioscience). The fixed cells were washed with Permeabilization buffer (eBioscience) and stained in Permeabilization buffer overnight at 4°C with anti-Foxp3-Alexa Fluor 647 (BioLegend). Cells were run on a LSR II (Becton Dickinson) flow cytometer and analyzed using BD FACSDiva and FlowJo software.

Statistical analysis

All data were analyzed with GraphPad Prism software. For viral burden analysis, cytokine measurements, and numbers of infiltrating leukocytes, data were analyzed by the Mann-Whitney test, ANOVA, or Kruskal-Wallis test with a Dunn's post hoc analysis. $P < 0.05$ indicated statistically significant differences.

Acknowledgments: We thank G. Sapparapu, P. Matta, H. King, and R. Lampley (Vanderbilt University) for technical support. **Funding:** This work was supported by grants from the NIH (R01 AI073755 and R01 AI104972 to M.S.D., and R01 AI114816 to J.E.C. and M.S.D.) and the Rheumatology Research Foundation (Innovative Research Grant to D.J.L.). J.J.M. was supported by a Rheumatology Research Foundation Scientist Development Award. A.R.Y. was supported by a NIGMS Cellular, Biochemical, and Molecular (CMB) Sciences Predoctoral Research Training Grant (GM: 007 067). Histological sections were prepared by the Washington University Musculoskeletal Research Center (NIH P30 AR057235).

3.6 Figures

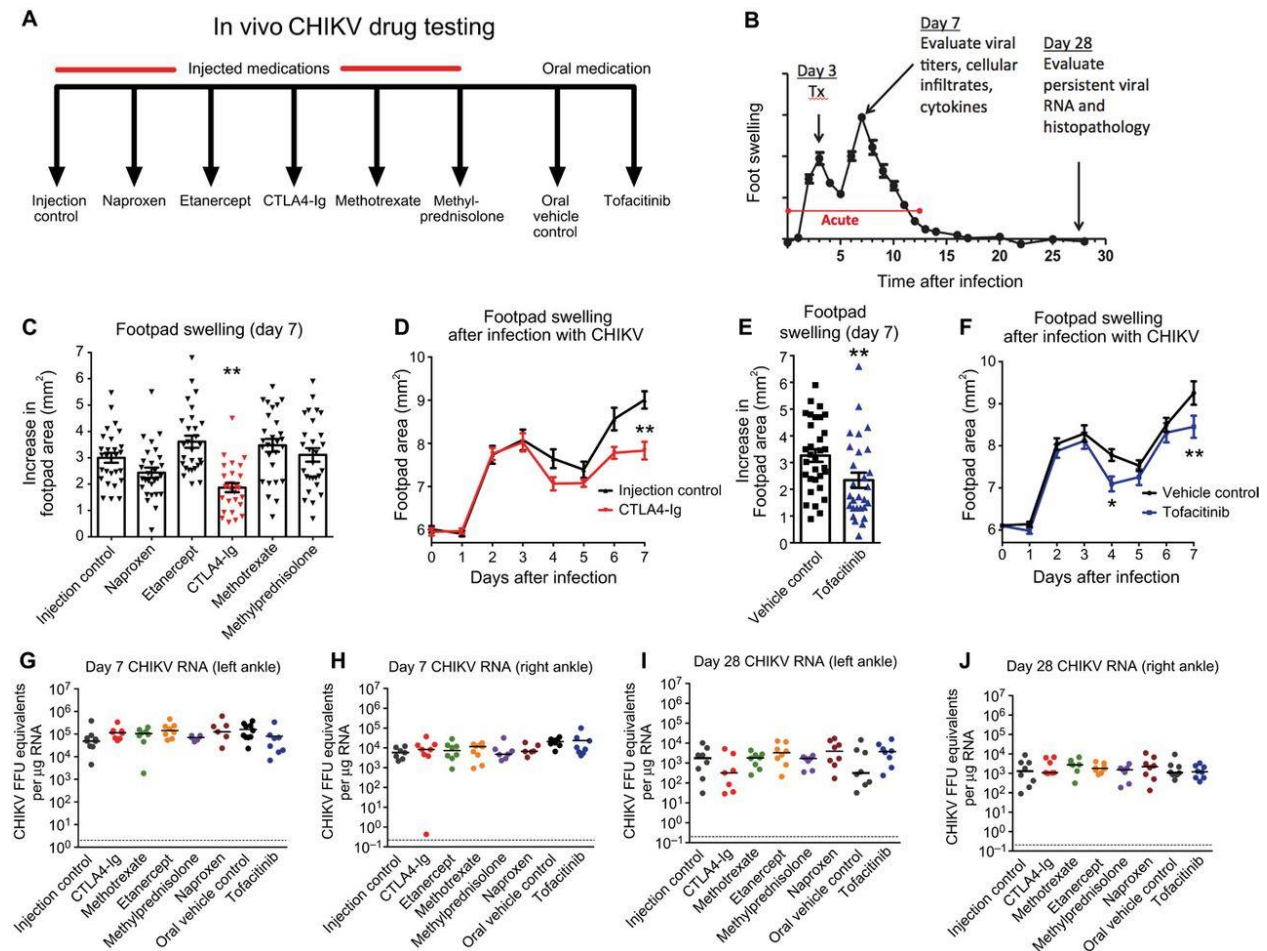


Figure 3.1 Screen of candidate oral and biological DMARDs for treatment of acute CHIKV arthritis in mice

Mice were inoculated with 10^3 FFU of CHIKV via a subcutaneous route. (A) Schematic depicting the two controls and six treatment arms. Medications and doses were methylprednisolone (0.5 mg/kg, IP) daily from 3-7 dpi, naproxen (10 mg/kg, IP) daily from 3-7 dpi, methotrexate (0.3 mg/kg, IP) once weekly (2 doses: 3, 10 dpi), etanercept (300 μ g, IP) 1 dose on day 3, CTLA4-Ig (300 μ g, IP) 1 dose on day 3, and tofacitinib (50 mg/kg) oral gavage daily from 3-7 dpi. For subsequent studies of CTLA4-Ig, an isotype control antibody was used. (B) Experimental design included treatment at 3 dpi and harvests on 7 and 28 dpi for the indicated analyses. Throughout the time course, foot swelling was measured using digital calipers. (C) Foot swelling (area in mm^2) on day 7 compared to day 0 for all injected therapies. (D) Foot swelling over time for injection control and CTLA4-Ig-treated animals. (E) Foot swelling on day 7 compared to day 0 for tofacitinib and oral vehicle control. (F) Foot swelling over time for oral vehicle control and tofacitinib-treated animals. (G to J) qRT-PCR analysis of viral RNA levels in the left and right ankles at 7 and 28 dpi for all treatment groups. Results in (C) to (J) are from at least two independent experiments with $n = 28$ per treatment group for measurement data from days 0 to 7 and $n = 7-8$ for viral burden analysis on days 7 and 28. Data represent the means (C to F) or median (G to J) \pm SEM. * $P < 0.05$, ** $P < 0.005$, **** $P < 0.0001$ [two-way ANOVA for analysis of swelling curves, Mann-Whitney for day 7 tofacitinib analysis, and Kruskal-Wallis with Dunn's post hoc analysis for day 7 injected medication and viral burden analysis].

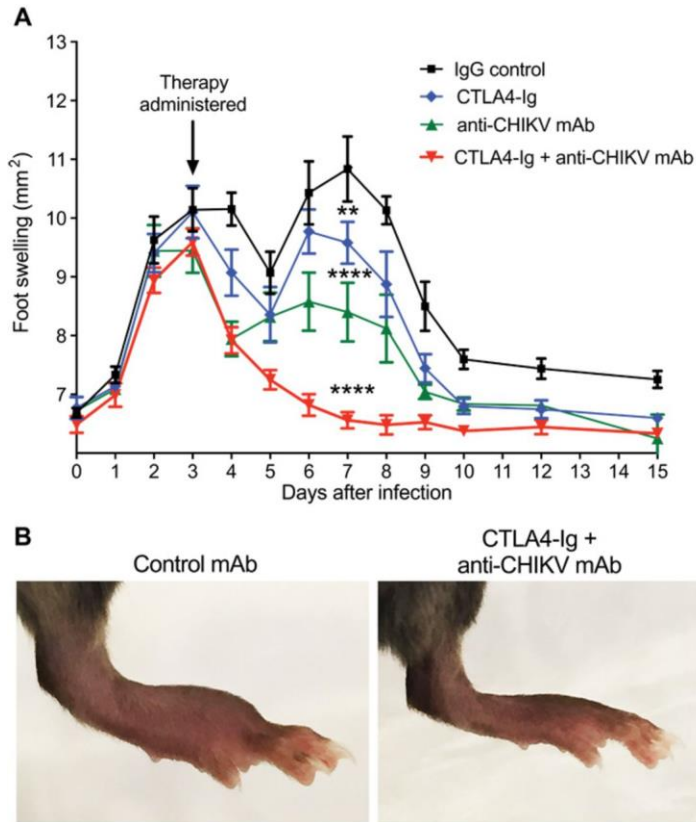


Figure 3.2 Combination therapy with CTLA4-Ig and an anti-CHIKV human mAb ameliorates acute CHIKV arthritis in mice

Mice were inoculated with 10^3 FFU of CHIKV via a subcutaneous route. (A) Foot swelling (area in mm^2) from day 0 through day 15 in mice receiving at day 3 a single IP injection of 600 μg of isotype control antibody, 300 μg of CTLA4-Ig, 300 μg of anti-CHIKV mAb (4N12), or a combination of 300 μg of CTLA4-Ig and 300 μg of anti-CHIKV mAb. Data are pooled from two independent experiments ($n = 15$ to 19 animals per group). (B) Representative photographs of ipsilateral foot swelling in the control mAb or combination therapy (CTLA4-Ig + anti-CHIKV mAb) groups. Data represent the means \pm SEM. $**P < 0.005$, $****P < 0.0001$ (two-way ANOVA with multiple comparisons).

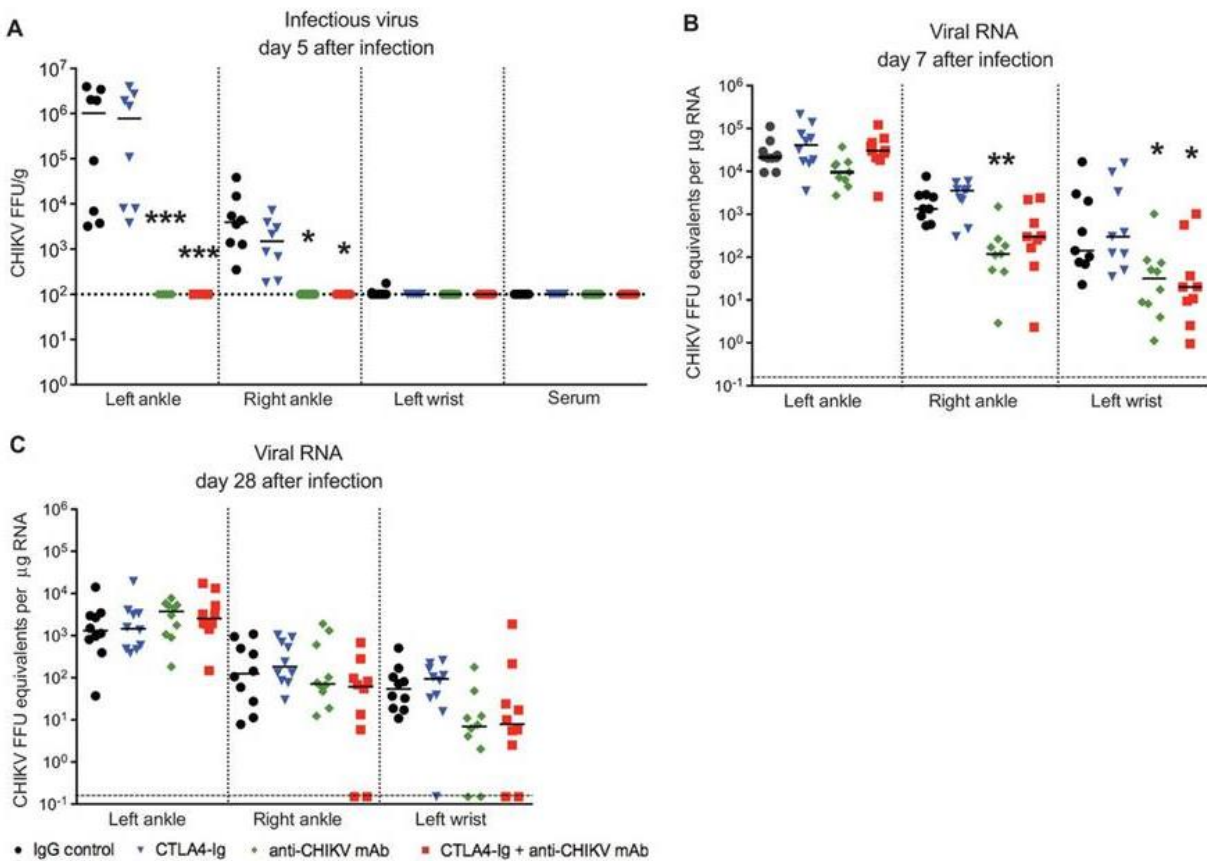


Figure 3.3 Viral burden in CHIKV-infected mice treated with CTLA4-Ig and anti-CHIKV mAb

Mice were inoculated with 10^3 FFU of CHIKV via a subcutaneous route. Mice received at day 3 a single IP injection of 600 µg of isotype control antibody, 300 µg of CTLA4-Ig, 300 µg of anti-CHIKV mAb, or a combination of 300 µg of CTLA4-Ig and 300 µg of anti-CHIKV mAb. (A) Infectious virus in joints and serum quantitated by focus-forming assay on day 5 after infection. (B and C) Real-time qRT-PCR analysis of viral RNA levels in the ipsilateral (left) and contralateral (right) ankles and left wrist at days 7 and 28 after infection. Results are pooled from two independent experiments with $n = 10$ per treatment group for viral RNA data and $n = 8$ for focus-forming assay data. Data represent the median \pm SEM. * $P < 0.05$, ** $P < 0.005$, *** $P < 0.0005$ (Kruskal-Wallis with Dunn's post hoc analysis).

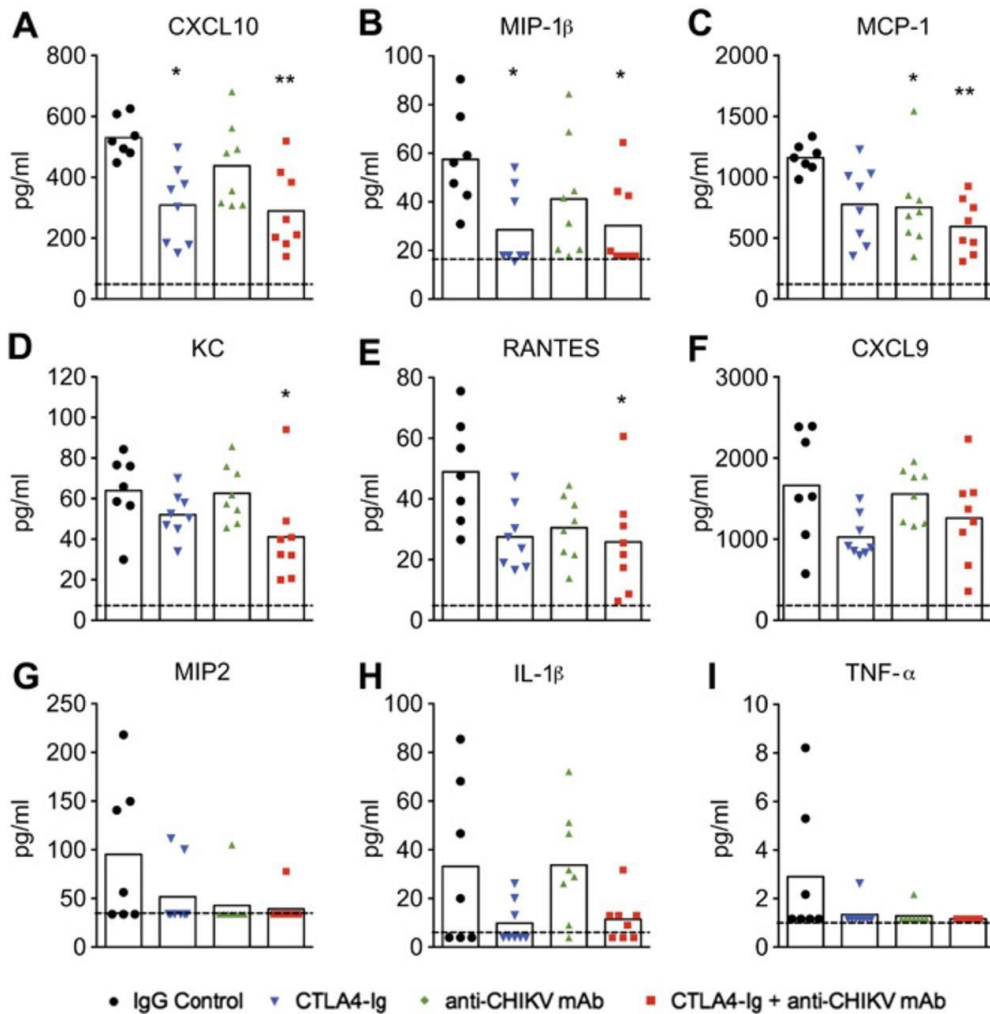


Figure 3.4 Cytokine and chemokine analysis in CHIKV-infected mice treated with CTLA4-Ig and anti-CHIKV mAb

Mice were inoculated with 10^3 FFU of CHIKV via a subcutaneous route. Mice received at day 3 a single IP injection of 600 μ g of isotype control antibody, 300 μ g of CTLA4-Ig, 300 μ g of anti-CHIKV mAb, or a combination of 300 μ g of CTLA4-Ig and 300 μ g of anti-CHIKV mAb. (A to I) Cytokine and chemokine levels on day 7 in the ipsilateral foot of mice in each treatment group. Analytes included CXCL10 (A), MIP-1 β (B), MCP-1 (C), KC (D), RANTES (E), CXCL9 (F), MIP2 (G), IL-1 β (H), and TNF- α (I). Results are pooled from two independent experiments with $n = 8$ mice per treatment group. Data represent the means \pm SEM. * $P < 0.05$, ** $P < 0.005$ (Kruskal-Wallis with Dunn's post hoc analysis).

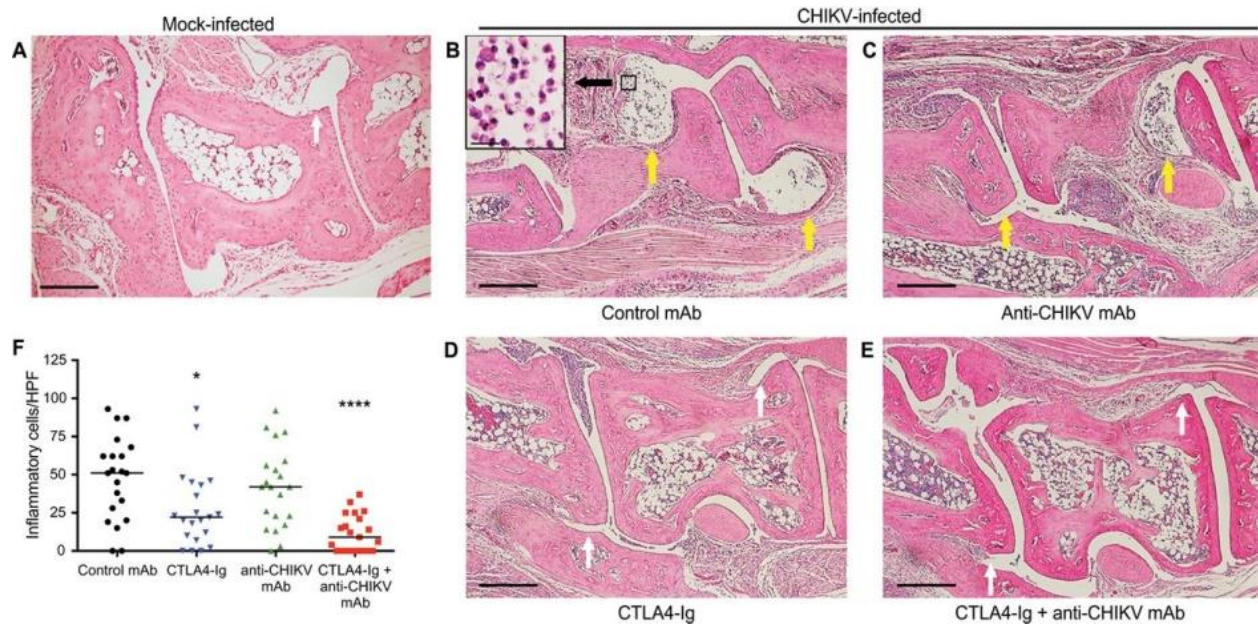


Figure 3.5 Representative H&E staining of the ipsilateral midfoot joints in CHIKV-infected mice treated with CTLA4-Ig and anti-CHIKV mAb

(A to F) Mice were inoculated with either PBS (A; mock) or 10^3 FFU of CHIKV (B to F) via a subcutaneous route. Animals were sacrificed, and histology of the ipsilateral foot was performed on day 7 after infection. CHIKV-infected mice received at day 3 a single intraperitoneal injection of 600 μ g of isotype control antibody (B), 300 μ g of anti-CHIKV mAb (C), 300 μ g of CTLA4-Ig (D), or a combination of 300 μ g of CTLA4-Ig and 300 μ g of anti-CHIKV mAb (E). The number of inflammatory cells per HPF in the midfoot synovial space was quantitated in a blinded fashion (F). Results are representative of at least two independent experiments with $n = 4$ per treatment group and two sections assessed per foot. Scale bars, 200 μ m. Yellow arrows, moderate to severe synovitis; white arrows, absent or mild synovitis * $P < 0.05$, **** $P < 0.0001$ (Kruskal-Wallis with Dunn's post hoc analysis).

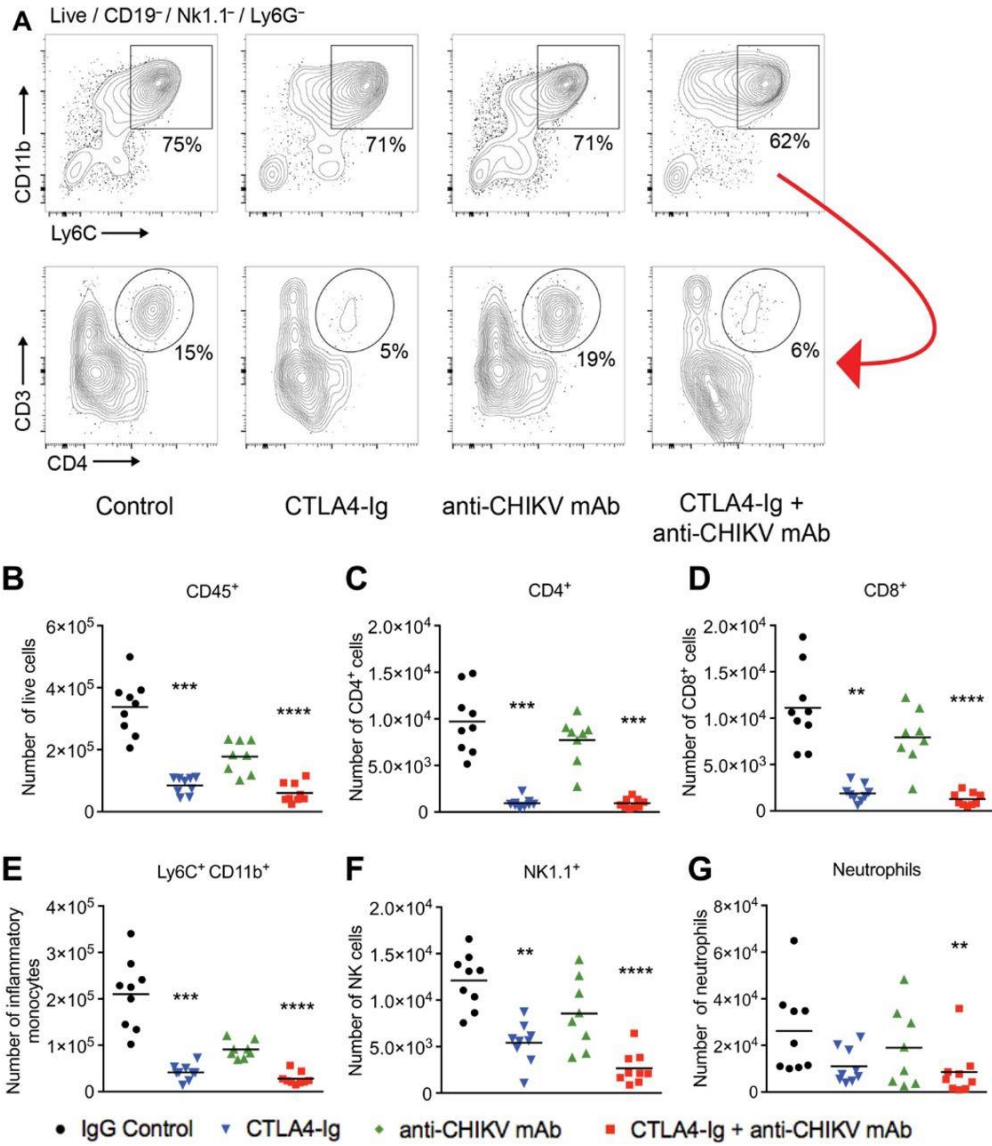


Figure 3.6 Flow cytometry analysis of infiltrating leukocytes in the feet of mice on day 7 after infection with CHIKV

Mice were inoculated with 10^3 FFU of CHIKV via a subcutaneous route. Mice received at day 3 a single intraperitoneal injection of 600 μ g of isotype control antibody, 300 μ g of CTLA4-Ig, 300 μ g of anti-CHIKV mAb, or 300 μ g of CTLA4-Ig and 300 μ g of anti-CHIKV mAb. (A) Gating strategy showing subpopulations of live $CD45^+$ cells, including the percentages of $CD11b^+Ly6C^+$ inflammatory monocytes, followed by CD3 and CD4 expression (lower panel) in the remaining Ly6C-negative cells (red arrow) isolated from the feet of mice from each treatment group. (B to G) Total number of isolated $CD45^+$, $CD4^+$, $CD8^+$, $Ly6C^+CD11b^+$, $NK1.1^+$, and $Ly6G^+$ cells from the feet of CHIKV-infected mice in each treatment group. Results are pooled from two independent experiments with 4 to 5 mice per group in each experiment. Data represent the means \pm SEM. ** $P < 0.005$, *** $P < 0.0005$, **** $P < 0.0001$ (Kruskal-Wallis with Dunn's post hoc analysis).

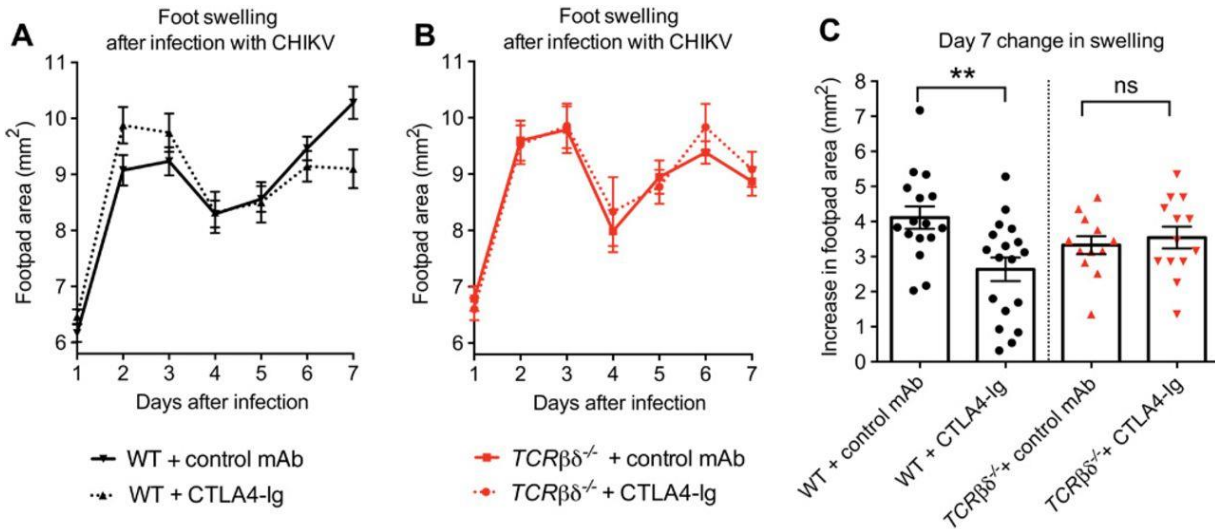


Figure 3.7 Clinical assessment of the response to CTLA4-Ig treatment in CHIKV-infected WT and $TCR\beta\delta^{-/-}$ mice

Mice were inoculated with 10^3 FFU of CHIKV via a subcutaneous route. (**A** and **B**) Foot swelling in WT (**A**) and $TCR\beta\delta^{-/-}$ (**B**) mice from day 1 through 7 in mice receiving at day 3 a single IP injection of 300 μ g of isotype control antibody or 300 μ g of CTLA4-Ig. (**C**) Increase in foot swelling (area in square millimeter) on day 7 after infection in control- and CTLA4-Ig-treated WT and $TCR\beta\delta^{-/-}$ mice. ns, not significant. Measurements were conducted in a blinded fashion. Results are pooled from two or three independent experiments with total $n = 16$ to 18 per group for WT animals and $n = 12$ to 13 per group for $TCR\beta\delta^{-/-}$ animals. Data represent the means \pm SEM. $**P < 0.005$ (two-way ANOVA with multiple comparisons for swelling curves; Mann-Whitney test for day 7 swelling).

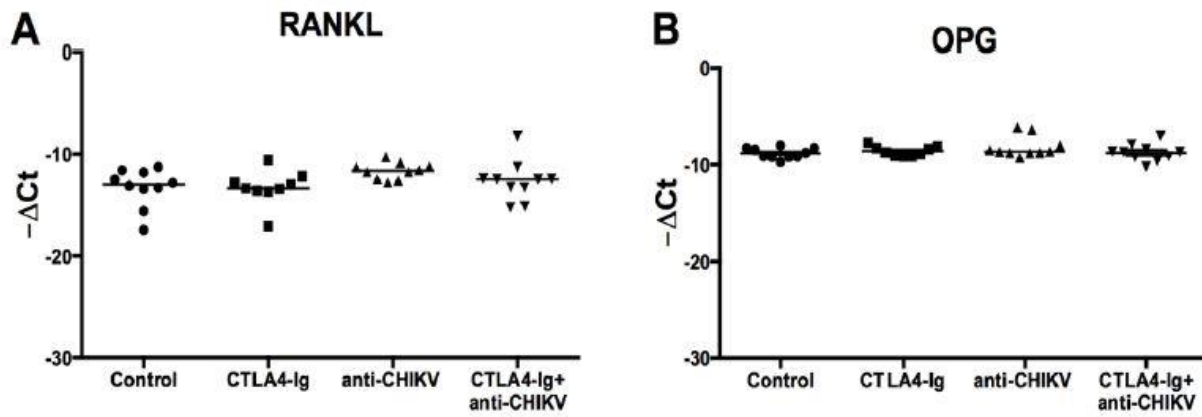


Figure S3.1 RANKL and OPG expression in CHIKV-infected joints

Mice were inoculated with 10^3 FFU of CHIKV via a subcutaneous route. At day 3 after infection, a single IP injection of 600 μ g of isotype control antibody, 300 μ g of CTLA4-Ig, 300 μ g of anti-CHIKV mAb, or a combination of 300 μ g CTLA4-Ig and 300 μ g anti-CHIKV mAb was administered. On day 7 after infection, RNA was isolated from the left foot. RANKL (**A**) and OPG (**B**) expression were measured by qRT-PCR and normalized to GAPDH. Data were pooled from two independent experiments ($n = 10$ animals per group) and analyzed by ANOVA with a multiple comparisons test. $P > 0.1$ for all groups.

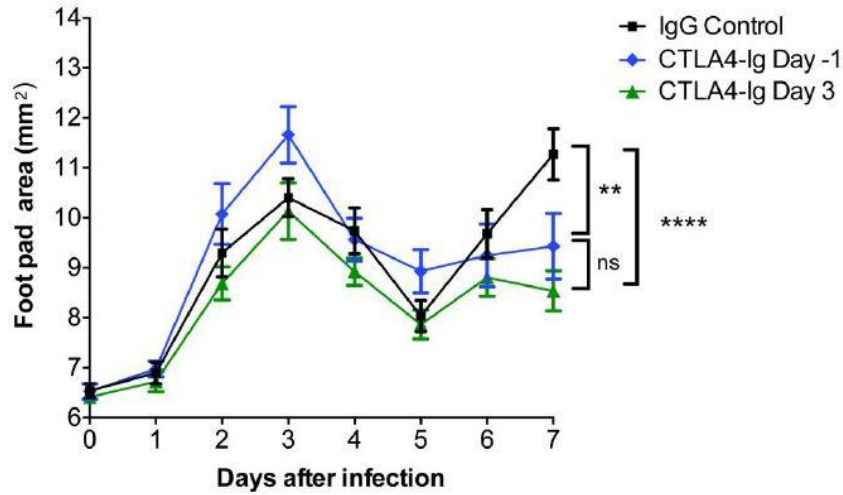


Figure S3.2 Foot swelling with CTLA4-Ig therapy administered before or during CHIKV infection

Five week-old mice were inoculated with 10^3 FFU of CHIKV via a subcutaneous route. (A) Foot swelling (area in mm^2) from day 0 through day 7 in mice receiving a single IP injection of 300 μg of isotype control antibody or 300 μg of CTLA4-Ig at day -1 or day 3. Data are pooled from two independent experiments ($n = 9$ or 10 animals per group). Data represent the mean \pm SEM. **, $P < 0.005$; **** $P < 0.0001$ (2-way ANOVA with multiple comparisons test).

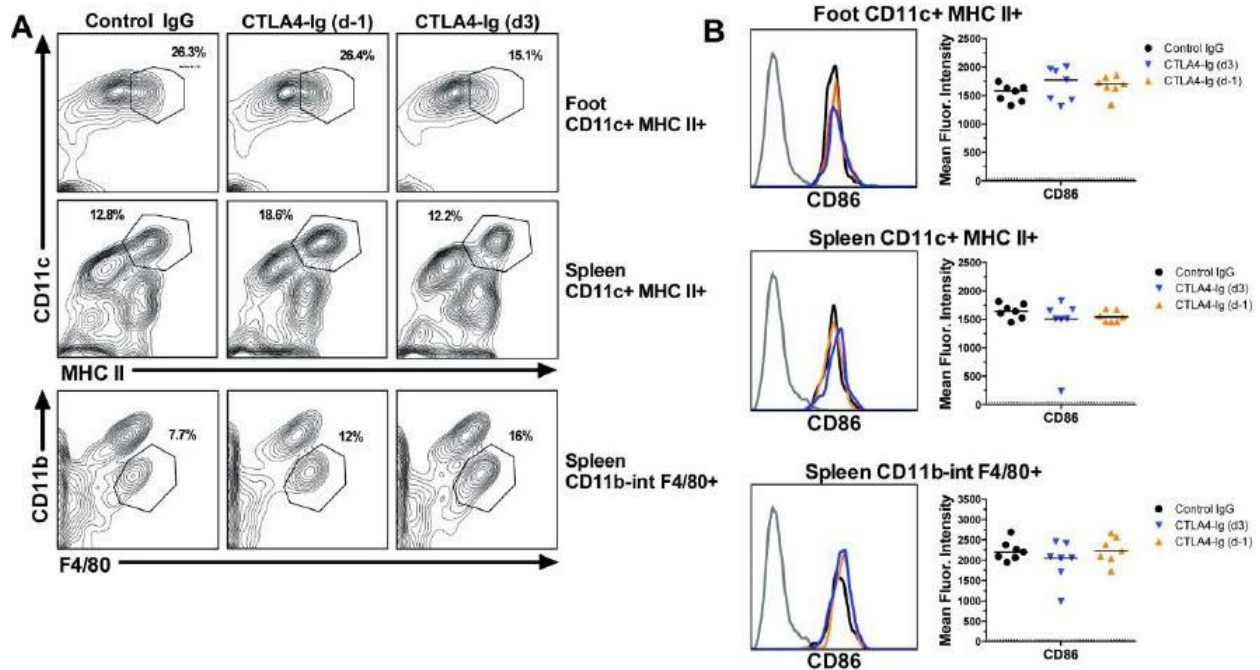


Figure S3.3 Flow cytometry analysis of APC activation in the spleen and ankles of mice on day 7 after infection with CHIKV

Mice were inoculated with 103 FFU of CHIKV via a subcutaneous route. Mice received at day 3 a single IP injection of 300 µg of isotype control antibody 300 µg of CTLA4-Ig on either day -1 or day 3 after infection. (A) Representative contour plots showing the percentages of CD11c⁺MHCII⁺ dendritic cells and CD11b^{int}F4/80⁺ macrophages in the left foot and spleen of infected animals from each treatment group. (B) Representative histograms (left panel) and geometric mean fluorescence intensity of CD86 expression on CD11c⁺MHCII⁺ dendritic cells and CD11b^{int}F4/80⁺ macrophages in the left foot and spleen of infected animals from each treatment group. Results are pooled from two independent experiments with 3 to 4 mice per group per experiment. No statistically significant differences were observed in the treatment groups (Kruskal-Wallis with Dunn's post-hoc analysis).

Chapter 4

Summary and Future Directions

4.1 Summary

CHIKV has rapidly emerged as a global pathogen in little more than a decade, ultimately infecting millions of people worldwide. Infected individuals experience debilitating myalgia and polyarthritis that can persist for months to years after infection. An IFN-I response is absolutely required to control CHIKV and other alphavirus infections. IFN-Is are composed of 14 IFN- α subtypes and single forms of IFN- β , IFN- ϵ , IFN- κ , and IFN- ω , and despite their central role in protection against CHIKV, little is known about the biological roles of individual IFN-I subtypes during viral infection.

We evaluated the pathogenesis of CHIKV in mice that lack either IFN- α (through IRF7 knockout or IFN- α blocking mAb) or IFN- β (through IFN- β knockout or IFN- β blocking mAb). We demonstrated that loss of IFN- α greatly impacted CHIKV replication and dissemination. In contrast, loss of IFN- β exacerbated acute CHIKV disease but without having much impact on viral loads, suggesting a protective immunomodulatory role. We demonstrated that IFN- β is protective in CHIKV infection by signaling on nonhematopoietic cells and ultimately limiting neutrophil recruitment into site of inflammation. Further, the increased clinical disease observed in IFN- β knockout mice could be rescued with neutrophil depletion. This is distinct from the immunomodulatory action of IFN- β during LCMV infection, where IFN- β promotes viral persistence, presumably by increasing infection of CD8 α^{-} DCs. Our findings support the growing evidence of differential functions for IFN- α versus IFN- β and also highlight that distinct mechanisms can underlie these differences depending on the biological context.

Pathogenesis of CHIKV is still poorly understood but is thought to reflect an interplay between viral replication and a detrimental immune response. Currently, no approved treatment is

effective in preventing or controlling CHIKV infection or disease. We examined the efficacy of several U.S. Food and Drug Administration (FDA)–approved RA therapies in a mouse model of CHIKV infection. We identified two DMARDs (CTLA4-Ig and tofacitinib) with efficacy during acute CHIKV arthritis. In particular, CTLA4-Ig, when paired with the neutralizing anti-CHIKV human mAb 4N12, was highly effective at reducing joint inflammation, periarticular swelling, migration of inflammatory leukocytes, and infection even when administered several days after virus inoculation. The concept of combination antiviral and immunomodulatory therapy is a unique approach for the treatment of infectious diseases. The near-complete effectiveness of combination therapy in our mouse model of acute CHIKV arthritis has implications for treatment of other viral infections in which both virus- and immune-mediated pathology result in morbidity and mortality (for example, influenza and severe acute respiratory syndrome coronavirus). Given the large number of clinically available biological and small molecular DMARDs, this work may provide greater impetus for studies that test combination antiviral and immunomodulatory therapies for the treatment of infectious diseases.

Collectively, these studies highlight that both viral replication and the host immune responses play important roles in CHIKV pathogenesis. The host immune response has evolved mechanisms, including IFN-I and likely others, that impede both host- and viral-mediated pathology. Continued pursuit of delineating host-pathogen interactions will be paramount in developing effective therapeutic and vaccine strategies to combat emerging tropical diseases, which remain a global health and economic burden.

4.2 Future Directions

Our findings demonstrate that IFN- α and IFN- β have distinct protective activities during acute CHIKV infection. IFN- α appears to be more important for initiating antiviral responses, whereas IFN- β functions as an immunomodulatory molecule to indirectly limit neutrophil-mediated pathology. Additionally, our findings suggest that nonhematopoietic cells are central to IFN-I mediated control of CHIKV arthritis, consistent with previously published bone marrow chimera experiments. While these findings have taken important steps to increase our understanding of IFN-I biology and CHIKV pathogenesis, there are several new questions raised from these observations. The following sections identify some of these outstanding questions and discuss future experiments that will aid in further characterizing the actions of IFN-I subtypes during CHIKV infection.

4.2.1 When and where are IFN-I subtypes induced during CHIKV infection?

Studies of IFN- ϵ demonstrated that the cell type and context of expression can dramatically impact the function of an IFN-I subtype. IFN- ϵ is the only subtype demonstrated to not be regulated by PRR pathways, but rather, it is constitutively expressed by the epithelium of reproductive organs and further regulated by sex hormones¹³⁷. Likely a consequence of its unique regulation, IFN- ϵ is the only type I IFN subtype shown to play a protective role against *Chlamydia* infection, whereas the other subtypes may worsen disease^{137,138}. There is very little known about differential expression of IFN- α versus IFN- β *in vivo*, and their differential properties during LCMV and CHIKV infection may be due to the timing and location of expression. It may be that loss of IFN- α greatly impacts viral replication because the IFN- α 's, but not IFN- β , are primarily expressed near the cells that are targeted by CHIKV. With the tools currently available, the best way to

discriminate between the IFN-I subtypes is at the transcript level, through the use of sequence specific probes. Use of fluorescent *in situ* hybridization (FISH) for IFN- β , IFN- $\alpha 4$, and at least one of the IFN- α subtypes induced downstream of IFN- $\alpha 4/\beta$ signaling (e.g. IFN- $\alpha 2$), paired with cell identifying marker staining would determine the specific cells expressing the various IFN-I subtypes. Using mRNA FISH detection has its caveats, since transcriptional induction is not equivalent to cytokine activity, but even with these limitations, this type of *in vivo* analysis has not been performed before and would still be informative.

Since transcriptional regulation does not perfectly correlate to cytokine activity, tools that visualize or detect the different IFN-I subtypes at the protein level *in vivo* are greatly needed. The advent of CRISPR-Cas9 technology has enabled precise targeted editing or deletion of genes with rapid results, and Washington University has several core facilities offering these services. Using this technology we could develop several mice strains that express fluorescently tagged IFN-I subtypes. IFN- β , IFN- $\alpha 4$, and a non-initiating subtype, like IFN- $\alpha 2$, would be the important subtypes to initially analyze. Tagging the IFN-I proteins themselves would avoid the caveats of relying on transcription as a readout of activity or expression, but may alter the activity of the protein. Most of the available fluorescent labels are much larger than the IFN-I subtypes, so extensive *in vitro* characterization would be required to first ensure that the tagged IFN-I is still functional. Alternatively, we could develop mice that fluorescently report induction of a particular IFN-I subtype. This scheme would have caveats similar to the FISH transcript detection method, but would avoid altering the function of the protein and might have better sensitivity compared to FISH. While there are caveats and limitations for each reporter mouse scheme, both methods would bypass the brute force screening needed to generate IFN-I subtype specific mAbs. Altogether, these types of tools will allow spatial and temporal evaluation of IFN-I subtype

induction during a viral infection *in vivo*, and may reveal novel properties that previous expression readouts from whole tissues might have missed.

4.2.2 How is IFN- α limiting CHIKV replication and dissemination?

The increase in viral replication and spread with the loss of IFN- α could be due to alterations in tropism, such as spread to immune cells, or be due to increased infection of cells normally infected by CHIKV (muscle and fibroblasts). This would be determined by immunohistochemistry (IHC) analysis with CHIKV and CD45 co-staining of the ipsilateral foot at several time points during acute infection. Given the results with Vav-Cre expressing mice (Fig. 2.4), we expect to see increased CHIKV staining in CD45⁻ cells in IRF7-KO mice and mice treated with anti-IFN- α mAb compared to WT mice, and we anticipate similar CHIKV staining between WT and IFN- β -KO mice, given the similarity in viral loads (Fig. 2.3A). These data will allow us to more conclusively say that nonhematopoietic cells are the key cell types responding to IFN-I during acute CHIKV infection. An important next question would then be what is the impact of loss of IFN-I signaling on these specific cell types during CHIKV infection *in vivo*? To address this, we would cross the IFNAR^{fl/fl} mice to Ckm (muscle creatine kinase) Cre mice, which target skeletal and cardiac muscle, or Coll1a2 (collagen, type 1, alpha 2) Cre mice, which target many fibroblast cell types^{205,206}. These types of experiments have not been done before and would allow us to study the impact of IFN-I responses in relevant cell types *in vivo*.

IFN-I ultimately exert their biological effects through the induction and regulation of ISGs. There have only been a handful of ISGs described to have anti-CHIKV activity *in vitro* and *in vivo*, including viperin, PKR, GADD34, IFITM3, and tetherin/BST2^{121,123-127}. ISG15 has also been described to play a protect role during CHIKV infection, but rather than functioning to limit viral replication, as it does in several other viral systems, the absence of ISG15 during neonatal CHIKV

infection resulted in increased lethality from a cytokine storm-like phenotype⁵⁸. There have been examples of differential ISG induction by IFN- β compared to IFN- α subtypes *in vitro*. For example, IFN- β was shown to have more potent osteoclastogenesis activity by its preferential upregulation of CXCL11 compared to IFN- $\alpha 2$ ¹³⁵. Cell type-dependent effects are thought to be the result of variation in IFNAR surface expression and composition of downstream effector molecules, such as STATs¹⁵⁷. In order to fully understand how IFN- α and IFN- β display distinct functions *in vivo*, a more comprehensive evaluation of the ISGs induced downstream of IFN- α versus IFN- β in the relevant cell types (such as muscle) is warranted. Our lab has established protocols for culturing primary synovial fibroblasts and myofibers. RNAseq analysis of infected primary cell cultures in the presence or absence of anti-IFN- α or anti-IFN- β blocking mAb will allow us to determine if there are IFN- α - or IFN- β -dependent sets of ISGs induced in response to CHIKV infection. Furthermore, we will be able to evaluate if ISG induction or subtype differences display cell type specificity (synovial fibroblasts versus myofibers).

4.2.3 What is the role of neutrophils in the pathogenesis of CHIKV-infected IFN- β -KO mice?

Neutrophils are essential for the increased clinical disease observed in the IFN- β -KO mice since the phenotype could be rescued with neutrophil depletion. IRF7-KO mice were not originally included in the analysis of cellular infiltrates and cytokine and chemokine induction because the drastic difference in viral load between IRF7-KO and WT mice would make it challenging to interpret the data. Nevertheless, we did run IRF7-KO samples as we were analyzing the WT and IFN- β -KO samples, and *Irf7*^{-/-} mice not only recruited more neutrophils but also showed fewer inflammatory monocytes compared to WT mice (Fig. 4.1A). In contrast with what we observed in IFN- β -KO mice (Figure 2.6), analysis of cytokine and chemokine induction in the ipsilateral foot

of IRF7-KO mice revealed elevated CXCL1 and substantially increased G-CSF levels (Fig. 4.1B). The likely scenario in the IRF7-KO mice is that elevated viral burden is driving increased inflammation, cell death, and edema, which collectively alter cellular recruitment. Importantly, despite the increase in neutrophil number, neutrophil depletion had no impact on foot swelling in IRF7-KO mice (Fig 2.7), which raises the idea that increased neutrophil number alone might not be responsible for the phenotype in the IFN- β -KO mice. Indeed, we observed elevated IL-9 levels, and one study demonstrated that synovial fluid from RA patients could increase the activation and survival of neutrophils *ex vivo*, but this effect was lost when anti-IL-9 neutralizing antibody was added¹⁶¹. To determine if the neutrophils themselves are altered in the IFN- β -KO mice, flow cytometry analysis of neutrophil activation markers and apoptosis, such as iNOS/NOS2 (eBiosciences) or Annexin V staining, would be used.

To understand the molecular mechanism of IFN- β -mediated protection during CHIKV infection, we need to know how many steps are between IFN- β and altered neutrophil recruitment and/or function. First, we need to determine if IL-9 is directly involved in the pathogenesis of CHIKV infection in IFN- β -KO mice, which could be determined by administering a commercially available anti-IL-9 neutralizing mAb (9C1; Bio X Cell) to IFN- β -KO mice during CHIKV infection²⁰⁷. If IL-9 is directly involved in the neutrophil phenotype, we should see complete or partial alleviation of increased foot swelling and neutrophil recruitment in the IFN- β -KO mice. If this turns out to be the case, the next question would be which cells are making IL-9? To answer this, we would infect IL-9 fate reporter mice [available at Medical Research Council (MRC), Mill Hill, UK] with CHIKV in the presence of anti-IFN- β blocking mAb or isotype control antibody. In a model of lung inflammation, ILC2s were identified as the predominant source of IL-9¹⁷³, and this would be consistent with the timing of elevated IL-9 in the IFN- β -KO mice (2 dpi) (Fig. 2.6).

The potential involvement of ILC2s in the pathogenesis of CHIKV in IFN- β -KO mice again raises the question of which cell types are responding to IFN- β ? Based on the Vav-Cre⁺ IFNAR1^{fl/fl} mice (Fig. 2.4), we believe that IFN- β is signaling on nonhematopoietic cells. ILC2s are known to produce IL-9 when stimulated with IL-25, IL-33, and thymic stromal lymphopoietin (TSLP), which are typically secreted by damaged epithelium barriers¹⁷⁴. Synovial fibroblasts isolated from RA patients have been shown to produce both IL-33 and TSLP^{175,176}. So if we determine that IL-9 and ILC2s are directly involved in the pathogenesis in the IFN- β -KO mice, determining the *in vivo* source of IL-33, IL-25, or TSLP would identify potential cellular targets of IFN- β . IFN- γ has previously been shown to downregulate IL-33 induction in lung fibroblasts in a STAT1-dependent manner²⁰⁸, and IFN-I signaling is also able to activate phosphorylated STAT1 homodimers¹⁰⁴. These data suggest that IFN- β -mediated regulation of IL-33 is not outside the realm of possibility. We would use IHC or immunofluorescence co-staining of IL-33 or IL-25 with cell identifying markers to determine the cells making these cytokines in ipsilateral foot sections of WT and IFN- β -KO mice.

If flow cytometry does not reveal differences in neutrophil activation and if IL-9 neutralization is protective, we would need to employ RNAseq analysis of isolated neutrophils (Ly6G⁺ enrichment, Miltenyi) to understand how neutrophils are contributing to the pathogenesis in IFN- β -KO mice. Alternatively, if IL-9 blockade has no effect, we would perform RNAseq on the whole foot tissue to delineate the mechanisms underlying the increased neutrophil recruitment and/or function in the IFN- β -KO mice compared to WT and IRF7-KO mice. Collectively, these experiments will yield a more complete picture of how loss of IFN- β activity leads to neutrophil-mediated immunopathology during CHIKV infection.

4.2.4 What roles do IFN-I play during chronic CHIKV disease?

The pathogenesis of chronic CHIKV disease is still poorly understood. CHIKV RNA, but not infectious virus, persists in the joints and musculoskeletal tissues of patients and animals infected with various strains of CHIKV^{52,55,66}. This RNA might serve as a PAMP and cause chronic symptoms by continuously activating the immune system. Consistent with this paradigm, microarray analysis of the ipsilateral foot of WT mice at 30 days post infection showed not only elevated expression of IFN-I-related genes, such as IRF7, IFNAR1, and IFN- β , but also downregulation of known IFN-I negative regulators SOCS1 and TRIM24⁵⁵. IFN-I can have detrimental effects during some chronic infections, such as LCMV, by promoting constant inflammation, but IFN-I are also important for augmenting protective adaptive immune responses, like the generation of neutralizing antibodies^{151,152,209}. Because *Ifnar1*^{-/-} mice die so quickly following CHIKV infection, most studies have focused on understanding the roles of IFN-I during acute CHIKV pathogenesis and do not examine chronic disease.

To determine the impact of loss of IFN- α or IFN- β on chronic CHIKV disease, we infected WT, IFN- β -KO, and IRF7-KO mice with 10^3 pfu CHIKV via a subcutaneous route and then sacrificed the mice at 28 dpi for persistent CHIKV E1 RNA analysis by qRT-PCR. We found that IRF7-KO mice had significantly more chronic CHIKV E1 RNA copies present in the ipsilateral ankle (Fig. 4.2A, left panel, $P < 0.01$), whereas IFN- β -KO mice displayed no change in chronic RNA compared to WT mice (Fig. 4.2A, left panel, $P > 0.05$). Additionally, IRF7-KO mice had substantially more persistent RNA in the contralateral ankle (Fig. 4.2A, right panel, $p < 0.0001$), and in contrast, the IFN- β -KO mice showed only a modest increase in RNA burden compared to WT mice, which was to a much lesser degree than the increase observed in the IRF7-KO mice (Fig. 4.2A, right panel, $P < 0.01$). Importantly, administering anti-IFN- α or anti-IFN- β mAb at 1

day before infection and again at 1 dpi phenocopied the IRF7-KO and IFN- β -KO mice, respectively (Fig 4.2B). These data are consistent with what we observed during acute infection, and the IFN- α 's seem to be more important in limiting persistent CHIKV RNA during chronic disease compared to IFN- β .

IFN-I are also known to augment antibody production and isotype switching in B cells¹⁰⁸. Neutralizing antibodies are important for clearing infectious virus and limiting persistent CHIKV RNA, so the elevated CHIKV RNA could either be due to the increased infection of cells early during infection or be due to a failure to properly control or clear the RNA through adaptive immune responses²¹⁰. To assess these possibilities, we infected WT mice with CHIKV and then administered anti-IFN- α mAb or isotype control antibody at 2 dpi, which is when elevated viral load is first observed in the IRF7-KO mice but before the generation of adaptive immune responses (Fig. 2.3A). Blockade of IFN- α at 2 dpi had no impact on foot swelling compared to isotype control treated mice (Fig. 4.2C), which is in stark contrast to the severe increase in foot swelling seen with the day -1/+1 blockade regimen (Fig. 2.1B). IFN- α blockade at day 2 also showed no increase in the viral RNA burden in the ipsilateral ankle (Fig. 4.2D, left panel). Detailed analysis of acute infectious virus with this blockade regimen still needs to be performed, but these data imply that IFN- α acts within the first 48 hours to limit clinical foot swelling, presumably through limiting viral replication at the site of infection. Furthermore, the antiviral activity of IFN- α during the first 48 hours of infection is able limit persistent CHIKV RNA in the ipsilateral ankle at 28 dpi. In contrast, the contralateral ankle still showed elevated persistent CHIKV RNA with day 2 blockade of IFN- α (Fig. 4.2D, right panel, $P < 0.0001$), suggesting that IFN- α activity is needed beyond 2 dpi to limit CHIKV dissemination.

The increased persistent viral RNA from loss of IFN- α could be due to more cells harboring CHIKV RNA during chronic time points. Our lab has developed a system to permanently label cells that survive CHIKV infection using a Cre-expressing CHIKV strain and fluorescent fate-reporter mouse. Using this system in conjunction with anti-IFN- α and anti-IFN- β blockade, we will be able to assess how many and what types of cells are surviving CHIKV infection and how loss of IFN- α or IFN- β impacts those cells populations. No difference in marked (Cre⁺) cells could indicate that IFN- α is impacting the amount of virus produced by an infected cell, rather than limiting the number of cells infected. Tropism studies during acute infection (discussed in section 4.2.2), would aid in interpreting the results from these chronic experiments. Much more work is needed to characterize the immune and viral factors contributing to chronic CHIKV disease, and there are limitations in using mice to study a human virus. However, these studies will still be beneficial in understanding how IFN-I subtypes function during chronic CHIKV pathogenesis.

4.2.5 Are there dual protective and detrimental roles for IFN- β during CHIKV infection?

Of all the IFN-I subtypes, IFN- β has the highest known natural affinity for IFNAR, and as such has been described as the most potent IFN-I subtype for a number of functions, including anti-proliferative and pro-apoptotic activities. In particular, IFN- β has potent immunomodulatory activity and is used as a therapeutic agent in multiple sclerosis, providing beneficial immunomodulatory effects¹⁷¹. In contrast, recent work with LCMV persistent infection determined that IFN- β was detrimental and promoted viral persistence¹⁵⁰. Blockade of IFN- β , but not IFN- α , improved antiviral T cell responses and lead to clearance of LCMV, recapitulating what was observed with IFNAR1 blockade¹⁵⁰⁻¹⁵². We did not see a significant change in persistent CHIKV RNA at 28 dpi with the loss of IFN- β (Fig. 4.2A, 4.2B), but given this history of IFN- β in

mediating chronic inflammation, we expanded our evaluations to ensure we were not missing a phenotype.

When we performed our chronic CHIKV experiments for WT, IFN- β -KO, and IRF7-KO mice, we also collected samples for histological analysis. We had a blinded pathologist score the day 28 H&E slides, and we were surprised to see that 100% of the IFN- β -KO mice received a score of 0 (no inflammation), whereas the WT and IRF7-KO mice received an average score of around 1 (mild inflammation) (Fig. 4.3A). This is preliminary data and needs to be repeated to increase the sample size, but this was a striking observation. For LCMV infection, the clue that prompted evaluation of a detrimental role for IFN- β during chronic infection came from evaluating IFN- α versus IFN- β induction. Infection with clone 13 LCMV infection, which yields persistent infection, revealed a substantial elevation in IFN- β induction compared to the amount that is induced during infection with the Armstrong strain of LCMV, which yields an acute infection¹⁵⁰. With this in mind, we next evaluated the induction of IFN- β , IFN- $\alpha 4$, and the IFN- α subtypes that are induced downstream of IFN- $\alpha 4/\beta$ signaling (pan non-IFN- $\alpha 4$) by qRT-PCR at 12 hours post infection and 28 dpi. Surprisingly, we found that IFN-I induction was much higher at the chronic time point than at the acute time point, and IFN- β had the highest chronic expression among the subtypes analyzed (Fig. 4.3B). A hallmark for detrimental IFN-I responses is sustained elevated expression, and our preliminary data suggest that this might be the case during CHIKV infection.

We know from our acute CHIKV studies, that IFN- β -KO mice have elevated neutrophil recruitment at 2 dpi. We next asked what would happen if we blocked IFN- β at around the time it had already performed this beneficial immunomodulatory function. We infected WT mice and then administered anti-IFN- β mAb at 2 dpi, and we monitored the mice for clinical foot swelling and then sacrificed them at 28 dpi for persistent RNA analysis. We found that day 2 IFN- β

blockade promoted quicker resolution of foot swelling compared to isotype control treated mice (Fig. 4.3C). Persistent RNA analysis at 28 dpi revealed no change in viral RNA burden, indicating that again, IFN- β seems to be modulating pathology, but not viral load (Fig. 4.3D). It is worth noting that the protective foot swelling phenotype seen with day 2 IFN- β blockade is modest compared to other beneficial treatments, such as depleting CD4⁺ T cells⁷⁹. However, these preliminary data suggest that IFN- β may be playing a detrimental role during the resolution of inflammation. We performed preliminary FACS analysis of immune infiltrates at 7 dpi in control treated mice or mice that received anti-IFN- β at 2 dpi, and we did not see any drastic changes in numbers for the expected immune cell populations at this time point, such as CD4⁺ T cells, CD8⁺ T cells, NK cells, macrophages, monocytes, or neutrophils (data not shown).

There have been very few studies performed to characterize the resolution phase of clinical CHIKV disease. At this point, we can only speculate why IFN- β has this paradoxical dual protective and pathogenic role. It could be that the presence of IFN- β at later time points skews the activation state of certain cell types that inhibits their ability to promote resolution of inflammation. Redesigning our flow cytometry panel to allow for more careful evaluation of the various cell populations that may be involved in resolution inflammation, such as myeloid suppressor cells or regulatory T cells, will be important in determining how IFN- β is mediating these detrimental effects. There are so many permutations of myeloid cell phenotypes, that standard flow cytometry may be insufficient to capture the phenotype. If we are unable to identify altered cell recruitment or activation by flow cytometry, then we may need to use CYTOF (mass cytometry) analysis to parse this phenotype.

Collectively, the data from acute CHIKV disease and these preliminary findings with chronic CHIKV disease suggest that the biological activity of IFN- β is more complicated than

originally thought. Its protective versus pathogenic functions are likely related to the timing, concentration, and cellular source of its expression, as well as its unique signaling potential as the highest affinity IFN-I subtype. IFN- β is administered intramuscularly or subcutaneously as a treatment for multiple sclerosis, and thus, CHIKV is a relevant model to study the functions of IFN- β , given the route of infection and tissues and cell types involved in its pathogenesis. Further delineation of the actions of IFN- β during acute and persistent CHIKV disease will likely yield important insight into its potential use as a therapeutic agent or target.

4.3 Materials and Methods

Mice

All animal experiments were performed in accordance and with approval of Washington University Institutional Animal Care and Use Committee guidelines, and all mouse infection studies were performed in an animal biosafety level 3 laboratory. All experiments were performed with 4-week-old male mice. C57BL/6J (WT), interferon beta knockout (*Ifnb*^{-/-}), and IRF7 knockout (*Irf7*^{-/-}) mice were bred and maintained in our mouse colony before being transferred to the animal biosafety level 3 laboratory for experiments. *Ifnb*^{-/-} and *Irf7*^{-/-} mice bred onto the C57BL/6J background were generously provided by Michael S. Diamond (Washington University School of Medicine).

Virus experiments

A recombinant strain of CHIKV (LR2006 OPY1) was generously provided by S. Higgs (Kansas State University) and generated from *in vitro* transcribed cDNA, as previously described¹⁷⁷. At 4 weeks of age, mice were inoculated in the left rear footpad with 10³ PFU of the LR2006 OPY1 strain of CHIKV in a volume of 10 μ l. Infected mice were monitored daily for foot

swelling with digital calipers for 28 days. At the termination of experiments mice were sedated with a ketamine-xylazine cocktail and euthanized, and then perfused via intracardiac injection with PBS. Tissues (ipsilateral left ankle and contralateral right ankle) were snap frozen in liquid nitrogen and stored at -80°C until processing for viral RNA burden. “Ankle” refers to distal foot with the skin and digits removed. Histological analysis and scoring, immune cell infiltrate analysis, and cytokine and chemokine analysis are detailed in section 2.5.

Real-time qRT-PCR analysis

RNA was extracted from tissue using TRIzol Reagent and an RNeasy Mini Kit (Qiagen). The TRIzol Reagent manufacturer’s protocol was followed up until removal of the RNA-containing aqueous phase, to which an equal volume of 100% RNase-free ethanol was added. This solution was added to the RNeasy column, after which the RNeasy Mini Kit instructions were followed. The quantity of CHIKV RNA was determined by qRT-PCR using the TaqMan RNA-to-CT 1-Step Kit (Applied Biosystems) with an E1-specific primer/probe set²⁰³. Absolute copies of CHIKV E1 was determined by with a copy number standard curve generated from CHIKV genomic RNA synthesized *in vitro*. Copy number was calculated using an online program (IDT) by taking into account the concentration of the RNA ($\text{ng}/\mu\text{L}$), the length of the RNA (11,800 bp for CHIKV), and nature of the RNA (ssRNA) (<http://scienceprimer.com/copy-number-calculator-for-realttime-pcr>).

For IFN-I expression by pRT-PCR, RNA was extracted using a TRIzol and RNeasy Mini Kit (Qiagen) hybrid protocol outlined above. Two microliters of the extracted RNA from CHIKV-infected or mock-infected mice were analyzed by qRT-PCR. An arbitrary standard curve was generated for each primer/probe set to generate arbitrary values (SQ) for each gene of interest or the housekeeping gene, GAPDH (glyceraldehyde-3-phosphate dehydrogenase). Mock and

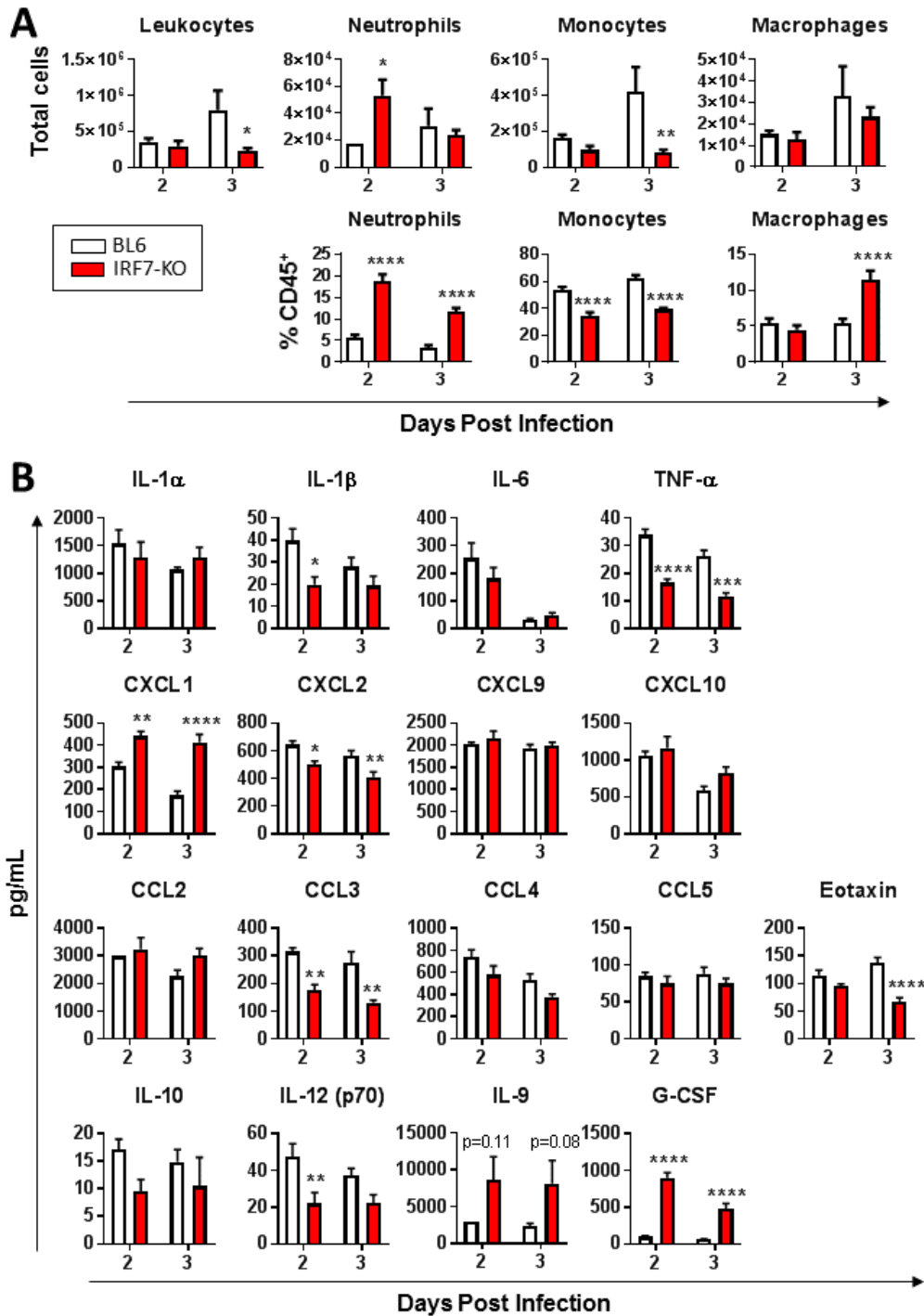
infected SQ values for the gene of interest and GAPDH values were used to calculate $\Delta\Delta C_t$, and normalized fold change was calculated by $2^{-\Delta\Delta C_t}$.

IFN- β Fwd: 5'-GGC TTC CAT CAT GAA CAA CAG-3' **Rev:** 5'-GTT GAT GGA GAG GGC TGT G-3' **Probe:** 5'-/56FAM/CTG CGT TCC TGC TGT GCT TCT C/36-TAMSp/-3'

IFN- $\alpha 4$ Fwd: 5'-TGT GTG ATG CAG GAA CCT CCT-3' **Rev:** 5'-GGT ACA CAG TGA TCC TGT GG-3' **Probe:** 5'-/56-FAM/AAG ACT CCC TGC TGG CTG TGA GG/36-TAMSp/-3'

Pan non-IFN $\alpha 4$ Fwd: 5'-ARS YTG TST GAT GCA RCA GGT-3' **Rev:** 5'-GGW ACA CAG TGA TCC TGT GG-3' **Probe:** 5'-/56-FAM/CAG GAA CCT CCT CTG ACC CAG GA/36-TAMSp/-3'

4.4 Figures



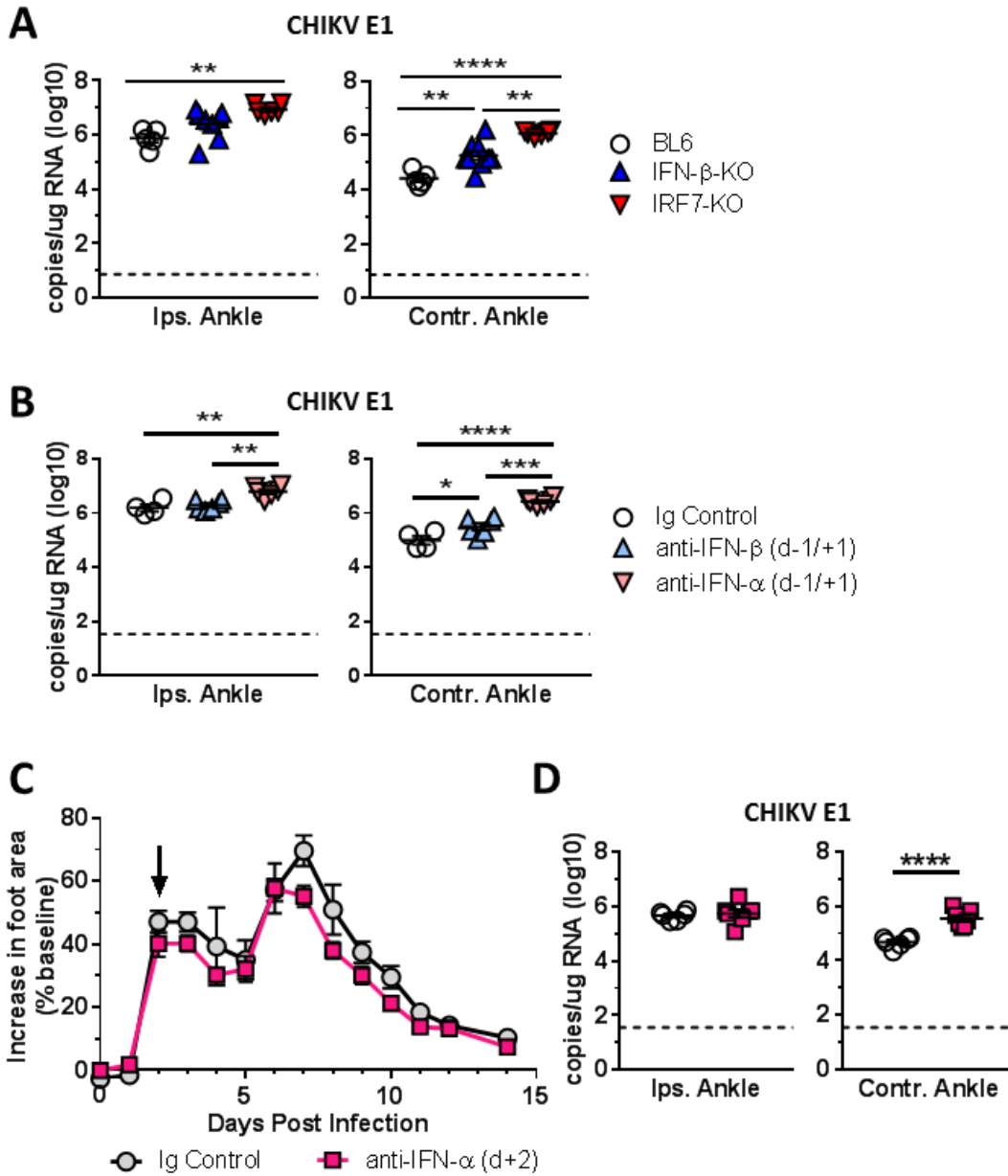


Figure 4.2 *IFN- α limits persistent CHIKV RNA in the ipsilateral ankle within the first 48 hours following CHIKV infection*

(A) WT, IFN- β -KO, or IRF7-KO mice were infected with 10^3 CHIKV and sacrificed at 28 dpi for CHIKV RNA analysis. (B) WT mice were treated with 1 mg of anti-mouse IFN- α (TIF-3C5), 1 mg anti-mouse IFN- β (HD β -4A7), or 1 mg isotype control antibody at 24h prior to and again 24h post infection by IP route and then sacrificed at 28 dpi for CHIKV RNA analysis. (C) WT mice were treated with 1 mg of anti-mouse IFN- α (TIF-3C5) or 1 mg isotype control antibody at 2 dpi and measured daily for foot swelling and then (D) sacrificed at 28 dpi for CHIKV RNA analysis. (A,B, D) Absolute copies of CHIKV E1 was determined by qRT-PCR and a standard curve generated from CHIKV genomic RNA synthesized *in vitro*. Dashed line represents the limit of detection. Ips, ipsilateral; contr, contralateral. *, $p < 0.05$; **, $p < 0.01$; ***, $p < 0.001$; ****, $p < 0.0001$ (1-way ANOVA with Tukey's post-hoc multiple comparisons analysis for RNA analysis; 2-way ANOVA with Dunnett's multiple comparisons for foot swelling).

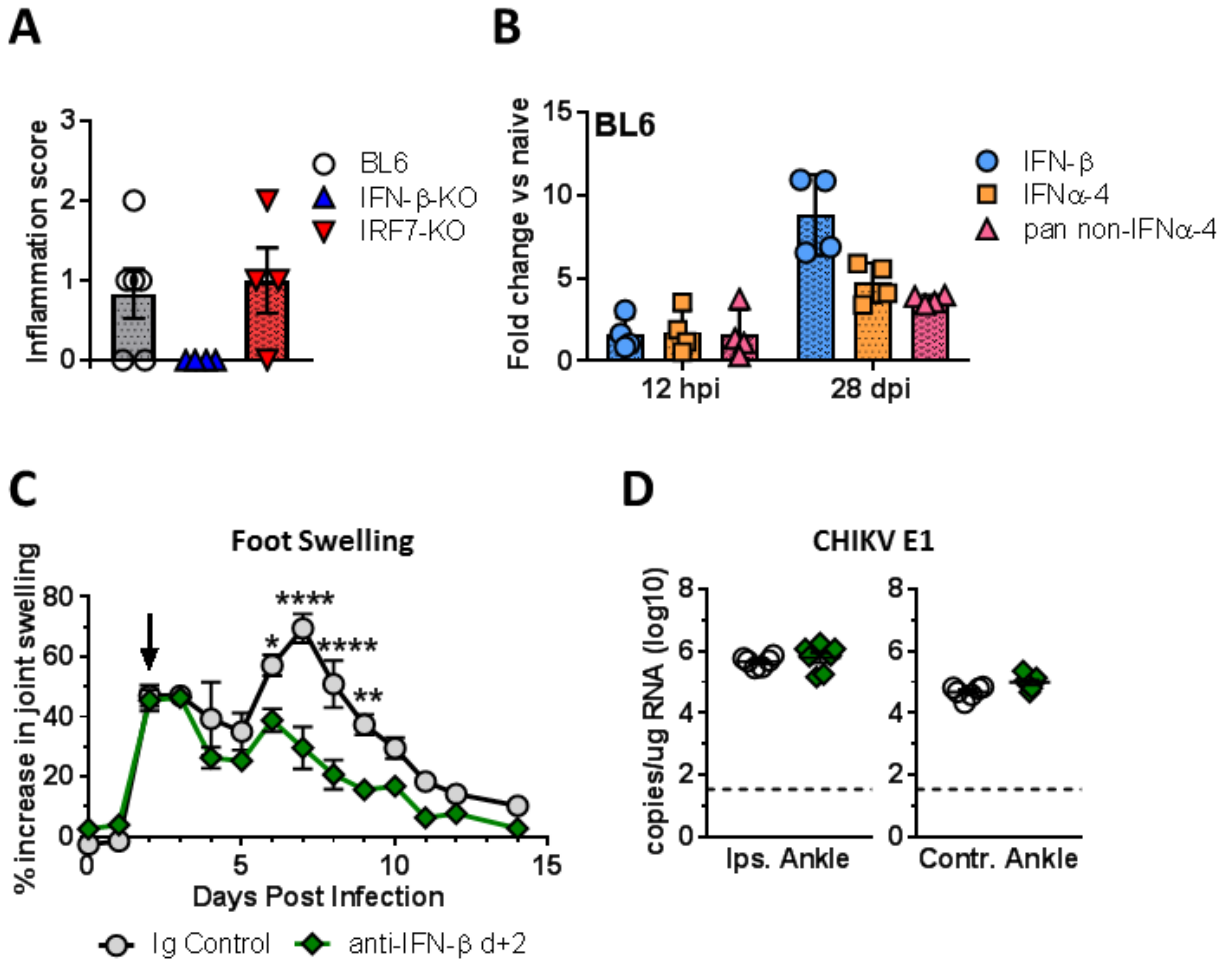


Figure 4.3 *IFN-β may have detrimental effects during chronic CHIKV pathogenesis*

(A) WT, IFN-β-KO, or IRF7-KO mice were infected with 10^3 pfu of CHIKV subcutaneously in the left rear foot, and the infected foot was harvested at 28 dpi for histological analysis. H&E slides from d28 were scored on a scale of 0 to 3 by a blinded pathologist for overall inflammation, taking into consideration joint space inflammation, myositis, and synovitis for scoring. Criteria were: 0, no inflammation; 1, mild inflammation; 2, moderate inflammation; 3, severe inflammation. Data are pooled from 2 independent experiments with $n = 4-5$ per group. (B) WT mice were infected with CHIKV and the infected ankle was harvested at 12 hours or 28 days post infection for RNA extraction. RT-PCR was used to determine the expression of IFN-β, IFN-α, or pan non-IFN-α4 subtypes. $n = 4$ per group. (C) WT mice were treated with 1 mg of anti-mouse IFN-β (HDb-4A7) or 1 mg isotype control antibody at 48 hours post infection, and the infected foot was measured daily with digital calipers and then (D) sacrificed for CHIKV E1 RNA at 28 dpi. All data are represented as mean \pm SEM, and if no error bar is present that indicates the error is smaller than the height of the symbol. The data are pooled from 2 independent experiments with $n = 6-7$ mice per group. *, $p < 0.05$; **, $p < 0.01$; ****, $p < 0.0001$ (2-way repeated measure ANOVA with Dunnett's post-hoc multiple comparisons analysis for foot swelling; 1-way ANOVA with Tukey's multiple comparisons for inflammation score; Mann-Whitney test for CHIKV E1 RNA burden).

References

1. Robinson, M. C. An epidemic of virus disease in Southern Province, Tanganyika Territory, in 1952-53. I. Clinical features. *Trans. R. Soc. Trop. Med. Hyg.* **49**, 28–32 (1955).
2. Morrison, T. E. Reemergence of Chikungunya Virus. *J. Virol.* **88**, 11644–11647 (2014).
3. Josseran, L. *et al.* Chikungunya disease outbreak, Reunion Island. *Emerg. Infect. Dis.* **12**, 1994–5 (2006).
4. Kariuki Njenga, M. *et al.* Tracking epidemic Chikungunya virus into the Indian Ocean from East Africa. *J. Gen. Virol.* **89**, 2754–60 (2008).
5. Economopoulou, A. *et al.* Atypical Chikungunya virus infections: clinical manifestations, mortality and risk factors for severe disease during the 2005-2006 outbreak on Réunion. *Epidemiol. Infect.* **137**, 534–41 (2009).
6. Das, T. *et al.* Chikungunya fever: CNS infection and pathologies of a re-emerging arbovirus. *Prog. Neurobiol.* **91**, 121–9 (2010).
7. Rohatgi, A. *et al.* Infection of Myofibers Contributes to Increased Pathogenicity during Infection with an Epidemic Strain of Chikungunya Virus. *J. Virol.* **88**, 2414–2425 (2014).
8. Staples, J. E., Breiman, R. F. & Powers, A. M. Chikungunya Fever: An Epidemiological Review of a Re-Emerging Infectious Disease. *Clin. Infect. Dis.* **49**, 942–948 (2009).
9. Leparc-Goffart, I., Nougairede, A., Cassadou, S., Prat, C. & de Lamballerie, X. Chikungunya in the Americas. *Lancet (London, England)* **383**, 514 (2014).
10. Kendrick, K., Stanek, D., Blackmore, C. & Centers for Disease Control and Prevention (CDC). Notes from the field: Transmission of chikungunya virus in the continental United States--Florida, 2014. *MMWR. Morb. Mortal. Wkly. Rep.* **63**, 1137 (2014).
11. Tsetsarkin, K. A., Vanlandingham, D. L., McGee, C. E. & Higgs, S. A single mutation in chikungunya virus affects vector specificity and epidemic potential. *PLoS Pathog.* **3**, e201 (2007).
12. Tsetsarkin, K. A. *et al.* Chikungunya virus emergence is constrained in Asia by lineage-specific adaptive landscapes. *Proc. Natl. Acad. Sci.* **108**, 7872–7877 (2011).
13. Nunes, M. R. T. *et al.* Emergence and potential for spread of Chikungunya virus in Brazil. *BMC Med.* **13**, 102 (2015).
14. Burt, F. J., Rolph, M. S., Rulli, N. E., Mahalingam, S. & Heise, M. T. Chikungunya: A re-emerging virus. *Lancet* **379**, 662–671 (2012).
15. Simon, F., Javelle, E., Oliver, M., Leparc-Goffart, I. & Marimoutou, C. Chikungunya virus infection. *Curr. Infect. Dis. Rep.* **13**, 218–28 (2011).
16. Caglioti, C. *et al.* Chikungunya virus infection: an overview. *New Microbiol.* **36**, 211–27 (2013).

17. Suhrbier, A., Jaffar-Bandjee, M. C. & Gasque, P. Arthritogenic alphaviruses-an overview. *Nat. Rev. Rheumatol.* **8**, 420–429 (2012).
18. Schilte, C. *et al.* Chikungunya Virus-associated Long-term Arthralgia: A 36-month Prospective Longitudinal Study. *PLoS Negl. Trop. Dis.* **7**, (2013).
19. Pialoux, G., Gaüzère, B. A., Jauréguiberry, S. & Strobel, M. Chikungunya, an epidemic arbovirosis. *Lancet Infect. Dis.* **7**, 319–327 (2007).
20. Borgherini, G. *et al.* Persistent arthralgia associated with chikungunya virus: a study of 88 adult patients on reunion island. *Clin. Infect. Dis.* **47**, 469–75 (2008).
21. Kennedy, A. C., Fleming, J. & Solomon, L. Chikungunya viral arthropathy: a clinical description. *J. Rheumatol.* **7**, 231–6 (1980).
22. Rodriguez-Morales, A. J., Cardona-Ospina, J. A., Villamil-Gómez, W. & Paniz-Mondolfi, A. E. How many patients with post-chikungunya chronic inflammatory rheumatism can we expect in the new endemic areas of Latin America? *Rheumatol. Int.* **35**, 2091–4 (2015).
23. Miner, J. J. *et al.* Brief report: Chikungunya viral arthritis in the United States: A mimic of seronegative rheumatoid arthritis. *Arthritis Rheumatol.* **67**, 1214–1220 (2015).
24. Brighton, S. W. Chloroquine phosphate treatment of chronic Chikungunya arthritis. An open pilot study. *South African Med. J.* **66**, 217–8 (1984).
25. De Lamballerie, X. *et al.* On chikungunya acute infection and chloroquine treatment. *Vector Borne Zoonotic Dis.* **8**, 837–9 (2008).
26. Chopra, A., Saluja, M. & Venugopalan, A. Effectiveness of chloroquine and inflammatory cytokine response in patients with early persistent musculoskeletal pain and arthritis following chikungunya virus infection. *Arthritis Rheumatol.* **66**, 319–326 (2014).
27. Powers, A. M. Vaccine and Therapeutic Options To Control Chikungunya Virus. *Clin. Microbiol. Rev.* **31**, e00104-16 (2017).
28. Smith, S. A. *et al.* Isolation and characterization of broad and ultrapotent human monoclonal antibodies with therapeutic activity against chikungunya virus. *Cell Host Microbe* **18**, 86–95 (2015).
29. Selvarajah, S. *et al.* A Neutralizing Monoclonal Antibody Targeting the Acid-Sensitive Region in Chikungunya Virus E2 Protects from Disease. *PLoS Negl. Trop. Dis.* **7**, e2423 (2013).
30. Karlas, A. *et al.* A human genome-wide loss-of-function screen identifies effective chikungunya antiviral drugs. *Nat. Commun.* **7**, 11320 (2016).
31. Silva, L. A. & Dermody, T. S. Chikungunya virus: epidemiology, replication, disease mechanisms, and prospective intervention strategies. *J. Clin. Invest.* **127**, 737–749 (2017).
32. Bernard, E. *et al.* Endocytosis of chikungunya virus into mammalian cells: role of clathrin and early endosomal compartments. *PLoS One* **5**, e11479 (2010).

33. Silva, L. A. *et al.* A Single-Amino-Acid Polymorphism in Chikungunya Virus E2 Glycoprotein Influences Glycosaminoglycan Utilization. *J. Virol.* **88**, 2385–2397 (2014).
34. Acharya, D., Paul, A. M., Anderson, J. F., Huang, F. & Bai, F. Loss of Glycosaminoglycan Receptor Binding after Mosquito Cell Passage Reduces Chikungunya Virus Infectivity. *PLoS Negl. Trop. Dis.* **9**, e0004139 (2015).
35. Ashbrook, A. W. *et al.* Residue 82 of the Chikungunya Virus E2 Attachment Protein Modulates Viral Dissemination and Arthritis in Mice. *J. Virol.* **88**, 12180–12192 (2014).
36. Gay, B. *et al.* pH-dependent entry of chikungunya virus into *Aedes albopictus* cells. *Infect. Genet. Evol.* **12**, 1275–81 (2012).
37. Wengler, G., Würkner, D. & Wengler, G. Identification of a sequence element in the alphavirus core protein which mediates interaction of cores with ribosomes and the disassembly of cores. *Virology* **191**, 880–8 (1992).
38. Singh, I. & Helenius, A. Role of ribosomes in Semliki Forest virus nucleocapsid uncoating. *J. Virol.* **66**, 7049–58 (1992).
39. Frolova, E. I., Gorchakov, R., Pereboeva, L., Atasheva, S. & Frolov, I. Functional Sindbis virus replicative complexes are formed at the plasma membrane. *J. Virol.* **84**, 11679–95 (2010).
40. Spuul, P., Balistreri, G., Kääriäinen, L. & Ahola, T. Phosphatidylinositol 3-kinase-, actin-, and microtubule-dependent transport of Semliki Forest Virus replication complexes from the plasma membrane to modified lysosomes. *J. Virol.* **84**, 7543–57 (2010).
41. Kujala, P. *et al.* Biogenesis of the Semliki Forest virus RNA replication complex. *J. Virol.* **75**, 3873–84 (2001).
42. Thaa, B. *et al.* Differential Phosphatidylinositol-3-Kinase-Akt-mTOR Activation by Semliki Forest and Chikungunya Viruses Is Dependent on nsP3 and Connected to Replication Complex Internalization. *J. Virol.* **89**, 11420–37 (2015).
43. Utt, A. *et al.* Versatile Trans-Replication Systems for Chikungunya Virus Allow Functional Analysis and Tagging of Every Replicase Protein. *PLoS One* **11**, e0151616 (2016).
44. Firth, A. E., Chung, B. Y., Fleeton, M. N. & Atkins, J. F. Discovery of frameshifting in Alphavirus 6K resolves a 20-year enigma. *Virol. J.* **5**, 108 (2008).
45. Snyder, J. E. *et al.* Functional characterization of the alphavirus TF protein. *J. Virol.* **87**, 8511–23 (2013).
46. Loewy, A., Smyth, J., von Bonsdorff, C. H., Liljestrom, P. & Schlesinger, M. J. The 6-kilodalton membrane protein of Semliki Forest virus is involved in the budding process. *J. Virol.* **69**, 469–75 (1995).
47. Soonsawad, P. *et al.* Structural evidence of glycoprotein assembly in cellular membrane compartments prior to Alphavirus budding. *J. Virol.* **84**, 11145–51 (2010).

48. Sjöberg, M. & Garoff, H. Interactions between the transmembrane segments of the alphavirus E1 and E2 proteins play a role in virus budding and fusion. *J. Virol.* **77**, 3441–50 (2003).
49. Voss, J. E. *et al.* Glycoprotein organization of Chikungunya virus particles revealed by X-ray crystallography. *Nature* **468**, 709–12 (2010).
50. Krejbich-Trotot, P. *et al.* Chikungunya virus mobilizes the apoptotic machinery to invade host cell defenses. *FASEB J.* **25**, 314–25 (2011).
51. Gardner, J. *et al.* Chikungunya Virus Arthritis in Adult Wild-Type Mice. *J. Virol.* **84**, 8021–8032 (2010).
52. Morrison, T. E. *et al.* A mouse model of chikungunya virus-induced musculoskeletal inflammatory disease: Evidence of arthritis, tenosynovitis, myositis, and persistence. *Am. J. Pathol.* **178**, 32–40 (2011).
53. Fox, J. M. & Diamond, M. S. Immune-Mediated Protection and Pathogenesis of Chikungunya Virus. *J. Immunol.* **197**, 4210–4218 (2016).
54. Hawman, D. W. *et al.* Chronic Joint Disease Caused by Persistent Chikungunya Virus Infection Is Controlled by the Adaptive Immune Response. *J. Virol.* **87**, 13878–13888 (2013).
55. Poo, Y. S. *et al.* Multiple Immune Factors Are Involved in Controlling Acute and Chronic Chikungunya Virus Infection. *PLoS Negl. Trop. Dis.* **8**, (2014).
56. Couderc, T. *et al.* A mouse model for Chikungunya: Young age and inefficient type-I interferon signaling are risk factors for severe disease. *PLoS Pathog.* **4**, (2008).
57. Ziegler, S. A., Lu, L., da Rosa, A. P. A. T., Xiao, S.-Y. & Tesh, R. B. An animal model for studying the pathogenesis of chikungunya virus infection. *Am. J. Trop. Med. Hyg.* **79**, 133–9 (2008).
58. Werneke, S. W. *et al.* ISG15 Is Critical in the Control of Chikungunya Virus Infection Independent of UBE1L Mediated Conjugation. *PLoS Pathog.* **7**, e1002322 (2011).
59. Labadie, K. *et al.* Chikungunya disease in nonhuman primates involves long-term viral persistence in macrophages. *J. Clin. Invest.* **120**, 894–906 (2010).
60. Messaoudi, I. *et al.* Chikungunya Virus Infection Results in Higher and Persistent Viral Replication in Aged Rhesus Macaques Due to Defects in Anti-Viral Immunity. *PLoS Negl. Trop. Dis.* **7**, (2013).
61. Sourisseau, M. *et al.* Characterization of reemerging chikungunya virus. *PLoS Pathog.* **3**, 0804–0817 (2007).
62. Bernard, E. *et al.* Human keratinocytes restrict chikungunya virus replication at a post-fusion step. *Virology* **476**, 1–10 (2015).
63. Noret, M. *et al.* Interleukin 6, RANKL, and Osteoprotegerin Expression by Chikungunya Virus-Infected Human Osteoblasts. *J. Infect. Dis.* **206**, 455–457 (2012).

64. Rudd, P. A. *et al.* Interferon Response Factors 3 and 7 Protect against Chikungunya Virus Hemorrhagic Fever and Shock. *J. Virol.* **86**, 9888–9898 (2012).
65. Her, Z. *et al.* Active Infection of Human Blood Monocytes by Chikungunya Virus Triggers an Innate Immune Response. *J. Immunol.* **184**, 5903–5913 (2010).
66. Hoarau, J. J. *et al.* Persistent Chronic Inflammation and Infection by Chikungunya Arthritogenic Alphavirus in Spite of a Robust Host Immune Response. *J. Immunol.* **184**, 5914–5927 (2010).
67. Ng, L. F. P. *et al.* IL-1 β , IL-6, and RANTES as Biomarkers of Chikungunya Severity. *PLoS One* **4**, e4261 (2009).
68. Chow, A. *et al.* Persistent Arthralgia Induced by Chikungunya Virus Infection is Associated with Interleukin-6 and Granulocyte Macrophage Colony-Stimulating Factor. *J. Infect. Dis.* **203**, 149–157 (2011).
69. Kelvin, A. A. *et al.* Inflammatory Cytokine Expression Is Associated with Chikungunya Virus Resolution and Symptom Severity. *PLoS Negl. Trop. Dis.* **5**, e1279 (2011).
70. Chen, W. *et al.* Bindarit, an Inhibitor of Monocyte Chemotactic Protein Synthesis, Protects against Bone Loss Induced by Chikungunya Virus Infection. *J. Virol.* **89**, 581–593 (2015).
71. Poo, Y. S. *et al.* CCR2 Deficiency Promotes Exacerbated Chronic Erosive Neutrophil-Dominated Chikungunya Virus Arthritis. *J. Virol.* **88**, 6862–6872 (2014).
72. Haist, K. C., Burrack, K. S., Davenport, B. J. & Morrison, T. E. Inflammatory monocytes mediate control of acute alphavirus infection in mice. *PLOS Pathog.* **13**, e1006748 (2017).
73. Thanapati, S., Das, R. & Tripathy, A. S. Phenotypic and functional analyses of NK and NKT-like populations during the early stages of chikungunya infection. *Front. Microbiol.* **6**, 1–11 (2015).
74. Petitdemange, C. *et al.* Unconventional Repertoire Profile Is Imprinted during Acute Chikungunya Infection for Natural Killer Cells Polarization toward Cytotoxicity. *PLoS Pathog.* **7**, e1002268 (2011).
75. Teo, T.-H. *et al.* Caribbean and La Réunion Chikungunya Virus Isolates Differ in Their Capacity To Induce Proinflammatory Th1 and NK Cell Responses and Acute Joint Pathology. *J. Virol.* **89**, 7955–7969 (2015).
76. Long, K. M. *et al.* $\gamma\delta$ T Cells Play a Protective Role in Chikungunya Virus-Induced Disease. *J. Virol.* **90**, 433–443 (2016).
77. Shikhagaie, M. M., Germar, K., Bal, S. M., Ros, X. R. & Spits, H. Innate lymphoid cells in autoimmunity: emerging regulators in rheumatic diseases. *Nat. Rev. Rheumatol.* **13**, 164–173 (2017).
78. Lee, W. W. L. *et al.* Expanding Regulatory T Cells Alleviates Chikungunya Virus-Induced Pathology in Mice. *J. Virol.* **89**, 7893–7904 (2015).
79. Teo, T.-H. *et al.* A Pathogenic Role for CD4⁺ T Cells during Chikungunya Virus Infection in

- Mice. *J. Immunol.* **190**, 259–269 (2013).
80. ISAACS, A. & LINDENMANN, J. Virus interference. I. The interferon. *Proc. R. Soc. London. Ser. B, Biol. Sci.* **147**, 258–67 (1957).
 81. ISAACS, A., LINDENMANN, J. & VALENTINE, R. C. Virus interference. II. Some properties of interferon. *Proc. R. Soc. London. Ser. B, Biol. Sci.* **147**, 268–73 (1957).
 82. Honda, K. & Taniguchi, T. IRFs: master regulators of signalling by Toll-like receptors and cytosolic pattern-recognition receptors. *Nat. Rev. Immunol.* **6**, 644–658 (2006).
 83. Desmet, C. J. & Ishii, K. J. Nucleic acid sensing at the interface between innate and adaptive immunity in vaccination. *Nat. Rev. Immunol.* **12**, 479–491 (2012).
 84. Paludan, S. R. Activation and Regulation of DNA-Driven Immune Responses. *Microbiol. Mol. Biol. Rev.* **79**, 225–241 (2015).
 85. Honda, K., Takaoka, A. & Taniguchi, T. Type I Interferon Gene Induction by the Interferon Regulatory Factor Family of Transcription Factors. *Immunity* **25**, 349–360 (2006).
 86. Takaoka, A. *et al.* DAI (DLM-1/ZBP1) is a cytosolic DNA sensor and an activator of innate immune response. *Nature* **448**, 501–505 (2007).
 87. Sun, L., Wu, J., Du, F., Chen, X. & Chen, Z. J. Cyclic GMP-AMP Synthase Is a Cytosolic DNA Sensor That Activates the Type I Interferon Pathway. *Science (80-.)*. **339**, 786–791 (2013).
 88. Wu, J. *et al.* Cyclic GMP-AMP is an endogenous second messenger in innate immune signaling by cytosolic DNA. *Science* **339**, 826–30 (2013).
 89. Hemmi, H. *et al.* A Toll-like receptor recognizes bacterial DNA. *Nature* **408**, 740–5 (2000).
 90. Liu, X. & Wang, C. The emerging roles of the STING adaptor protein in immunity and diseases. *Immunology* **147**, 285–291 (2016).
 91. Barbalat, R., Ewald, S. E., Mouchess, M. L. & Barton, G. M. Nucleic Acid Recognition by the Innate Immune System. *Annu. Rev. Immunol.* **29**, 185–214 (2011).
 92. Sato, M., Tanaka, N., Hata, N., Oda, E. & Taniguchi, T. Involvement of the IRF family transcription factor IRF-3 in virus-induced activation of the IFN- β gene. *FEBS Lett.* **425**, 112–116 (1998).
 93. Lin, R., Heylbroeck, C., Pitha, P. M. & Hiscott, J. Virus-Dependent Phosphorylation of the IRF-3 Transcription Factor Regulates Nuclear Translocation, Transactivation Potential, and Proteasome-Mediated Degradation. *Mol. Cell. Biol.* **18**, 2986–2996 (1998).
 94. Marie, I. Differential viral induction of distinct interferon-alpha genes by positive feedback through interferon regulatory factor-7. *EMBO J.* **17**, 6660–6669 (1998).
 95. Sato, M. *et al.* Positive feedback regulation of type I IFN genes by the IFN-inducible transcription factor IRF-7. *FEBS Lett.* **441**, 106–110 (1998).

96. Daffis, S. *et al.* Interferon Regulatory Factor IRF-7 Induces the Antiviral Alpha Interferon Response and Protects against Lethal West Nile Virus Infection. *J. Virol.* **82**, 8465–8475 (2008).
97. Schilte, C. *et al.* Cutting Edge: Independent Roles for IRF-3 and IRF-7 in Hematopoietic and Nonhematopoietic Cells during Host Response to Chikungunya Infection. *J. Immunol.* **188**, 2967–2971 (2012).
98. Sheehan, K. C. F., Lazear, H. M., Diamond, M. S. & Schreiber, R. D. Selective blockade of Interferon- α and - β reveals their non-redundant functions in a mouse model of West Nile virus infection. *PLoS One* **10**, 1–19 (2015).
99. Ciancanelli, M. J. *et al.* Life-threatening influenza and impaired interferon amplification in human IRF7 deficiency. *Science (80-.)*. **348**, 448–453 (2015).
100. Gilliet, M., Cao, W. & Liu, Y.-J. Plasmacytoid dendritic cells: sensing nucleic acids in viral infection and autoimmune diseases. *Nat. Rev. Immunol.* **8**, 594–606 (2008).
101. Swiecki, M., Wang, Y., Gilfillan, S. & Colonna, M. Plasmacytoid Dendritic Cells Contribute to Systemic but Not Local Antiviral Responses to HSV Infections. *PLoS Pathog.* **9**, 2–11 (2013).
102. Swiecki, M. & Colonna, M. The multifaceted biology of plasmacytoid dendritic cells. *Nat. Rev. Immunol.* **15**, 471–485 (2015).
103. Uzé, G., Schreiber, G., Piehler, J. & Pellegrini, S. The Receptor of the Type I Interferon Family. in *Interferon: The 50th Anniversary* **316 VN-r**, 71–95 (Springer Berlin Heidelberg, 2007).
104. Plataniias, L. C. Mechanisms of type-I- and type-II-interferon-mediated signalling. *Nat. Rev. Immunol.* **5**, 375–386 (2005).
105. Haque, S. J. & Williams, B. R. Identification and characterization of an interferon (IFN)-stimulated response element-IFN-stimulated gene factor 3-independent signaling pathway for IFN- α . *J. Biol. Chem.* **269**, 19523–9 (1994).
106. Wen, Z., Zhong, Z. & Darnell, J. E. Maximal activation of transcription by Stat1 and Stat3 requires both tyrosine and serine phosphorylation. *Cell* **82**, 241–50 (1995).
107. Wen, Z. & Darnell, J. E. Mapping of Stat3 serine phosphorylation to a single residue (727) and evidence that serine phosphorylation has no influence on DNA binding of Stat1 and Stat3. *Nucleic Acids Res.* **25**, 2062–7 (1997).
108. González-Navajas, J. M., Lee, J., David, M. & Raz, E. Immunomodulatory functions of type I interferons. *Nat. Rev. Immunol.* **12**, 125–35 (2012).
109. Uddin, S. *et al.* Activation of the p38 mitogen-activated protein kinase by type I interferons. *J. Biol. Chem.* **274**, 30127–31 (1999).
110. Goh, K. C., Haque, S. J. & Williams, B. R. p38 MAP kinase is required for STAT1 serine phosphorylation and transcriptional activation induced by interferons. *EMBO J.* **18**, 5601–8 (1999).

111. Nguyen, H., Ramana, C. V., Bayes, J. & Stark, G. R. Roles of phosphatidylinositol 3-kinase in interferon-gamma-dependent phosphorylation of STAT1 on serine 727 and activation of gene expression. *J. Biol. Chem.* **276**, 33361–8 (2001).
112. Ahmad, S., Alsayed, Y. M., Druker, B. J. & Plataniias, L. C. The type I interferon receptor mediates tyrosine phosphorylation of the CrkL adaptor protein. *J. Biol. Chem.* **272**, 29991–4 (1997).
113. Fros, J. J. & Pijlman, G. P. Alphavirus infection: Host cell shut-off and inhibition of antiviral responses. *Viruses* **8**, 166 (2016).
114. Fros, J. J., van der Maten, E., Vlak, J. M. & Pijlman, G. P. The C-Terminal Domain of Chikungunya Virus nsP2 Independently Governs Viral RNA Replication, Cytopathicity, and Inhibition of Interferon Signaling. *J. Virol.* **87**, 10394–10400 (2013).
115. Fros, J. J. *et al.* Chikungunya Virus Nonstructural Protein 2 Inhibits Type I/II Interferon-Stimulated JAK-STAT Signaling. *J. Virol.* **84**, 10877–10887 (2010).
116. Schilte, C. *et al.* Type I IFN controls chikungunya virus via its action on nonhematopoietic cells. *J. Exp. Med.* **207**, 429–442 (2010).
117. Her, Z. *et al.* Loss of TLR3 aggravates CHIKV replication and pathology due to an altered virus-specific neutralizing antibody response. *EMBO Mol. Med.* **7**, 24–41 (2015).
118. Ryman, K. D., Klimstra, W. B., Nguyen, K. B., Biron, C. a & Johnston, R. E. Alpha/beta interferon protects adult mice from fatal Sindbis virus infection and is an important determinant of cell and tissue tropism. *J. Virol.* **74**, 3366–78 (2000).
119. Muller, U. *et al.* Functional Role of Type I and Type 11 in Antiviral Interferons Defense. **264**, 1918–1921 (1994).
120. Grieder, F. B. & Vogel, S. N. Role of interferon and interferon regulatory factors in early protection against Venezuelan equine encephalitis virus infection. *Virology* **257**, 106–18 (1999).
121. Teng, T. S. *et al.* Viperin restricts chikungunya virus replication and pathology. *J. Clin. Invest.* **122**, 4447–4460 (2012).
122. Pindel, A. & Sadler, A. The Role of Protein Kinase R in the Interferon Response. *J. Interf. Cytokine Res.* **31**, 59–70 (2011).
123. White, L. K. *et al.* Chikungunya Virus Induces IPS-1-Dependent Innate Immune Activation and Protein Kinase R-Independent Translational Shutoff. *J. Virol.* **85**, 606–620 (2011).
124. Clavarino, G. *et al.* Induction of GADD34 is necessary for dsRNA-dependent interferon- β production and participates in the control of Chikungunya virus infection. *PLoS Pathog.* **8**, (2012).
125. Poddar, S., Hyde, J. L., Gorman, M. J., Farzan, M. & Diamond, M. S. The Interferon-Stimulated Gene IFITM3 Restricts Infection and Pathogenesis of Arthritogenic and Encephalitic Alphaviruses. *J. Virol.* **90**, 8780–8794 (2016).

126. Jones, P. H. *et al.* BST-2/tetherin-mediated restriction of chikungunya (CHIKV) VLP budding is counteracted by CHIKV non-structural protein 1 (nsP1). *Virology* **438**, 37–49 (2013).
127. Mahauad-Fernandez, W. D., Jones, P. H. & Okeoma, C. M. Critical role for bone marrow stromal antigen 2 in acute Chikungunya virus infection. *J. Gen. Virol.* **95**, 2450–2461 (2014).
128. Morales, D. J. & Lenschow, D. J. The antiviral activities of ISG15. *J. Mol. Biol.* **425**, 4995–5008 (2013).
129. Shabman, R. S. *et al.* Differential Induction of Type I Interferon Responses in Myeloid Dendritic Cells by Mosquito and Mammalian-Cell-Derived Alphaviruses. *J. Virol.* **81**, 237–247 (2007).
130. Samuel, M. a & Diamond, M. S. Alpha/Beta Interferon Protects against Lethal West Nile Virus Infection by Restricting Cellular Tropism and Enhancing Neuronal Survival. *J. Virol.* **79**, 13350–13361 (2005).
131. Piehler, J., Roisman, L. C. & Schreiber, G. New Structural and Functional Aspects of the Type I Interferon-Receptor Interaction Revealed by Comprehensive Mutational Analysis of the Binding Interface. *J. Biol. Chem.* **275**, 40425–40433 (2000).
132. Roisman, L. C., Jaitin, D. A., Baker, D. P. & Schreiber, G. Mutational Analysis of the IFNAR1 Binding Site on IFN α 2 Reveals the Architecture of a Weak Ligand–Receptor Binding-site. *J. Mol. Biol.* **353**, 271–281 (2005).
133. Gavutis, M., Jaks, E., Lamken, P. & Piehler, J. Determination of the Two-Dimensional Interaction Rate Constants of a Cytokine Receptor Complex. *Biophys. J.* **90**, 3345–3355 (2006).
134. Strunk, J. J. *et al.* Ligand Binding Induces a Conformational Change in ifnar1 that Is Propagated to Its Membrane-Proximal Domain. *J. Mol. Biol.* **377**, 725–739 (2008).
135. Coelho, L. F. L., Magno de Freitas Almeida, G., Mennechet, F. J. D., Blangy, A. & Uzé, G. Interferon-alpha and -beta differentially regulate osteoclastogenesis: role of differential induction of chemokine CXCL11 expression. *Proc. Natl. Acad. Sci. U. S. A.* **102**, 11917–22 (2005).
136. Schreiber, G. & Piehler, J. The molecular basis for functional plasticity in type I interferon signaling. *Trends Immunol.* **36**, 139–149 (2015).
137. Fung, K. Y. *et al.* Interferon-epsilon Protects the Female Reproductive Tract from Viral and Bacterial Infection. *Science (80-.).* **339**, 1088–1092 (2013).
138. Hermant, P., Francius, C., Clotman, F. & Michiels, T. IFN- ϵ Is Constitutively Expressed by Cells of the Reproductive Tract and Is Inefficiently Secreted by Fibroblasts and Cell Lines. *PLoS One* **8**, 1–9 (2013).
139. Stifter, S. A. *et al.* Defining the distinct, intrinsic properties of the novel type I interferon, IFN ϵ . *J. Biol. Chem.* **293**, 3168–3179 (2018).
140. Yang, L. *et al.* Molecular and functional characterization of canine interferon-epsilon. *J. Interferon Cytokine Res.* **33**, 760–8 (2013).

141. Takaoka, A. *et al.* Cross talk between interferon-gamma and -alpha/beta signaling components in caveolar membrane domains. *Science* **288**, 2357–60 (2000).
142. Lazear, H. M., Pinto, A. K., Vogt, M. R., Gale, M. & Diamond, M. S. Beta Interferon Controls West Nile Virus Infection and Pathogenesis in Mice. *J. Virol.* **85**, 7186–7194 (2011).
143. Daffis, S., Samuel, M. A., Keller, B. C., Gale, M. & Diamond, M. S. Cell-Specific IRF-3 Responses Protect against West Nile Virus Infection by Interferon-Dependent and -Independent Mechanisms. *PLoS Pathog.* **3**, e106 (2007).
144. Deonarain, R. *et al.* Impaired Antiviral Response and Alpha / Beta Interferon Induction in Mice Lacking Beta Interferon Impaired Antiviral Response and Alpha / Beta Interferon Induction in Mice Lacking Beta Interferon. (2000). doi:10.1128/JVI.74.7.3404-3409.2000.Updated
145. Deonarain, R., Cerullo, D., Fuse, K., Liu, P. P. & Fish, E. N. Protective role for interferon- β in coxsackievirus B3 infection. *Circulation* **110**, 3540–3543 (2004).
146. Davidson, S., Maini, M. K. & Wack, A. Disease-Promoting Effects of Type I Interferons in Viral, Bacterial, and Coinfections. *J. Interf. Cytokine Res.* **35**, 252–264 (2015).
147. Tumpey, T. M. *et al.* The Mx1 Gene Protects Mice against the Pandemic 1918 and Highly Lethal Human H5N1 Influenza Viruses. *J. Virol.* **81**, 10818–10821 (2007).
148. Davidson, S., Crotta, S., McCabe, T. M. & Wack, A. Pathogenic potential of interferon $\alpha\beta$ in acute influenza infection. *Nat. Commun.* **5**, (2014).
149. Koerner, I., Kochs, G., Kalinke, U., Weiss, S. & Staeheli, P. Protective Role of Beta Interferon in Host Defense against Influenza A Virus. *J. Virol.* **81**, 2025–2030 (2007).
150. Ng, C. T. *et al.* Blockade of Interferon Beta, but Not Interferon Alpha, Signaling Controls Persistent Viral Infection. *Cell Host Microbe* **17**, 653–661 (2015).
151. Wilson, E. B. *et al.* Blockade of Chronic Type I Interferon Signaling to Control Persistent LCMV Infection. *Science (80-.)*. **340**, 202–207 (2013).
152. Teijaro, J. R. *et al.* Persistent LCMV Infection Is Controlled by Blockade of Type I Interferon Signaling. *Science (80-.)*. **340**, 207–211 (2013).
153. Wijesundara, D. K., Xi, Y. & Ranasinghe, C. Unravelling the convoluted biological roles of type I interferons (IFN-Is) in infection and immunity: A way forward for therapeutics and vaccine design. *Front. Immunol.* **5 VN-re**, 412 (2014).
154. Jaitin, D. A. *et al.* Inquiring into the differential action of interferons (IFNs): an IFN-alpha2 mutant with enhanced affinity to IFNAR1 is functionally similar to IFN-beta. *Mol. Cell. Biol.* **26**, 1888–97 (2006).
155. Thomas, C. *et al.* Structural linkage between ligand discrimination and receptor activation by Type I interferons. *Cell* **146**, 621–632 (2011).
156. Piehler, J., Thomas, C., Garcia, K. C. & Schreiber, G. Structural and dynamic determinants of type

- I interferon receptor assembly and their functional interpretation. *Immunol. Rev.* **250**, 317–334 (2012).
157. Schreiber, G. The molecular basis for differential type I interferon signaling. *J. Biol. Chem.* **292**, 7285–7294 (2017).
 158. Bego, M. G., Mercier, J. & Cohen, E. A. Virus-Activated Interferon Regulatory Factor 7 Upregulates Expression of the Interferon-Regulated BST2 Gene Independently of Interferon Signaling. *J. Virol.* **86**, 3513–3527 (2012).
 159. Georgiades, P. *et al.* vavCre Transgenic mice: A tool for mutagenesis in hematopoietic and endothelial lineages. *genesis* **34**, 251–256 (2002).
 160. Ciccia, F. *et al.* Interleukin-9 and T helper type 9 cells in rheumatic diseases. *Clin. Exp. Immunol.* **185**, 125–132 (2016).
 161. Chowdhury, K. *et al.* Synovial IL-9 facilitates neutrophil survival, function and differentiation of Th17 cells in rheumatoid arthritis. *Arthritis Res. Ther.* **20**, 18 (2018).
 162. Yang, Y., Du, L., Sun, M., Kijlstra, A. & Yang, P. IFN- β Inhibits the Increased Expression of IL-9 during Experimental Autoimmune Uveoretinitis. *PLoS One* **7**, 3–8 (2012).
 163. Zust, R. *et al.* Type I Interferon Signals in Macrophages and Dendritic Cells Control Dengue Virus Infection: Implications for a New Mouse Model To Test Dengue Vaccines. *J. Virol.* **88**, 7276–7285 (2014).
 164. Ospelt, C. Synovial fibroblasts in 2017. *RMD open* **3**, e000471 (2017).
 165. Carrión, M. *et al.* RNA sensors in human osteoarthritis and rheumatoid arthritis synovial fibroblasts: Immune regulation by vasoactive intestinal peptide. *Arthritis Rheum.* **63**, 1626–1636 (2011).
 166. Adams, V. *et al.* Induction of iNOS expression in skeletal muscle by IL-1beta and NFkappaB activation: an in vitro and in vivo study. *Cardiovasc. Res.* **54**, 95–104 (2002).
 167. Lim, P.-Y., Behr, M. J., Chadwick, C. M., Shi, P.-Y. & Bernard, K. A. Keratinocytes are cell targets of West Nile virus in vivo. *J. Virol.* **85**, 5197–201 (2011).
 168. Surasombatpattana, P. *et al.* Dengue virus replication in infected human keratinocytes leads to activation of antiviral innate immune responses. *Infect. Genet. Evol.* **11**, 1664–73 (2011).
 169. Ng, C. T. & Oldstone, M. B. A. Infected CD8 α - dendritic cells are the predominant source of IL-10 during establishment of persistent viral infection. *Proc. Natl. Acad. Sci.* **109**, 14116–14121 (2012).
 170. Prinz, M. *et al.* Distinct and Nonredundant In Vivo Functions of IFNAR on Myeloid Cells Limit Autoimmunity in the Central Nervous System. *Immunity* **28**, 675–686 (2008).
 171. Kasper, L. H. & Reder, A. T. Immunomodulatory activity of interferon-beta. *Ann. Clin. Transl. Neurol.* **1**, 622–631 (2014).

172. Goswami, R. & Kaplan, M. H. A Brief History of IL-9. *J. Immunol.* **186**, 3283–3288 (2011).
173. Wilhelm, C. *et al.* An IL-9 fate reporter demonstrates the induction of an innate IL-9 response in lung inflammation. *Nat. Immunol.* **12**, 1071–1077 (2011).
174. Licona-Limón, P., Kim, L. K., Palm, N. W. & Flavell, R. A. TH2, allergy and group 2 innate lymphoid cells. *Nat. Immunol.* **14**, 536–542 (2013).
175. Ozawa, T. *et al.* Thymic stromal lymphopoietin secretion of synovial fibroblasts is positively and negatively regulated by Toll-like receptors/nuclear factor-kappaB pathway and interferon-gamma/dexamethasone. *Mod. Rheumatol.* **17**, 459–63 (2007).
176. Campo, G. M. *et al.* 6-Mer hyaluronan oligosaccharides increase IL-18 and IL-33 production in mouse synovial fibroblasts subjected to collagen-induced arthritis. *Innate Immun.* **18**, 675–684 (2012).
177. Vanlandingham, D. L. *et al.* Development and characterization of a double subgenomic chikungunya virus infectious clone to express heterologous genes in *Aedes aegypti* mosquitoes. *Insect Biochem. Mol. Biol.* **35**, 1162–70 (2005).
178. ROSS, R. W. The Newala epidemic. III. The virus: isolation, pathogenic properties and relationship to the epidemic. *J. Hyg. (Lond).* **54**, 177–91 (1956).
179. Petersen, L. R. & Powers, A. M. Chikungunya: epidemiology. *F1000Research* **5**, (2016).
180. Rodriguez-Morales, A. J. *et al.* Post-chikungunya chronic inflammatory rheumatism: results from a retrospective follow-up study of 283 adult and child cases in La Virginia, Risaralda, Colombia. *F1000Research* **5**, 360 (2016).
181. Sissoko, D. *et al.* Post-epidemic Chikungunya disease on Reunion Island: course of rheumatic manifestations and associated factors over a 15-month period. *PLoS Negl. Trop. Dis.* **3**, e389 (2009).
182. Manimunda, S. P. *et al.* Clinical progression of chikungunya fever during acute and chronic arthritic stages and the changes in joint morphology as revealed by imaging. *Trans. R. Soc. Trop. Med. Hyg.* **104**, 392–399 (2010).
183. Fourie, E. D. & Morrison, J. G. Rheumatoid arthritic syndrome after chikungunya fever. *South African Med. J.* **56**, 130–2 (1979).
184. Bouquillard, E. & Combe, B. Rheumatoid arthritis after Chikungunya fever: a prospective follow-up study of 21 cases. *Ann. Rheum. Dis.* **68**, 1505–6 (2009).
185. Larsen, A. & Thoen, J. Hand radiography of 200 patients with rheumatoid arthritis repeated after an interval of one year. *Scand. J. Rheumatol.* **16**, 395–401 (1987).
186. Dowty, M. E. *et al.* Preclinical to clinical translation of tofacitinib, a Janus kinase inhibitor, in rheumatoid arthritis. *J. Pharmacol. Exp. Ther.* **348**, 165–73 (2014).
187. Fleischmann, R. *et al.* Placebo-controlled trial of tofacitinib monotherapy in rheumatoid arthritis.

- N. Engl. J. Med.* **367**, 495–507 (2012).
188. Pandya, S. Methotrexate and hydroxychloroquine combination therapy in chronic chikungunya arthritis: a 16 week study. *Indian J. Rheumatol.* **3**, 93–97 (2008).
 189. Goupil, B. A. *et al.* Novel lesions of bones and joints associated with chikungunya virus infection in two mouse models of disease: New insights into disease pathogenesis. *PLoS One* **11**, 1–21 (2016).
 190. Nakaya, H. I. *et al.* Gene profiling of Chikungunya virus arthritis in a mouse model reveals significant overlap with rheumatoid arthritis. *Arthritis Rheum.* **64**, 3553–63 (2012).
 191. Rulli, N. E. *et al.* Protection From Arthritis and Myositis in a Mouse Model of Acute Chikungunya Virus Disease by Bindarit, an Inhibitor of Monocyte Chemotactic Protein-1 Synthesis. *J. Infect. Dis.* **204**, 1026–1030 (2011).
 192. Pal, P. *et al.* Development of a Highly Protective Combination Monoclonal Antibody Therapy against Chikungunya Virus. *PLoS Pathog.* **9**, e1003312 (2013).
 193. Goh, L. Y. H. *et al.* Neutralizing monoclonal antibodies to the E2 protein of chikungunya virus protects against disease in a mouse model. *Clin. Immunol.* **149**, 487–97 (2013).
 194. Lenschow, D. *et al.* Long-term survival of xenogeneic pancreatic islet grafts induced by CTLA4lg. *Science (80-.).* **257**, 789–792 (1992).
 195. Liu, R., Bal, H. S., Desta, T., Behl, Y. & Graves, D. T. Tumor necrosis factor-alpha mediates diabetes-enhanced apoptosis of matrix-producing cells and impairs diabetic healing. *Am. J. Pathol.* **168**, 757–64 (2006).
 196. Cutolo, M. *et al.* CTLA4-Ig interacts with cultured synovial macrophages from rheumatoid arthritis patients and downregulates cytokine production. *Arthritis Res. Ther.* **11**, R176 (2009).
 197. Liu, Y. *et al.* Co-stimulation of murine CD4 T cell growth: cooperation between B7 and heat-stable antigen. *Eur. J. Immunol.* **22**, 2855–9 (1992).
 198. Wu, Y., Guo, Y. & Liu, Y. A major costimulatory molecule on antigen-presenting cells, CTLA4 ligand A, is distinct from B7. *J. Exp. Med.* **178**, 1789–93 (1993).
 199. Teo, T. H. *et al.* Fingolimod treatment abrogates chikungunya virus-induced arthralgia. *Sci. Transl. Med.* **9**, 1–12 (2017).
 200. Lee, E. B. *et al.* Tofacitinib versus methotrexate in rheumatoid arthritis. *N. Engl. J. Med.* **370**, 2377–86 (2014).
 201. Blettery, M. *et al.* Brief Report: Management of Chronic Post-Chikungunya Rheumatic Disease: The Martinican Experience. *Arthritis Rheumatol.* **68**, 2817–2824 (2016).
 202. Zaid, A., Rulli, N. E., Rolph, M. S., Suhrbier, A. & Mahalingam, S. Disease exacerbation by etanercept in a mouse model of alphaviral arthritis and myositis. *Arthritis Rheum.* **63**, 488–91 (2011).

203. Bellini, R. *et al.* Impact of Chikungunya virus on *Aedes albopictus* females and possibility of vertical transmission using the actors of the 2007 outbreak in Italy. *PLoS One* **7**, e28360 (2012).
204. Oliphant, T. *et al.* Development of a humanized monoclonal antibody with therapeutic potential against West Nile virus. *Nat. Med.* **11**, 522–30 (2005).
205. Brüning, J. C. *et al.* A muscle-specific insulin receptor knockout exhibits features of the metabolic syndrome of NIDDM without altering glucose tolerance. *Mol. Cell* **2**, 559–69 (1998).
206. Zheng, B., Zhang, Z., Black, C. M., de Crombrughe, B. & Denton, C. P. Ligand-dependent genetic recombination in fibroblasts : a potentially powerful technique for investigating gene function in fibrosis. *Am. J. Pathol.* **160**, 1609–17 (2002).
207. Elyaman, W. *et al.* Notch Receptors and Smad3 Signaling Cooperate in the Induction of Interleukin-9-Producing T Cells. *Immunity* **36**, 623–634 (2012).
208. Kopach, P. *et al.* IFN- γ directly controls IL-33 protein level through a STAT1- and LMP2-dependent mechanism. *J. Biol. Chem.* **289**, 11829–43 (2014).
209. McNab, F., Mayer-Barber, K., Sher, A., Wack, A. & O’Garra, A. Type I interferons in infectious disease. *Nat. Rev. Immunol.* **15**, 87–103 (2015).
210. Hawman, D. W. *et al.* Pathogenic Chikungunya Virus Evades B Cell Responses to Establish Persistence. *Cell Rep.* **16**, 1326–1338 (2016).